

Josip Juraj Strossmayer University of Osijek, Croatia

University of Dubrovnik, Croatia

Ruđer Bošković Institute, Zagreb, Croatia

University Postgraduate Interdisciplinary Doctoral Study

Molecular Biosciences

Jelena Dragojević

**CHARACTERIZATION OF ORGANIC ANION TRANSPORTERS IN
ZEBRAFISH (*DANIO RERIO* HAMILTON, 1822)**

DOCTORAL THESIS

Osijek, 2018.

TEMELJNA DOKUMENTACIJSKA KARTICA

Sveučilište Josipa Jurja Strossmayera u Osijeku

Doktorska disertacija

Sveučilište u Dubrovniku

Institut Ruđer Bošković

Poslijediplomski interdisciplinarni sveučilišni studij Molekularne bioznanosti

Znanstveno područje: Prirodne znanosti

Znanstveno polje: Biologija

Karakterizacija prijenosnika organskih aniona zebrice (*Danio rerio* Hamilton, 1822)

Jelena Dragojević

Rad je izrađen u: Institut Ruđer Bošković, Zagreb

Mentor: dr. sc. Tvrtko Smital, znanstveni savjetnik

Kratki sažetak doktorskog rada:

Prijenosnici organskih aniona su membranski transportni proteini iz obitelji SLC21 (OATP, engl. *organic anion-transporting polypeptides*) i SLC22 (OAT, engl. *organic anion transporters*) unutar nadobitelji SLC (engl. *solute carriers*). Odgovorni su za unos endo- i ksenobiotika u stanicu. Usprkos ključnoj ulozi u toksikološkom odgovoru, njihova ekotoksikološka važnost i karakteristike su slabo istražene. Stoga je glavni cilj ovog istraživanja bila identifikacija i molekularna karakterizacija prijenosnika organskih aniona kod zebrice (*Danio rerio*). Dodatan cilj je bio stvaranje *knockout* zebrica za najbolje istraženi prijenosnik organskih aniona zebrice, Oatp1d1. Kod zebrice je prisutno sedam Oat proteina: Oat1, Oat2a, 2b, 2c, 2d, 2e i Oat3, a kodirani su genima *slc22a6*, *slc22a7(a-e)* i *slc22a8*. Identificirani su novi modelni fluorescentni supstrati za pet Oat transporterera zebrice te su razvijeni standardizirani visoko protočni *in vitro* testovi za identifikaciju interaktora tih 5 proteina. Oat transporteri zebrice su pokazali interakciju s raznovrsnim endogenim spojevima te raznim ksenobioticima. Stvorene su i prve *knockout* zebrice za Oatp1d1 pomoću CRISPR/Cas9 pristupa editiranja genoma.

Broj stranica: 110

Broj slika: 45

Broj tablica: 10

Broj literaturnih navoda: 122

Jezik izvornika: engleski

Ključne riječi: SLC prijenosnici, *Danio rerio*, filogenetska analiza, sintenija, tkivna ekspresija, funkcija, ADME, CRISPR/Cas9

Datum obrane: 14.12.2018.

Stručno povjerenstvo za obranu:

1. Andreja Ambriović Ristov, dr. sc., znanstvena savjetnica, Institut Ruđer Bošković, predsjednik
2. Davorka Breljak, dr. sc., znanstvena savjetnica, Institut za medicinska istraživanja i medicinu rada, Zagreb, član
3. Vera Cesar, dr. sc., redovita profesorica, Odjel za Biologiju, Sveučilište J. J. Strossmayera u Osijeku, član
4. Neda Slade, dr. sc., znanstvena savjetnica, Institut Ruđer Bošković, zamjena člana

Rad je pohranjen u: Nacionalnoj i sveučilišnoj knjižnici Zagreb, Ul. Hrvatske bratske zajednice 4, Zagreb; Gradskoj i sveučilišnoj knjižnici Osijek, Europska avenija 24, Osijek; Sveučilištu Josipa Jurja Strossmayera u Osijeku, Trg sv. Trojstva 3, Osijek.

BASIC DOCUMENTATION CARD

Josip Juraj Strossmayer University of Osijek

University of Dubrovnik

Ruđer Bošković Institute

University Postgraduate Interdisciplinary Doctoral Study of Molecular biosciences

PhD thesis

Scientific Area: Natural sciences

Scientific Field: Biology

Characterization of organic anion transporters in zebrafish (*Danio rerio* Hamilton, 1822)

Jelena Dragojević

Thesis performed at: Institut Ruđer Bošković, Zagreb

Supervisor: Tvrtko Smital, PhD, Senior Scientist

Short abstract:

Organic anion transporters (OATPs/OATs) are transmembrane proteins which belong to SLC21 and SLC22 subfamily of the SLC (Solute Carriers) family. They are responsible for the uptake of various endogenous and xenobiotic compounds into the cell. Despite their crucial role in toxicological response, their detailed ecotoxicological relevance and characteristics in non-mammalians are still unknown. Therefore, the main goal of this study was identification and molecular characterization of organic anion transporters in zebrafish (*Danio rerio*). Additional goal was the creation of zebrafish gene knockout for the best characterized zebrafish transporter of organic anions, Oatp1d1. Seven organic anion transporters are present in zebrafish: Oat1, Oat2a, 2b, 2c, 2d, 2e and Oat3, encoded by genes *slc22a6*, *slc22a7(a-e)* and *slc22a8*, respectively. New model fluorescent substrates were identified for 5 zebrafish Oats, and high throughput *in vitro* assays for identification of interactors of these proteins were developed. Zebrafish Oats showed interaction with various endo- and xenobiotics. The first CRISPR/Cas9 zebrafish Oatp1d1 knockouts were successfully generated.

Number of pages: 110

Number of figures: 45

Number of tables: 10

Number of references: 122

Original in: English

Key words: SLC transporters, *Danio rerio*, phylogenetic analysis, synteny analysis, tissue expression, function, ADME, CRISPR/Cas9

Date of the thesis defense: 14.12.2018.

Reviewers:

1. Andreja Ambriović Ristov, PhD, Senior Scientist, Ruđer Bošković Institute, Zagreb
2. Davorka Breljak, PhD, Senior Scientist, Institute for Medical Research and Occupational Health, Zagreb
3. Professor Vera Cesar, PhD, Josip Juraj Strossmayer University of Osijek
4. Neda Slade, PhD, Senior Scientist, Ruđer Bošković Institute, Zagreb

Thesis deposited in: National and University Library in Zagreb, Ul. Hrvatske bratske zajednice 4, Zagreb, Croatia; City and University Library of Osijek, Europska avenija 24, Osijek, Croatia; Josip Juraj Strossmayer University of Osijek, Trg sv. Trojstva 3, Osijek, Croatia.

Research for this PhD thesis was performed in the Laboratory for Molecular Ecotoxicology, Division of Marine and Environmental Research, Ruđer Bošković Institute, Zagreb, under the supervision of Tvrtko Smital, PhD. This work was supported by the Croatian National Science Foundation (Project No. 4806), the SCOPES programme joint research project granted by the Swiss National Science Foundation (SNSF) (Grant No. SCOPES - IZ73ZO_152274/1), and by STIM - REI, a project funded by European Union from European Structural and Investment Funds 2014 - 2020, Contract Number: KK.01.1.1.01.0003.

Acknowledgments

Firstly, I would like to express my sincere gratitude to my supervisor Tvrtko Smital for giving me the opportunity to work in his lab, for his guidance, patience and motivation. I am grateful for your helpful comments, suggestions and constructive criticism throughout these four years of my Ph.D study.

Besides my advisor, I would like to thank my fellow labmates Ivan, Jovica, Petra, Marta and Roko for all they taught me and for all the help, guidance and stimulating discussions.

Also, I thank my dear colleagues from Department of Biology in Osijek. In particular, I am grateful to Branimir K. Hackenberger for enlightening me the first glance of research.

Most of all I would like to thank my beautiful family: my parents Jadranka and Vlado and to my brother Nikola and sister Sonja for their unconditional love and support throughout writing this thesis and my entire education and life in general. If I could choose any family in the world, I would always choose you.

I thank my friends: Doris for all the support, care and relaxing fun times we spent together, and Petra for emotional support and understanding during the toughest times in my work and life in general. I am forever thankful to my late best friend Nanook for unconditional love, all the fun and relaxing times we spent together throughout the last 12 years, those moments I will always cherish. You helped me so much and made me a better person.

Last but not least, I thank Bartol for all the love, encouragement and emotional support. Thank you for standing next to me while following my dreams.

TABLE OF CONTENTS

1. Introduction

1.1. Cellular detoxification mechanism – ADME	1
1.2. Important barriers and role of transport proteins	2
1.2.1. Intestinal barrier	3
1.2.2. Blood-brain barrier	4
1.2.3. Hepatic barrier	4
1.2.4. Renal barrier	5
1.3. Uptake transporters of organic anions	6
1.3.1. The SLC21 subfamily: Organic anion transporting polypeptides	6
1.3.1.1. Zebrafish Oatp1d1	8
1.3.2. The SLC22 subfamily	8
1.3.2.1. Organic anion transporters (OATs)	10
1.3.2.1.1. Cellular and tissue distribution of OATs	11
1.3.2.1.2. Mechanism of transport	12
1.3.2.1.3. Substrate specificity	14
1.3.2.1.4. Structure and function	15
1.3.2.1.5. Regulation	17
1.3.2.1.5.1. Transcriptional regulation	17
1.3.2.1.5.2. Post-translational mechanisms	18
1.4. Studies on non-mammalian uptake transporters	20
1.5. Zebrafish as a vertebrate model organism	20
1.6. Genome editing in zebrafish – CRISPR/Cas9	23
1.7. Summary and aims	28

2. Materials and Methods

2.1. Materials	30
2.2. Methods	33
2.2.1. Phylogenetic and synteny analysis	33
2.2.2. Tissue-specific gene expression analysis	33
2.2.3. Cloning and heterologous expression	35
2.2.3.1. Transient transfection	36
2.2.3.2. Stable transfection	37
2.2.4. Transport activity assays	38
2.2.5. Western blot analysis	39
2.2.6. Immunofluorescence	39
2.2.7. Creating gene knockouts using CRISPR/Cas9 system	40

2.2.8. Data analysis.....	41
3. Results	
3.1. Phylogenetic analysis.....	43
3.2. Synteny analysis	45
3.3. Tissue expression profiles	48
3.4. Protein identification and cell localization	50
3.5. Functional characterization of zebrafish Oats.....	54
3.5.1. Fluorescent substrates	54
3.5.2. Inhibition tests.....	58
3.5.2.1. The interaction screen assay	58
3.5.2.2. Dose-response assays.....	65
3.5.3. Determining the type of interaction	70
3.6. Creating gene knockouts using CRISPR/Cas9 system.....	72
4. Discussion.....	76
5. Conclusions.....	86
6. References.....	88
7. Summary	96
8. Sažetak	100
9. Abbreviations	102
10. Supplement	105
11. Curriculum vitae.....	109

1. Introduction

1.1. Cellular detoxification mechanism – ADME

Elimination of endo- and xenobiotic substances from the cell is essentially a four-step process based on the combination and coordination of metabolism and transport processes (Doring and Petzinger, 2014). This concept is included under the acronym "ADME", which stands for absorption, distribution, metabolism and elimination. Metabolism and detoxification of xenobiotics requires the sequential biotransformation steps of phase I and phase II (Williams, 1959), whereas xenobiotic transport includes two transport steps of phase 0 (Petzinger and Geyer, 2006) and phase III (Ishikawa, 1992). Phase 0 entails uptake membrane transporters that mediate passing of the compounds through the cell plasma membrane into the cell; phase I contains oxidoreductases and hydrolases that modify the substance chemically by processes such as oxidation, reduction and hydrolysis or by the removal and addition of an active group; phase II entails the conjugation of a drug or a phase I metabolite with a polar group to render it possible for excretion, e.g., sulphates and glucuronide; finally, phase III is mediated by efflux transporters that expel compounds out of the cell, and they belong to ABC (ATP Binding Cassette) and SLC (Solute Carriers) families (Goodman and Gilman, 1994). Principal sites of metabolism in vertebrates are liver and kidney and once the drug is rendered hydrophilic it can be easily excreted out by the bile and urine without significant reabsorption (Goodman and Gilman, 1994).

For a long period it was believed that small non-charged xenobiotic molecules may enter cells by passive diffusion. The same was considered for all lipophilic organic and inorganic molecules due to hydrophobic nature of the cell membrane lipid bilayer. Although evidence for the carrier-mediated transport of xenobiotics culminated during the 1980s, it was not before the first cloning of the drug transporter MDR1/P-glycoprotein (P-gp; ABCB1) from the ABC family in 1985, that an additional elimination step was recognized to describe the excretion of drug metabolites by carrier-mediated efflux transport (Riordan et al., 1985). Whereas the term "phase III", affirmed in 1990s, described the efflux of drugs, the carrier-mediated uptake from the blood or gut lumen into the metabolizing cell was not considered until 2006, when Petzinger & Geyer termed that process the "phase 0 transport" (Petzinger & Geyer, 2006). In the liver and kidney cells, phase 0 carrier-mediated uptake occurs at the blood-facing basolateral membrane and is spatially separated from the bile-facing canalicular membrane and the urine-facing tubule brush border membrane (Fig. 1). Thus,

the sequence of the transport phases allows vectorial transcellular drug transfer (Doring and Petzinger, 2014).

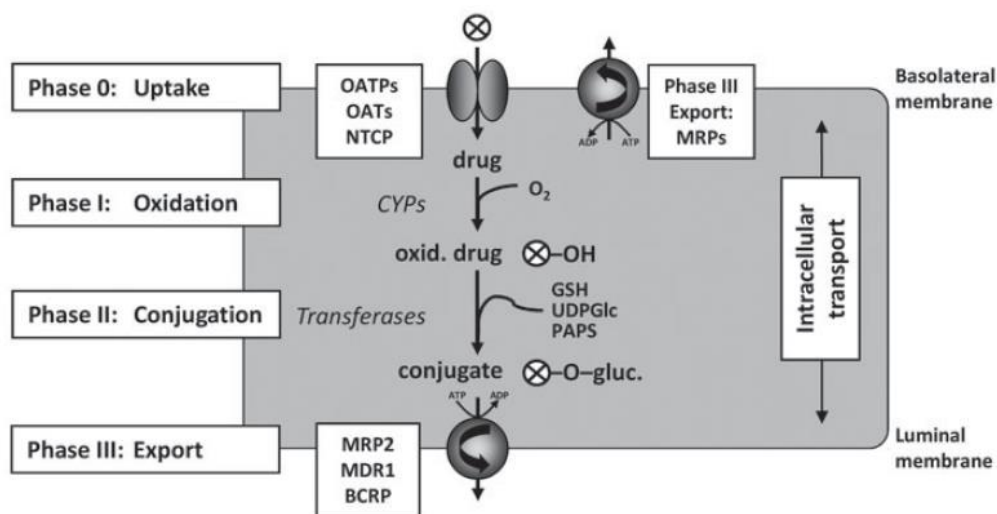


Figure 1. Sequential steps of elimination of xenobiotic substances by metabolism and membrane transport (adapted from Doring and Petzinger, 2014).

1.2. Important barriers and role of transport proteins

Transcellular permeation of chemicals has been viewed as the combination of passive and/or transporter-mediated processes (Sugano et al., 2010). More recently, it has been suggested that all drug transport is essentially carrier mediated, because of the large number of transporters (any particular cell may express dozens of transporters) and the broad substrate specificity of many transporters, as well as the energetically unfavorable transbilayer permeation of small charged molecules (Kell et al., 2011). Human genome sequencing yielded 833 putative transporter genes that, for the most part, belong to two main superfamilies of human membrane transporters: ABC transporters, mediating mainly cellular efflux, and the SLC, mainly mediating cellular uptake of their substrates (Gaborik et al., 2017).

Membrane transporters are well recognized determinants of drug disposition and effects (Giacomini et al., 2010; Klaassen and Aleksunes, 2010; Zolk and Fromm, 2011). Therefore, they have attracted great attention and are listed as critical elements to consider when evaluating drug-drug interactions by US FDA (Giacomini et al., 2010; Morrissey et al., 2013).

Membrane transporters can be divided into two groups based on their cellular location and function: uptake transporters that mediate the entry of their substrates into the cell (phase 0 of ADME), and efflux transporters that mediate the excretion of compounds out of the cell (phase 3 of ADME). Uptake transporters are mostly members of SLC22/Slc22 (organic cation transporters, OCTs; organic cation and zwitterion transporters, OCTNs; and organic anion transporters, OATs) and SLC21/Slc21 (organic anion transporting polypeptides, OATPs), while efflux transporters are usually members of ABC or MATE (multidrug and toxin compound extrusion) families. Considering function of these transporters, it is expected that they are expressed at the barrier tissues.

1.2.1. Intestinal barrier

In mammals, intestine is the site of absorption of orally administered drugs. Main cellular components of the intestinal barrier are enterocytes found in small intestine, which is considered the most important site of absorption due to its large surface area and a proximal position to stomach. However, as the activity of metabolic enzymes is lower in the colon, it is becoming an attractive site for absorption of controlled release drug formulations (Lin et al., 1999). Transporters that are expressed in human enterocytes are depicted in Fig. 2.

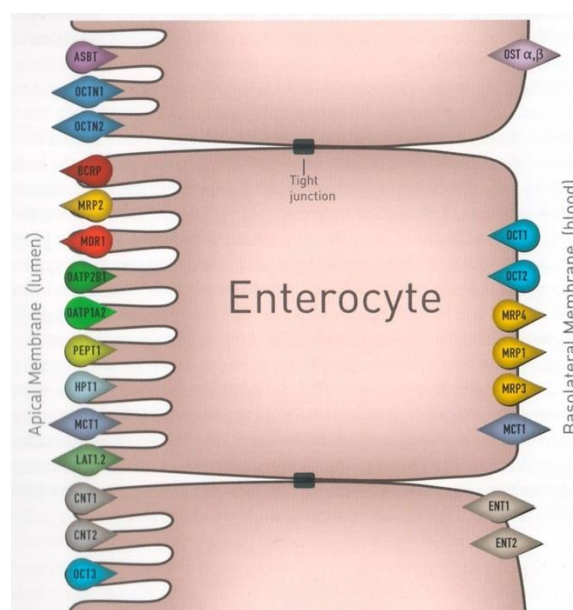


Figure 2. Transporters in human intestinal barrier (from Gaborik et al., 2017).

1.2.2. Blood-brain barrier

The two major interfaces connecting the blood and brain compartments in vertebrates are the blood-brain barrier (BBB) and the blood-cerebrospinal fluid barrier (BCSFB). As the surface area of BBB in mammals is approximately 100-fold larger than BCSFB and the distance between neurons and brain capillaries is less than 20 nm in the BBB while the distance between the brain ventricles and circumventricular organs is in the order of millimeters in the BCSFB, the BBB is considered as a far more important barrier (Pardridge, 2002). The barrier function at the BBB is provided by the microcapillary endothelial cells that contain no fenestrations. Transporters that are expressed in human enterocytes are depicted in Fig. 3.

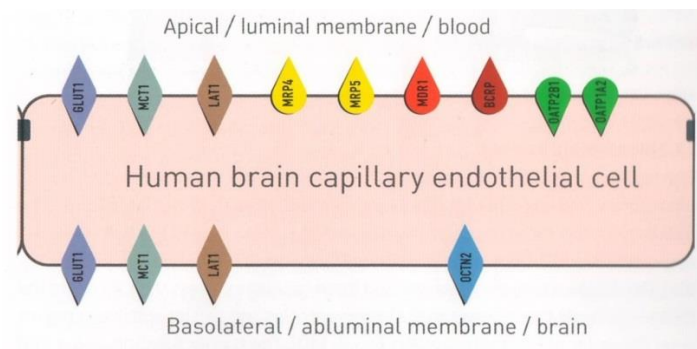


Figure 3. Transporters in human blood-brain barrier (from Gaborik et al., 2017).

1.2.3. Hepatic barrier

After the nutrients or drugs are absorbed by the gastrointestinal tract, they are taken up by the part of the bloodstream called the hepatic portal system. This system is designed to take digested foodstuff into the liver where it can be processed. The main cellular components of the hepatic barrier are hepatocytes. Hepatocytes make up 70-85% of the liver's mass and are the site of systemic absorption and excretion of most orally taken drugs and their metabolites. Transporters that are expressed in the parenchymal cells (hepatocytes) are depicted in Fig. 4.

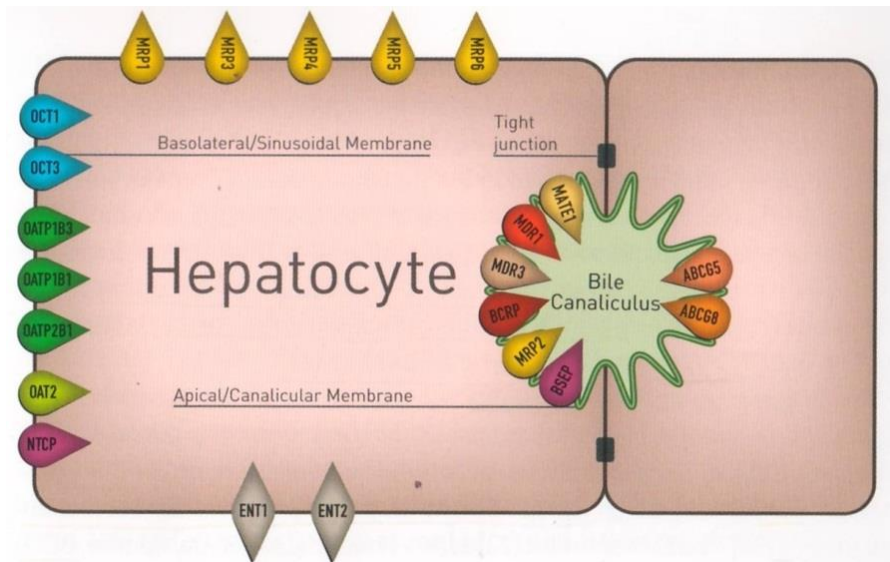


Figure 4. Transporters in human hepatic barrier (from Gaborik et al., 2017).

1.2.4. Renal barrier

The main cellular components of renal secretory transport are the proximal tubule cells. Uptake transporters (members of SLC22 family) with high expression levels in the plasma membrane of renal tubular epithelial cells are responsible for the substrate uptake from the blood or the glomerular filtrate, after which the substrates are excreted back into urine or blood by ABC transporters (Giacomini et al., 2010; Masereeuw and Russel, 2010; Morrissey et al., 2013). All transporters expressed in the renal barrier are depicted in Fig. 5.

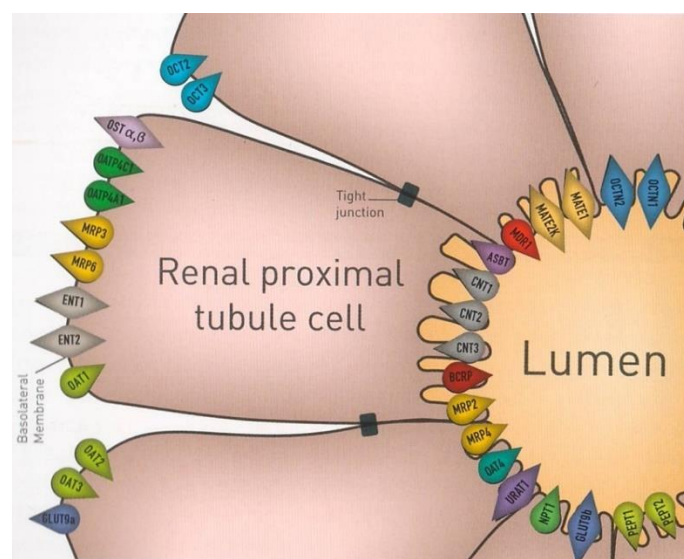


Figure 5. Transporters in human renal barrier (from Gaborik et al., 2017).

1.3. Uptake transporters of organic anions

Numerous endo- and xenobiotics, including many drugs, are organic anions. Their disposition and elimination from the body depend on the function of polyspecific drug transporters that belong to two subfamilies: SLC21 and SLC22 subfamily of the SLC family. They are responsible for the uptake of various endogenous and xenobiotic compounds into the cell. Despite their crucial role in toxicological response in mammals, research on their ecotoxicological relevance and characteristics in non-mammalian species is still scarce.

1.3.1. The SLC21 subfamily: Organic anion transporting polypeptides

Members of the OATP family (gene symbol *SLC21* or *SLCO*) transport large amphipatic molecules across plasma membrane of eukaryotes and mediate transport of wide range of endogenous (steroid hormones, bile salts, prostaglandins) and exogenous compounds (pharmaceuticals, natural toxins). So far, more than 160 OATP/Oatp proteins have been identified at a genome level in at least 25 animal species, which have been classified into 6 subfamilies (OATP1-6) (Hagenbuch et al., 2004). Typical Oatp transporter is composed of 643-722 amino acids, with molecular mass of 80-90 kDa. High resolution crystallography has revealed the structure of 12 transmembrane domanes (TMDs), with large extracellular loop 9 (LP9) between TMD 9 and 10 (Hagenbuch et al., 2008). Mechanism of transport is not completely solved, but it is assumed to be an anionic antiport. Majority of human OATPs, including OATP1A2, OATP1B1 and OATP1B3 work as $[\text{HCO}_3^-]$ antiporters (Satlin et al., 1997).

OATP family comprises of 6 subfamilies in mammals, OATP/Oatp1-6 with 11 transporters in human, 15 in mouse and 16 in rat. OATP/Oatp1 subfamily is the most studied due to its connection with human diseases and cancer, therefore the knockout animal models have been mostly created for members of this subfamily (Hagenbuch et al., 2008). OATP1 subfamily includes 4 human proteins: OATP1A2, OATP1B1, OATP1B3 and OATP1C1 (Hill et al., 2005); 6 in mouse (Oatp1a1, Oatp1a4-6, Oatp1b2, Oatp1c1) and 6 in rat (Oatp1a1, Oatp1a3-5, Oatp1b2 and Oatp1c1) (Hagenbuch et al., 2012). Ubiquitously expressed OATP1A2 transports physiologically important compounds such as conjugated steroid hormones (estrone-3-sulphate (E3S), dehydroepiandrostedione sulfate (DHEAS) and estradiol-17 β -glucuronide), thyroid hormones (T4, T3), bilirubin, bile salts (cholate (CH),

taurocholate (TC), taurochenodeoxycholate (TCDC)), and prostaglandin E2 (PGE2). Rodent Oatp1a substrates overlap with human OATP1A2 (Hagenbuch et al., 2008). Apart from physiological compounds, OATP1A2 also transmits various drugs (Satlin et al., 1997). Unlike OATP1A2, which is present in various tissues, OATP1B1 and OATP1B3, as well as Oatp1b2 rodents, are specific to the liver (Kobayashi et al., 2003). Human and rodent OATP1B/1b substrates are highly overlapping and include steroid hormone conjugates (E3S, DHEAS, estradiol-17 β -glucuronide), bile salts (CH, TC, TCDC) and bilirubin and its conjugates (Hagenbuch et al., 2004). hOATP1B1, hOATP1B3 and rodent Oatp1b2 have been most intensively investigated due to their large role in disposing of drugs and their elimination through bile. OATP1C1, unlike other OATPs, has a narrow substrate range that mainly involves thyroid hormones (T4, T3, reverse T3 and their conjugates) (Satlin et al., 1997).

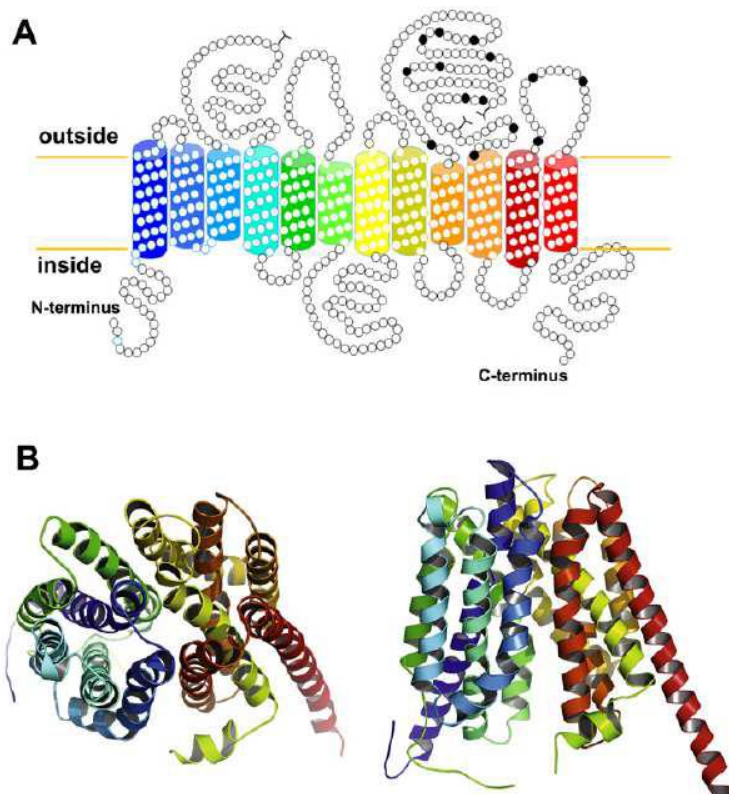


Figure 6. (A) Topology prediction for hOATP1B1 shows 12 TMDs, and a large extracellular loop 9 (LP9) between TMD 9 and 10 that carries conserved cysteine residues (black dots); (B) Homology model of hOATP1B1 which shows the protein from the extracellular side (left) and within the lipid bilayer (right) (Roth et al., 2012). Colors of the TMDs in the topology model (A) match colors in the homology model (B) (Hagenbuch and Stieger, 2013).

1.3.1.1. Zebrafish Oatp1d1

Oatp1d subfamily is only present in teleost fish and our group has made the first detailed characterization of Oatp1d1 protein in zebrafish (Popovic et al., 2013; Popovic et al., 2014). Zebrafish Oatp1d1 is similar to mammalian OATP1A/Oatp1a and OATP1B/Oatp1b and has a major physiological role in transport and preservation of the balance of steroid hormones (Leuthold et al., 2009; Popovic et al., 2013). Oatp1d1 is ubiquitously expressed in zebrafish, with the highest expression in liver and brain, it is present in dimeric and possibly oligomeric form in the cell membrane, and the suggested mechanism of Oatp1d1 mediated transport is bicarbonate exchange.

Oatp1d1, like other Oatps, is a polyspecific transporter that mediates the uptake of wide range of compounds. It transports endogenous compounds like conjugated steroid hormones and cortisol, as well as various xenobiotics like diclofenac, perfluorooctanesulfonic acid (PFOS), nonylphenol, gemfibrozil, 17 α -ethinylestradiol, carbaryl, diazinon, caffeine and metolachlor. Strong inhibitors of Oatp1d1 transport activity are perfluorooctanoic acid (PFOA), chlorpyrifos-methyl, estrone (E1) and 17 β -estradiol (E2).

1.3.2. The SLC22 subfamily

The solute carrier family 22 (SLC22) is a large family of organic ion transporters that belongs to the major facilitator superfamily (MFS) which is assigned as 2.A.1 in the Milton Saier “transporter classification system” (see <http://www.tcdb.org/>). The MFS is one of the two largest families of membrane transporters comprising uniporters, symporters, and antiporters from bacteria, lower eukaryotes, plants, to mammals in 18 families (Koepsell et al., 2003; Wright and Dantzer, 2004). The first identified member of the SLC22 family, the rat organic transporter Slc22a1 (rOct1), was cloned in 1994 by Gründemann et al. (1994).

Today it is known that members of the SLC22 family transport a variety of compounds including drugs, environmental toxins, and endogenous metabolites across the cell membrane (Koepsell et al., 2003; Wright and Dantzer, 2004). Most transporters of the SLC22 family are polyspecific, i.e., they transport multiple structurally different substrates, and numerous additional compounds can act as high and/or low affinity inhibitors (Koepsell

et al., 2007; Minuesa et al., 2009; Nies et al., 2010). Many *SLC22* genes are expressed in liver, kidneys, and intestine where they play important roles in absorption and excretion of drugs while they are also found in other organs such as brain and heart (Koepsell and Endou, 2004). The SLC22 proteins have been predicted to have 12 α -helical TMDs, a large extended extracellular loop between TMDs 1/2 and a large intracellular loop between TMDs 6/7 (Fig. 7). Extracellular LP1, located between TMD1 and TMD2, is important for N-linked glycosylation of the protein and in some cases for its homo-oligomerization (carries conserved cysteine residues for the formation of disulfide cross bridges), while intracellular LP6 is involved in posttranscriptional regulation (protein kinase-mediated phosphorylation) (Brast et al., 2012; Keller et al., 2011; Nigam et al., 2015). The family can be divided into three subgroups according to substrate specificity and function: the organic cation transporters (OCTs), the organic cation/carnitine transporters (OCTNs), and the organic anion transporters (OATs) (Grundemann et al., 1994). Moreover, there are several members of the SLC22 family with unidentified substrate specificity or function.

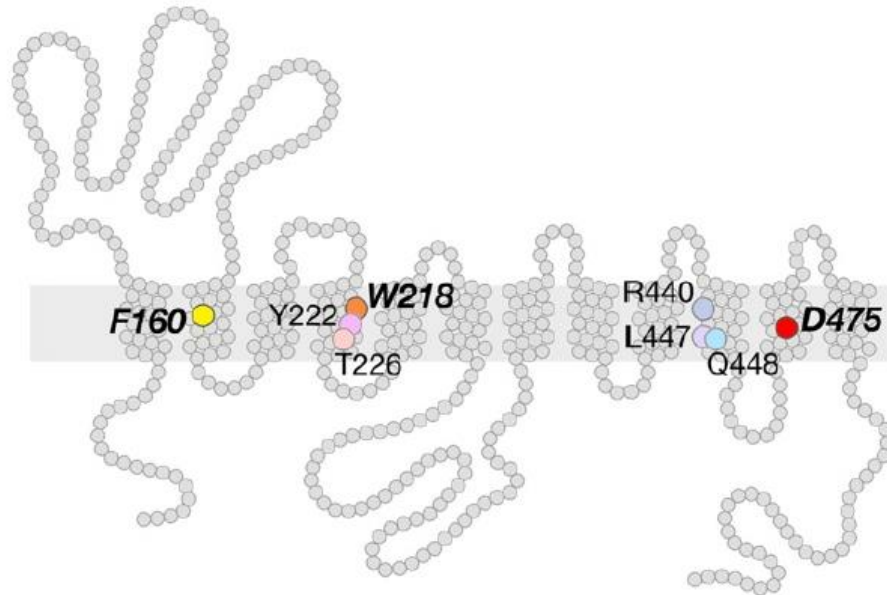


Figure 7. Predicted membrane topology of rat OCT1 with designated amino acids which influence substrate affinity. Modeling was performed using the tertiary structure of LacY (from Koepsell, 2013).

1.3.2.1. Organic anion transporters (OATs)

Organic anion transporters (OATs in humans, Oats in other animal species) are a family of transmembrane proteins able to transport a variety of compounds including drugs, environmental toxins and endogenous metabolites into the cell, playing an essential role in their elimination from the body. They received a lot of attention recently because of their role in transporting of common drugs (antibiotics, antivirals, diuretics, nonsteroidal anti-inflammatory drugs), toxins (mercury, aristolochic acid), and nutrients (vitamins, flavonoids). They share many structural characteristics with other MFS proteins (Nigam et al., 2015). Although their crystal structure is not solved yet, several homology models based on the related bacterial MFS protein glycerol-3-phosphate transporter (GlpT) or lactose permease (LacY) were reported, indicating the structure of 12 α -helices (Perry et al., 2006). Accordingly, OATs/Oats are composed of 540–560 amino acids, comprising 12 TMDs that form the pore and are characterized by two large interconnecting loops (one extracellular and one intracellular), similar to other bacterial and mammalian transporters (Lopez-Nieto et al., 1997).

Considering their tissue specific expression, although OATs/Oats were initially found in kidney, they are expressed in almost all barrier epithelia of the body (kidney, liver, choroid plexus, intestine, olfactory mucosa, brain, retina, placenta, even in muscle, bone and heart) (Burckhardt, 2012; Mihaljevic et al., 2016). In terms of the transport mechanism, prototypical OATs/Oats such as Oat1 are secondary active transporters. OATs/Oats mediated influx typically involves the exchange, or countertransport with another solute, in most cases intracellular organic anions (e.g., dicarboxylate or α -ketoglutarate (α -KG) for OAT1, OAT3, OAT4, Oat6, Oat8; or succinate for OAT2) against negative membrane potential inside the cell, and this transport requires the input of energy. The required intracellular to extracellular dicarboxylate gradient is maintained by the Na^+ /dicarboxylate co-transport (approximately 60%) and by the intracellular production via metabolism (approximately 40%) (Dantzler, 2002).

OATs/Oats are thought to be part of a so-called “tertiary” transport system involving the organic anion transporter, the Na^+ - K^+ -ATPase, and the sodium-dicarboxylate cotransporter (Nigam et al., 2015). They primarily transport organic anions, but are also capable of transporting a variety of organic cationic drugs (e.g., cimetidine), as well as metabolites like

creatinine, and possibly polyamines and carnitine (Ahn et al., 2009, 2011; Kusuhara et al., 1999; Vallon et al., 2012). Their substrates are characterized by a small size (< 500 Da), a hydrophobic region (optimally 8–10 Å in length), and a negative charge (Ullrich and Rumrich, 1988; Fritzsche et al., 1989), and are classified as "type I" organic anions (Wright et al., 2004, Sekine et al., 2004). Complete transport through epithelial cells involves transporters at the basolateral and apical surfaces, and is often a combination of the SLC ("uptake/influx") transporters and ABC ("efflux") transporters. For example, in kidneys it appears that basolateral Oat1 and Oat3 uptake of organic anions is coupled to apically located efflux transporters including ABCC2 and ABCC4 (Nigam et al., 2015).

1.3.2.1.1. Cellular and tissue distribution of OATs

The first organic anion transporter, named OAT1, was cloned in 1997 from a rat kidney cDNA library (Sekine et al., 1997; Sweet et al., 1997). Human OAT1 (hOAT1), rat Oat1 (rOat1) and mouse Oat1 (mOat1) transcripts are expressed abundantly in kidney and at lower levels in brain (Lopez-Nieto et al., 1997; Sekine et al., 1997; Sweet et al., 1997; Lu et al., 1999; Race et al., 1999). *In situ* hybridization demonstrated that rat *oat1* mRNA is expressed in renal proximal tubules (Lopez-Nieto et al., 1997; Sekine et al., 1997). Immunohistochemistry has shown that hOAT1, rOat1 and mOat1 are expressed at the basolateral membrane of renal proximal tubule cells (Sekine et al., 1997; Sweet et al., 1997; Geng et al., 1999; Hosoyamada et al., 1999). Recently, Hilgendorf et al. (2007) demonstrated by quantitative polymerase chain reaction (qPCR) that hOAT1 has the highest expression of 36 drug transporters found in human kidney. *Oat1* mRNA expression was also seen in mouse and rat choroid plexus by reverse transcriptase-polymerase chain reaction (RT-PCR) analysis (Sweet et al., 2002). Subsequently, *hOat1* mRNA was also detected in human choroid plexus by Alebouyeh et al. (2003), cerebral cortex and hippocampus (Bahn et al., 2005) and in the olfactory mucosa (Monte et al., 2004). Using radiation hybrid mapping, *hOat1* was localized to human chromosome 11q13.1-2, *roat1* to rat chromosome 1q43, and *moat1* to mouse chromosome 19 (Lopez-Nieto et al., 1997; Hosoyamada et al., 1999).

Rat and human *Oat2/oat2* mRNA are expressed predominantly in the liver, with lower levels in kidney and other tissues (Sekine et al., 1998; Sun et al., 2001). In contrast, *moat2* mRNA is

strongly expressed in kidney and weakly in liver, indicating that the expression pattern for OAT2 is both species and tissue specific. Human OAT2 was immunolocalized in basolateral membrane of proximal tubules (Enomoto et al., 2002a, 2002b), whereas in rats and mice Oat2 was found at the apical membrane in late S3 segments of proximal tubules (Ljubojevic et al., 2007), as well as in cortical thick ascending limbs of Henle's loop and collecting ducts (Kojima et al., 2002). OAT2/Oat2 in liver is presumed to be localized in the sinusoidal membrane of hepatocytes (basolateral membrane) (Burckhardt, 2012). Mouse Oat2 was mapped to mouse chromosome 17C using fluorescent *in situ* hybridization analysis (FISH) (Kobayashi et al. 2002).

hOat3 mRNA is predominantly expressed in kidney, with low expression in brain and skeletal muscle (Cha et al., 2001). *roat3* mRNA is mainly expressed in kidney, liver and brain (Kobayashi et al., 2002); whereas *moat3* mRNA is abundantly expressed in the kidney, brain, and eye tissues (Kobayashi et al., 2004). Recently, *hOat3* was also shown by qPCR to be expressed in adrenal tissue and a human adrenal cell line (NCI-H295R) (Asif et al., 2005). In the kidney, immunohistochemistry demonstrated that both *hOat3* and *roat3* are predominantly expressed at the basolateral membrane of the renal proximal tubule (Cha et al., 2001; Hasegawa et al., 2002). Moreover, quantitative PCR analysis has shown that hOAT3 is highly expressed in kidney — second only to hOAT1 among the 36 drug transporters assessed (Hilgendorf et al., 2007). In choroid plexus (CP), mOat3 is expressed at the apical membrane (Sweet et al., 2002), consistent with its physiological role in transport out of the cerebrospinal fluid (CSF) into the epithelium for efflux into the blood. *moat3* was mapped to chromosome 19, using single-strand conformation polymorphisms analysis (Brady et al., 1999). Radiation hybrid analysis demonstrated that the *hOat3* gene is on chromosome 11q11.7 (Cha et al., 2001).

1.3.2.1.2. Mechanism of transport

First *in vitro* studies using renal slices (Cross and Taggart, 1950) demonstrated that the transport process is dependent upon metabolic energy and on the presence of sodium in the extracellular space. They also showed that a number of metabolic intermediates stimulate this transport. Nevertheless, the detailed mechanism of organic anion transport remained

uncertain until the mid 1980s, when Burckhardt et al. (1987) and Pritchard (1988) demonstrated, using isolated basolateral membrane vesicles from rat renal cortex, that OATs transport was driven by uptake across the basolateral membrane in exchange for intracellular dicarboxylate (physiologically α -KG; Pritchard, 1990). The required intracellular/extracellular α -KG gradient is maintained by mediated uptake of α -KG into the cells across the basolateral membrane by Na^+ /dicarboxylate co-transport (approximately 60%) and by intracellular production via metabolism (approximately 40%) (Dantzler 2002). Finally, the inwardly directed Na^+ gradient driving this process is the product of ATP hydrolysis via the Na, K-ATPase at the basolateral membrane (Shimada et al., 1987; Pritchard, 1988, 1990; Pritchard and Miller, 1993; Schmitt and Burckhardt, 1993; Dantzler, 2002; Wright and Dantzler, 2004). Thus, as depicted in Fig. 8, the overall effect of these transporters acting in concert is the net entry of sodium and organic anion into the cell, energized by the hydrolysis of ATP. In contrast, the dicarboxylate counter-ion, α -KG, is recycled and undergoes no net change in concentration. The overall process may be termed tertiary active transport, since the transport of the organic anion substrate is separated from ATP hydrolysis by two intervening steps. Despite the complexity of this mechanism, it is very effective, resulting in complete clearance of good substrates like p-aminohippurate (PAH) from the renal plasma in a single pass through the kidney (Pritchard and Miller, 1993). Subsequent work, discussed below, has led to cloning of the basolateral OATs and demonstrated that the properties of the cloned basolateral OATs match precisely with the features of the overall process as defined by the membrane vesicle studies.

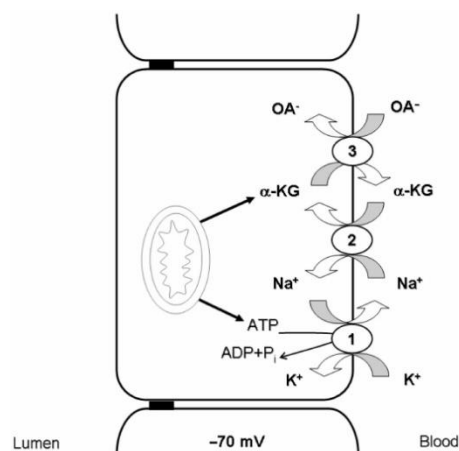


Figure 8. Classical model of basolateral OAT transport system. (From Srimaroeng et al., 2008).

1.3.2.1.3. Substrate specificity

OAT1/Oat1 is well known for its very broad substrate specificity as it interacts with several endogenous and multitude of exogenous compounds, drugs and toxins of various chemical structures. The prototypical test anion for OAT1/Oat1 is radiolabeled p-aminohippurate with determined mean K_m value of 28.5 μM for human OAT1 (Burckhardt et al., 2011). The interaction with dicarboxylates depended on the length of the carbon chain separating the two negatively charged carboxyl groups with a maximum inhibition by dicarboxylates with five or six carbons (Uwai et al., 1998). Known OAT1 substrates include nonsteroidal anti-inflammatory drugs (NSAIDs), antibiotics, diuretics, folate, α -KG, cyclic nucleotides, prostaglandins, gut microbial metabolites, uremic toxins, vitamins, dietary compounds, uric acid, mercury conjugates, and other toxins (reviewed in Nigam et al., 2015).

OAT2/Oat2 has received relatively little attention when compared to other OATs/Oats and solute carriers (Shen et al., 2016). Although its substrate specificity has not been extensively examined, initial studies indicate that, like other OATs, OAT2 transports a variety of organic anions (Sekine et al., 1998; Sun et al., 2001; Kimura et al., 2002; Kobayashi et al., 2002, 2005b; Burckhardt and Burckhardt, 2003). In human and male rats, OAT2/Oat2 is mainly expressed in liver, where it mediates hepatic excretion of endogenous substrates such as glutamate, glutarate, urate, L-ascorbate, cyclic nucleotides, PGE2 and PGF2, E3S, DHEAS and α -KG, along with transport of xenobiotics such as salicylate, erythromycin, tetracycline, ranitidine, 5-fluorouracil, methotrexate (MTX), taxol, aflatoxin B1 and other drugs and toxins (Nigam et al., 2015). Oat2 was also shown to interact with various drugs including diuretics, antibiotics, antiviral, antineoplastic and nonsteroidal anti-inflammatory drugs (Burckhardt, 2012).

The substrates for OAT3/Oat3 are as diverse as those of OAT1/Oat1 and substrate specificity of Oat3 overlaps with Oat1. Nevertheless, there are some substrates that clearly preferentially interact with either OAT1/Oat1 or OAT3/Oat3 (reviewed in Nigam et al., 2015). Oat3 mediates the uptake of endogenous metabolites such as conjugates of signaling sex steroids, as well as vitamins and other plant-derived metabolites (e.g., flavonoids) (Wu et al., 2013). It also transports PAH, E3S, DHEAS, estradiol glucuronide, MTX, ochratoxin A (OTA), PGE2, TC, glutarate, cAMP, urate, and a cationic compound, cimetidine (Kusuhara et al., 1999; Cha et al., 2001; Sugiyama et al., 2001; Kimura et al., 2002; Sweet et al., 2002). In

addition, Oat3 also transports aristolochic acid and OTA and is thus thought to be important in the pathogenesis of Balkan Nephropathy (Xue et al, 2011). While the ability of Oat1 to transport cations is quite restricted, Oat3 can bind and transport a number of cations, some with 10-fold greater affinity than that seen with Oat1, even though it is, like Oat1, predominantly an organic anion transporter (Ahn et al., 2013, Vallon et al., 2012). Presumably, the ability of Oat3 to bind organic cations better than Oat1 is reflected in the nature of the ligand binding site, but this awaits three-dimensional structural determination.

1.3.2.1.4. Structure and function

To date, more than 110 amino acids have been mutated in OATs from different species (reviewed in Srimaroeng et al., 2008). Unfortunately, many of the mutant transporters examined (>70%) have reduced surface expression, either from protein instability or trafficking problems. Fig. 9. summarizes mutants that have been shown to cause functional increases or decreases in substrate transport regardless of membrane expression levels.

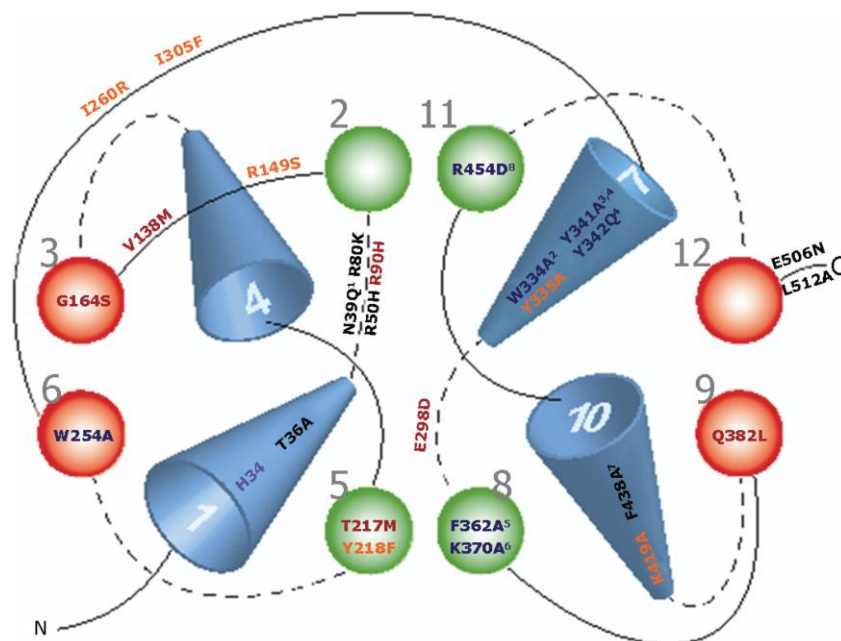


Figure 9. Amino acids critical for transport of SLC22 substrates shown in 3D arrangement of TMDs. Dotted lines depict extracellular loops and solid lines represent cytoplasmic loops. fOat1 mutants are shown in purple, rOat3 mutants in blue, hOAT3 mutants in orange, hOAT1 mutants in black, and URAT1 mutants in red. 1, N39Q of mOat1; 2, residue also mutated to F, which caused functional decreases; 3, residue also mutated to Y, which caused functional

decreases; 4, corresponds to Y353A/W/F and Y354A/W/F mutants in hOAT1, respectively; 5, residue also mutated to S, which caused functional decreases; 6, corresponds to K394A mutated in fOat1; 7, corresponds to F426 in hOAT3; 8, corresponds to R478D mutated in fOat1 and R466K mutated in hOAT1 (from Srimaroeng et al., 2008).

Two groups of amino acids, basic and aromatic, appeared to be dominant for transport function of OATs. Conserved basic amino acids in OAT1/Oat1, OAT2/Oat2 and OAT3/Oat3 isoforms from several species are: histidine in TMD 1, lysine in TMD 8, and arginine in TMD 11. Conservation of mentioned amino acids guided researchers to create site specific mutations at those residues. In result, mutations at H34 reduce PAH uptake by more than 50% in both fOat1 (Wolff et al., 2001) and hOAT1 (Hong et al., 2004). Additional experiments in fOat1 and rOat3 (K394A and K370A, respectively) described the contributions of the lysine in TMD 8 to Oat function (Feng et al., 2001; Wolff et al., 2001). PAH transport was significantly decreased in both isoforms. The importance of K394 in dicarboxylate interaction and conformational changes in fOat1 was also demonstrated (Feng et al., 2001; Wolff et al., 2001). Further experiments on rOat3 (Feng et al., 2001), fOat1 (Wolff et al., 2001) and hOAT1 (Rizwan et al., 2007) demonstrated a requirement for the arginine in TMD 11 for transport of Oat substrates and dicarboxylates. Decreases in PAH and glutarate uptake were also demonstrated in hOAT1 R466K mutant. Similar to the lysine in TMD 8 and arginine in TMD 11, the lysine in TMD 10 (K419) alters PAH transport. Glutarate is not transported by this mutant, and PAH and glutarate uptake are not restored to control levels by the K419R mutation (Astorga et al., 2007; Perry et al., 2007).

Among aromatic amino acids, tryptophan, tyrosine, and phenylalanine residues in TMD 7 and 8 have been examined to determine their contributions to substrate transport. In rOat3 mutants, importance of the hydroxyl group of Y342, the indole ring of W334 and the aromatic rings of Y335, Y341 and F362 were demonstrated for PAH and cimetidine transport (Feng et al., 2002). Additional studies of residues Y353, Y354 and W346 in hOAT1 (which correspond to Y341, Y342 and W334 of rOat3) indicated that transport by the Y353A mutant is restored upon mutation to Y353F. However, the Y354F mutant is not similar to wild-type (WT) hOAT1 in its transport. This finding implicates potential hydrogen bonding in substrate interaction at Y354 for hOAT1 and rOat3 (Hong et al., 2007b). Two additional hOAT1 and

hOAT3 aromatic residue mutants were reported (Y230A/Y218A, F438A/F426A) in TMD 5 and 10, respectively (Perry et al., 2006, 2007; Astorga et al., 2007). In these studies, kinetic analysis showed a reduced K_m for cidofovir transport in the hOAT1 F438 mutant.

Additional charged amino acids in loops were suggested to contribute to OAT/Oat function, including: arginines in the extracellular loop between TMD 1 and 2 (R50H, R80K, R90H), R149S in intracellular loop between TMD 2 and 3, and one charged E506 in the C-terminus (Yang et al., 2002; Bleasby et al., 2005; Erdman et al., 2006; Xu et al., 2006).

Computational models indicate that many of the aromatic and basic amino acids that alter OAT/Oat1 function, as described in the previous section, appear to surround the putative binding site (for hOAT1: R466, K382, Y353, Y354, and F374, as depicted in Fig. 10) (Perry et al., 2006).

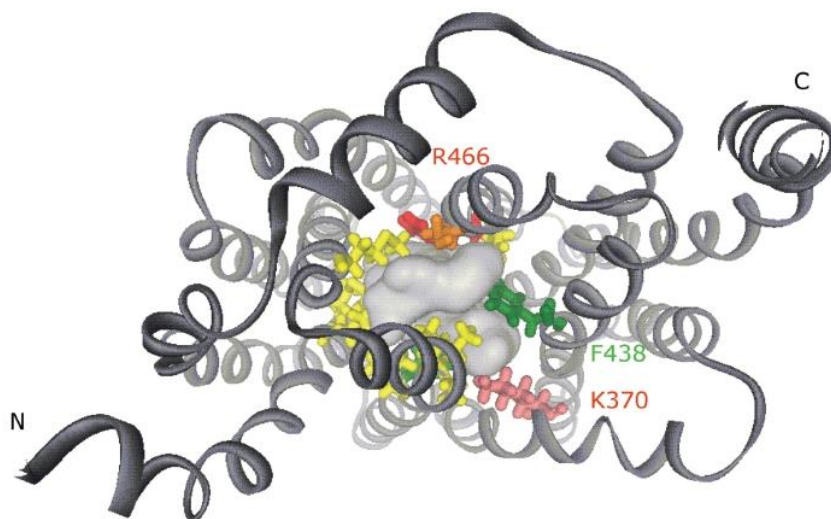


Figure 10. Three-dimensional structure of hOAT1, looking into the cytoplasmic open face. The putative binding site is surrounded by aliphatic amino acids (marked in yellow), polar amino acids (orange), positively charged amino acids (red; R466 and K370), and aromatic amino acids (green; Y230 and F438) (from Srimaroeng et al., 2008).

1.3.2.1.5. Regulation

1.3.2.1.5.1. Transcriptional regulation

Differences in transporter function that have been observed between individuals may be caused through up- or down-regulation of OAT expression based on prior exposure to drugs

and xenobiotics, or on differences in hormonal status. A few hepatocyte nuclear factors (HNFs) have been shown to initiate transcriptional regulation of OATs. HNF-4 α activates hOAT1, hOAT3 and hOAT2 promoter activity (Ogasawara et al., 2007; Nigam et al., 2018; Popowski et al., 2005). HNF-1 α and/or β , can also activate both hOAT1 and mOat1 promoters (Saji et al., 2008). The hOAT3 promoter is activated by the HNF-1 α homodimer, the HNF-1 β homodimer, and the HNF-1 α / β heterodimer, although the HNF-1 β homodimer is less effective (Kikuchi et al., 2006). Kikuchi et al. (2006) also noted that multiple CpG dinucleotides are present in the putative hOAT3 promoter region. Since these sites are a likely target for DNA methylation, they explored the possibility of epigenetic control of hOAT3 expression and function, and showed that hOAT3 promoter activity is abolished after methylation *in vitro*. Finally, Ogasawara et al. (2006) showed that a cAMP response element (CRE) affects basal and inducible transcriptional activity of the hOAT3 promoter, and that the hOAT3 promoter is activated by phosphorylation of CRE-binding protein (CRE-B1) and activating transcription factor (ATF1).

Gender differences have also been seen for several OATs and they very likely reflect nuclear transcription factor signaling. For example, in adult rats Oat1 expression is lower in female rats than in male (Buist et al., 2002), with a correspondingly smaller PAH clearance in females as well (Reyes et al., 1998; Cerrutti et al., 2001, 2002a, b). Moreover, androgen seems to up-regulate rOat1 and rOat3 expression, whereas estrogen reduced expression. In mice, the expression of mOat1 was stronger in males, downregulated by castration, and upregulated by testosterone treatment, while mOat3 expression showed an opposite pattern, with lower expression in males, upregulated by castration and downregulated by testosterone (Breljak et al., 2013). However, there are no gender differences in rbOat1 and rbOat3 expression and function (Groves et al., 2006). In contrast to OAT1 and OAT3, rOat2 showed androgen inhibition and estrogen stimulation (Buist et al., 2002; Ljubojevic et al., 2004). mOat2 showed an expression pattern similar to rOat2 (Ljubojevic et al., 2007). Data on gender differences in the renal transport were reviewed by Sabolic et al. (2007).

1.3.2.1.5.2. Post-translational mechanisms

As mentioned above, several potential N-glycosylation sites have been predicted in extracellular loop and a number of potential phosphorylation sites are present in intracellular loops. N-glycosylation appears to play a critical role in membrane

targeting/trafficking, protein folding and possibly regulation of OAT function, as has been demonstrated for mOat1 (Kuze et al., 1999), hOAT1 (Tanaka et al., 2004a), and hOAT4 (Zhou et al., 2005), although the molecular basis for the changes in folding and trafficking are not yet fully understood.

A variety of data suggest that phosphorylation of the large intracellular loop and interactions of the OATs with protein partners can alter OAT function. For example, it has been known since 1990s that the conventional PKC (cPKC) is an important regulator of OAT1 and OAT3 function, as its activation inhibits OAT1-mediated PAH transport in various expression systems (Uwai et al., 1998; Lu et al., 1999; Wolff et al., 2003; You et al., 2000), as well as OAT3-mediated uptake of ES (Takeda et al., 2000). In addition, it has been demonstrated that cPKC activation leads to inhibition of basolateral uptake of fluorescein, which is a substrate for both OAT1 and OAT3 (Gekle et al., 1999; Shuprisha et al., 2000). Interestingly, activation of cPKC does not lead to reduced OAT1 and OAT3 transport through phosphorylation of transporter itself, but it appears to be mediated by retrieval of the transporter from the membrane (You et al., 2000; Wolff et al., 2003).

Epidermal growth factor (EGF), unlike cPKC, stimulates basolateral PAH uptake *via* Oat1 in rabbit tubules. This effect is mediated through a complex signaling pathway through activation of mitogen-activated/extracellular-signal regulated kinase (MEK), extracellular signal-regulated kinase isoforms 1 and 2 (ERK1/2), and phospholipase A2 (PLA2), resulting in increased arachidonic acid (AA) release. Subsequently, AA is metabolized to PGE2 *via* cyclooxygenase I (COX I). In turn, PGE2 activates adenylate cyclase, leading to cAMP production and activation of PKA and ultimately increased basolateral rbOat1-mediated PAH uptake (Sauvant et al., 2002, 2003, 2006; Dantzler and Wright, 2003). EGF also stimulates OAT3-mediated transport of ES and the signaling process is identical to that described for OAT1 up-regulation (Soodvilai et al., 2004). Srimaroeng et al. (2008) have shown that both insulin and EGF are able to stimulate ES transport in rat renal cortical slices through the activation of PKC ζ , which is downstream of PKA in the same signaling pathway identified by Soodvilai et al. (2004) through PKA activation.

There are some other types of regulation that are known to alter function of transporters but have not yet been evaluated for the OATs, but these possibilities need to be explored experimentally (Srimaroeng et al., 2008).

1.4. Studies on non-mammalian uptake transporters

Despite their physiological importance and role in cellular detoxification, knowledge about uptake transporters in non-mammalian species is scarce, and the same is true for zebrafish (*Danio rerio*) as an increasingly important vertebrate model species.

To date, the only well characterized non-mammalian Oat is winter flounder Oat (fOat) (Wolff et al., 1997; Aslamkhan et al., 2006), later called flounder Oat1. Flounder Oat1 has substantial sequence homology to mammalian orthologs OAT1/Oat1 and OAT3/Oat3, as well as functional properties of both mammalian forms.

There is a growing interest in zebrafish due to numerous advantages of this model organism (explained in detail in the next section), and finally a fully sequenced genome. In addition, the teleost specific whole genome duplication (WGD) provided the evolutionary driving force in generating enormous number of newly functional genes, whose research can provide new understanding of human gene changes linked to numerous diseases. Nevertheless, the WGD is the reason why zebrafish often has two paralogs that correspond to the single gene in other vertebrate species, including humans (Ravi and Venkatesh, 2008). Despite the additional round of the genome duplication in fish, however, large portions of vertebrate genes and cellular pathways are evolutionary conserved in vertebrates, and findings on zebrafish can generally be translated to other vertebrate species (Busby et al., 2010).

1.5. Zebrafish as a vertebrate model organism

Zebrafish is an important and widely used model species in biomedical and environmental research, as well as in other areas including genetic regulation of aging, regeneration, animal behavior, vertebrate development and disease. The use of zebrafish as a model organism began in the 1960s as it has been recognized to have many characteristics that make it a valuable model for studying human genetics and disease. Zebrafish is a popular model because of the ease of laboratory maintenance, small size and low cost, the ability to obtain hundreds of embryos on daily basis, and the accessibility, translucency, and rapid early development (Holtzman et al., 2016).

Zebrafish is a tropical species native to south-east Asia, about 2.5 to 4 cm long. It has transparent larval stages, and as it matures to an adult it develops blue stripes that run along the length of the body. Males are slender and torpedo-shaped usually with a pink or yellow tinge. Females tend to be less pink than the males and are fatter due to the eggs they carry (Fig. 11). The complete genome sequence of the zebrafish was published in 2013 and is 1,505,581,940 base pairs in length and contains 26,247 protein-coding genes (Ensembl, www.ensembl.org) (Holtzman et al., 2016).

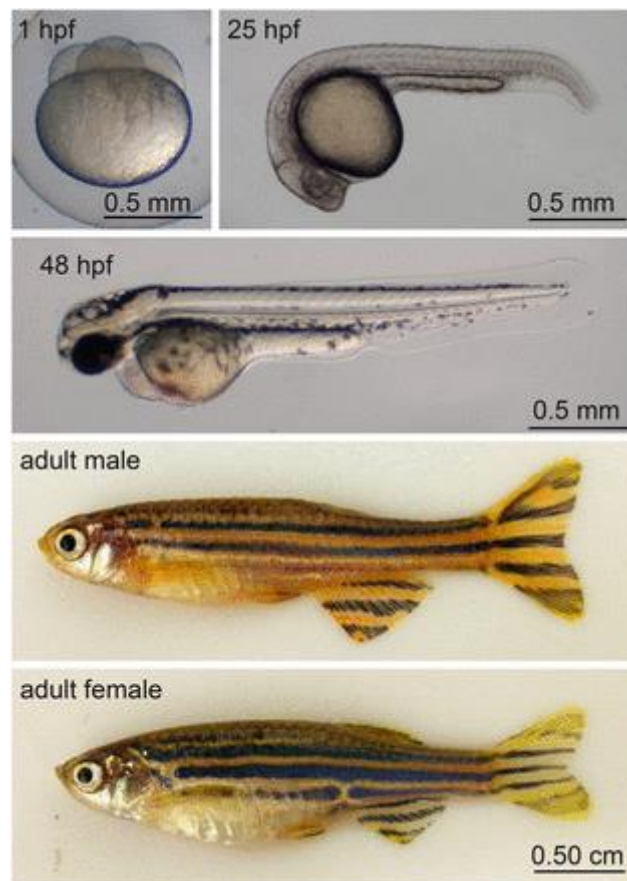


Figure 11. Life stages of zebrafish (*Danio rerio*). A zebrafish embryo at the four-cell stage (1 hr postfertilization (hpf)) has four cells at the animal pole that sit atop a single yolk cell and are formed through discoidal cleavage. By 25 hpf, the body axis of the embryo has formed. Embryos at 48 hpf have rudiments of most major organs (e.g., note the heart tube just ventral to the eyes). Zebrafish reach adulthood at 3-4 months postfertilization. Adult males have a streamlined shape and a yellow hue, while adult females are larger and have a whiter hue. Lateral views with animal pole to the top (four-cell-stage embryo) or anterior to the left and dorsal to the top (all other images) (Adapted from Holtzman et al., 2016).

Danio rerio (initially designated *Brachydanio rerio*) were first described by English physician Sir Francis Hamilton in a book about fishes of the Ganges River (Hamilton, 1822). In the wild, zebrafish are a tropical freshwater fish living in small rivers, streams, paddy fields, and channels in South Asia, including India, Myanmar, Bangladesh, and Nepal (Engeszer et al., 2007; Spence et al., 2008; Arunachalam et al. 2013). The natural environments for breeding are ponds that form during monsoons, are still and shallow with pebble, sand, or silt substrata that likely protects the clear eggs from predation. The breeding is likely to correspond to the more abundant availability of food during the monsoon season (Spence et al., 2006). Their diet in the wild consists mainly of insects, insect larvae, nematodes, and small crustaceans.

In the laboratory, zebrafish are kept in clear, alkaline (pH ~ 8.0) water with temperatures around 28.5°C (they tolerate 20 to 33°C). They are fed artificial food that is typically supplemented with live food such as brine shrimp or mealworms for a more balanced diet (McClure et al., 2006; Spence et al., 2008). Because adult zebrafish are in average <3.5 cm in length, many thousands can be kept in a confined laboratory space. Breeding in laboratories includes the use of specially designed breeding tanks and is stimulated by light (break of daylight triggers mating in wild zebrafish). They produce hundreds of offspring at weekly intervals providing scientists with an ample supply of embryos to study. Zebrafish embryos grow at extremely fast rate, developing as much in a day as a human embryo develops in one month and are nearly transparent up to 5 dpf which allows researchers to easily examine the development of internal structures.

Many WT, mutant, and transgenic strains of zebrafish are available through the Zebrafish International Resource Center in Eugene, Oregon (<http://zebrafish.org/home/guide.php>) and European Zebrafish Resource Center (<https://www.ezrc.kit.edu/>) at Karlsruhe Institute for Technology (Germany). Excellent literature sources on zebrafish are available, including The Zebrafish Book (Westerfield, 2000), Zebrafish: A Practical Approach (Nusslein-Volhard and Dahm, 2002), the Zebrafish Model Organism Database (<http://zfin.org>), and a comprehensive review on zebrafish husbandry by Lawrence (2011).

1.6. Genome editing in zebrafish – CRISPR/Cas9

The development of efficient and reliable ways to make precise, targeted changes to the genome of living cells is a long-standing goal for life science researchers. Precise and efficient genome-engineering technologies, including the custom-made zinc-finger nucleases (ZFNs) and transcription activator-like effectors (TALENs), have been successfully applied in a variety of mammalian cells and non-mammalian model organisms, including zebrafish (Joung et al., 2012). It has been demonstrated that gene-specific alterations, including insertions or deletions (indels), can be generated via non-homologous end-joining (NHEJ) induced by ZFN- or TALEN-mediated double-stranded breaks (DSBs). If a double- or single-stranded DNA donor is provided, precise nucleotide substitutions or insertions at or near the break site are achieved via homologous recombination (HR) DNA repair in mammalian cells and in zebrafish embryos, suggesting possible improvement in target-specific gene *knockin* and *knockout in vivo*. Precise insertion of a reporter gene or mutant loxP (mloxP) site is especially important for investigating endogenous gene expression, or generating conditional gene knockouts in model organisms such as zebrafish (Chang et al., 2013). However, although ZFNs and TALENs enable researchers to generate permanent mutations, these approaches are costly and time-consuming, limiting their widespread use, particularly for large scale, high-throughput studies.

New tool for genome editing recently emerged, called CRISPR (Clustered Regularly Interspaced Short Palindromic Repeats). CRISPR is a family of DNA sequences in bacteria and archaea that contain snippets of DNA from viruses that have attacked them, and are used to detect and destroy DNA from similar viruses during subsequent attacks (Barrangou, 2015). Therefore, CRISPR presents an adaptive immune system or a 'genetic memory' that ensures the rejection of new, returning and everpresent invading DNA molecules. It can be reprogrammed to reject invading DNA molecules that have not been previously encountered. CRISPRs are separated by short spacer sequences that match bacteriophage or plasmid sequences and specify the targets of interference. Typically, a repeat cluster is preceded by a 'leader' sequence, an AT-rich region several hundred base pairs long with intraspecies (Jansen et al., 2002). A set of CRISPR-associated (*cas*) genes immediately precedes or follows the repeats. These genes are conserved, can be classified into different

families and subtypes, and encode the protein machinery responsible for CRISPR activity (Fig. 12) (Marraffini et al., 2010).

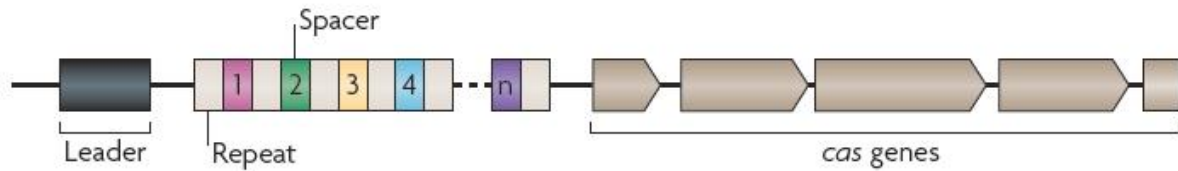


Figure 12. Features of CRISPR loci. Clustered regularly interspaced short palindromic repeats (CRISPRs, grey boxes) are preceded by a leader sequence (black box) that is AT-rich. Repeats are separated by non-repetitive spacers (colored boxes) that share sequence identity with fragments of plasmids and bacteriophage genomes and specify the targets of CRISPR interference. A set of CRISPR-associated (*cas*) genes immediately precedes or follows the repeats. (From Marraffini et al., 2010)

These repeats were initially discovered in the 1980s in *E. coli* (Ishino et al., 1987), but their function was unknown until 2007, when Barrangou and colleagues demonstrated that *Streptococcus thermophilus* can acquire resistance against a bacteriophage by integrating a genome fragment of an infectious virus into its CRISPR locus (Barrangou et al., 2007). Three types of CRISPR mechanisms have been identified, of which type II is most studied. In type II CRISPR system, invading DNA from viruses or plasmids is cut into small fragments and incorporated into a CRISPR locus amidst a series of short repeats (around 20 bps). The loci are transcribed, and transcripts are then processed to generate small RNAs (crRNA – CRISPR RNA), which are used to guide effector endonucleases that target invading DNA based on sequence complementarity (Fig. 11) (Jinek et al., 2012). The type II CRISPR mechanism is unique compared to other CRISPR systems, as only one Cas protein (Cas9) is required for gene silencing. To achieve site-specific DNA recognition and cleavage, Cas9 must be complexed with both a crRNA and a separate trans-activating crRNA (tracrRNA or trRNA), that is partially complementary to the crRNA and is required for crRNA maturation (Jinek et al., 2012). Several studies have demonstrated that Cas9 guided by gRNA is sufficient to execute *in vitro* sequence-specific cleavage of target DNA (Jinek et al., 2012; Gasiunas et al.,

2012), and site-specific DNA cleavage in mammalian cells as reported most recently (Cong et al., 2013; Mali et al., 2013).

Cas9 function relies on the presence of two nuclease domains, a RuvC-like nuclease domain located at the amino terminus and a HNH-like nuclease domain that resides in the mid-region of the protein (Sapranauskas et al., 2011). During the destruction of target DNA, the HNH and RuvC-like nuclease domains cut both DNA strands, generating double-stranded breaks (DSBs) at sites defined by a 20-nucleotide target sequence within an associated crRNA transcript (Jinek et al., 2012). The HNH domain cleaves the complementary strand, while the RuvC domain cleaves the noncomplementary strand. The double-stranded endonuclease activity of Cas9 requires that a short conserved sequence, (2–5 nts) known as protospacer-associated motif (PAM), follows immediately 3' of the crRNA complementary sequence (Swarts et al., 2012).

An important feature of Cas9, crucial for its use in genome editing, is its programmability. In 2012, Doudna and Charpentier developed a simple two-component system by combining trRNA and crRNA into a single synthetic single guide RNA (sgRNA). sgRNA programmed Cas9 was shown to be as effective as Cas9 programmed with separate trRNA and crRNA in guiding targeted gene alterations (Fig. 13).

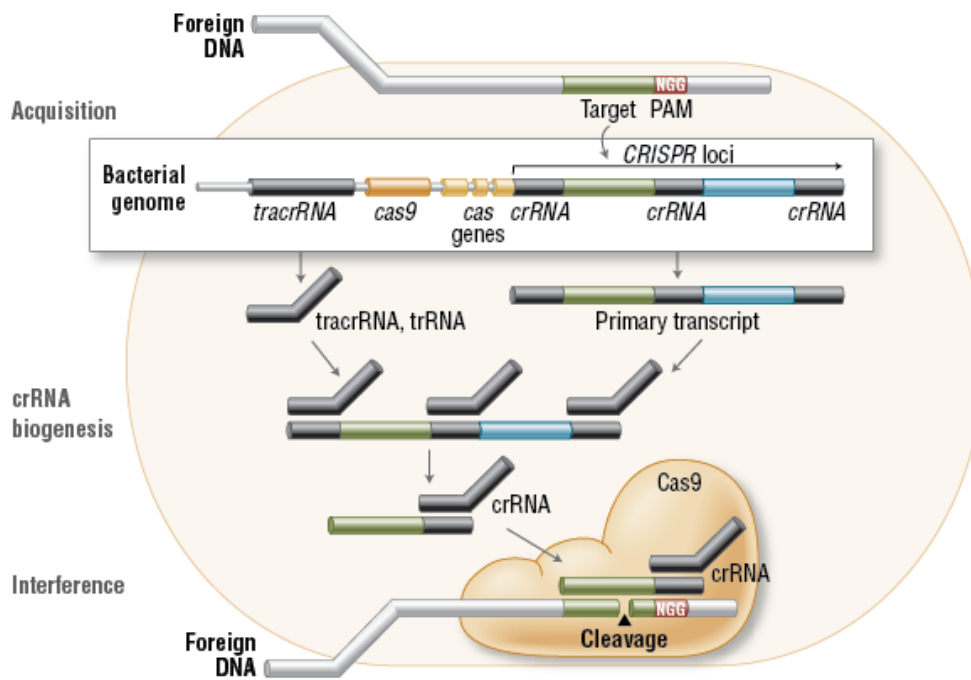


Figure 13. Cas9 *in vivo*: Bacterial Adaptive Immunity. In the acquisition phase, foreign DNA is incorporated into the bacterial genome at the CRISPR loci. CRISPR loci is then transcribed and processed into crRNA during crRNA biogenesis. During interference, Cas9 endonuclease complexed with a crRNA and separate *tracrRNA* cleaves foreign DNA containing a 20-nucleotide crRNA complementary sequence adjacent to the PAM sequence (From Jinek et al., 2012).

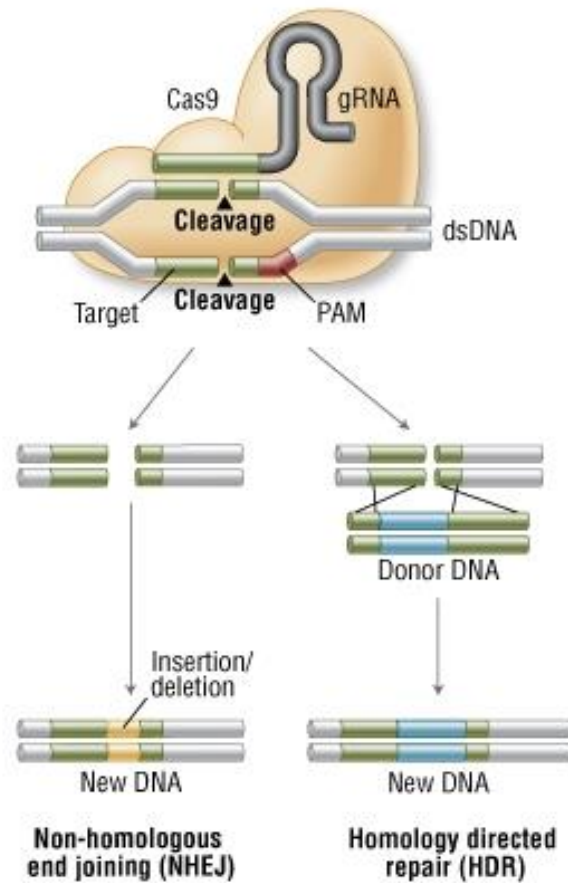


Figure 14. Genome engineering with Cas9 nuclease. Cas9 nuclease site specifically cleaves double-stranded DNA activating double-strand break repair machinery. In the absence of a homologous repair template non-homologous end joining can result in indels disrupting the target sequence. Alternatively, precise mutations and knock-ins can be made by providing a homologous repair template and exploiting the homology directed repair pathway.

1.7. Summary and aims

In summary, transporters of organic anions, which belong to two SLC/Slc families, SLC21/Slc21 and SLC22/Slc22, are polyspecific transporters that mediate uptake of a vast number of endogenous and exogenous compounds and play a crucial role in ADME processes, as well as in physiological homeostasis of organic anions in humans and other animals. Although their substrates partially overlap, the main difference between these two families of transporters is the size of their substrates. OATs/Oats mainly transport small molecules (smaller than 500 Da), while OATPs/Oatps transport larger amphipathic compounds.

Majority of knowledge on uptake transporters has been obtained using mammalian research models (mouse, rat, human), and studies on non-mammalian uptake transporters are still scarce. The same is true for zebrafish as an increasingly important vertebrate model species frequently used in both biomedical and environmental research. Secondly, in spite of a widely recognized and accepted role of uptake transporters in mammalian toxicology, their putative ecotoxicological relevance is poorly understood and studied.

Taking into account the described deficiencies and gaps in knowledge, the main goal of this study was identification and molecular characterization of Oats from the Slc22 family in zebrafish as an important model organism. Furthermore, based on the previous work of our group on zebrafish Oatp1d1, a member of Slc21 family that has been well characterized *in vitro*, to foster *in vivo* research directed to understanding of the role of uptake transporters an additional aim of this doctoral thesis was directed to generation of the first zebrafish Oatp1d1 knockout using state-of-the-art CRISP/Cas9 gene editing approach.

To accomplish the described general goal, several specific goals were defined:

- 1) To establish phylogenetic relationships between zebrafish Oats and OATs/Oats in other vertebrates;
- 2) To perform conserved synteny analysis in order to determine chromosomal locations of *Oat* genes and determine level of gene order preservation among zebrafish, human and other fish *OAT/Oat* genes;

- 3) To determine the tissue expression profile of *Oat* genes in zebrafish that would enable identifying dominantly expressed genes in tissues that are of particular toxicological importance (liver, kidney, intestine and gills);
- 4) To perform functional characterization of zebrafish Oat transporters by identification of novel fluorescent substrates, and identification of their interactors among various endogenous and xenobiotic compounds using transient and stable transfected cell lines;
- 5) To generate the first zebrafish Oatp1d1 gene *knockout* by implementing CRISPR/Cas9 gene editing technology.

2. Materials and Methods

2.1. Materials

All fluorescent dyes were purchased from Sigma-Aldrich (Taufkirchen, Germany) except ethidium bromide, which was purchased from Serva Electrophoresis GmbH (Heidelberg, Germany). The other used chemicals were purchased from Sigma-Aldrich (Taufkirchen, Germany) or Carl Roth GMBH (Karlsruhe, Germany).

Plasmids used in this study are listed in Table 2.1., enzymes are listed in Table 2.2., commercial kits in Table 2.3. and antibodies used for Western blotting analysis and immunocytochemistry in Table 2.4. Primers used for cloning of full length amplicons/genes and for the quantitative PCR analysis are listed in Table 2.5. and 2.6., respectively.

For the purpose of multiplication, DH5 α *E. coli* competent cells (Life Technologies, CA, USA) were used. These cells were grown on agar plates (Sigma-Aldrich, Taufkirchen, Germany) or in liquid Luria-Bretani medium (Becton, Dickinson and Company, Sparks, USA), supplemented with 100 μ g/mL of ampicilin (Sigma-Aldrich, Taufkirchen, Germany).

Human Embryonic Kidney cells (HEK293T) (ATCC, CRL-1573) were used in all experiments for purpose of heterologous expression. This cell line was selected due to short duplication time (<24 h) and high transfection efficiency (Tom et al., 2008). The cells were cultivated in DMEM-FBS medium, which is Dulbecco's modified Eagle medium (DMEM) with high glucose (Life technologies, CA, USA) and 10% fetal bovine serum (FBS) (Lonza, Basel, Switzerland), at 37°C and 5% CO₂ maintained atmosphere. Transient transfection of HEK293 cells was achieved using branched polyethyleneimine (PEI) transfection reagent (Sigma-Aldrich, Taufkirchen, Germany) in 48-well plates. The transfection was achieved using PEI's ability to encapsulate negatively charged plasmid DNA into positive particles, which interact with negatively charged cell surface and enter the cell through endocytosis (Boussif et al., 1995).

Protein concentrations were determined with the Bradford assay (Bradford, 1976). For that purpose, Bradford reagent was made by dissolving 100 mg Coomassie Brilliant Blue G250 (Sigma-Aldrich, Taufkirchen, Germany) in 50 mL ethanol (96%; Kemika, Zagreb). Afterwards, 100 mL of phosphorous acid was added to ethanol solution. Finally, 850 mL of mQ water was added to the mixture and filtered through membrane filter (pore diameter 0.2 μ m; TPP Techno Plastic Products AG, Switzerland).

Western blot analysis was performed using Mini-PROTEAN 3 Cell electrophoresis chamber (Bio-Rad Laboratories, CA, USA) for polyacrylamide gel electrophoresis, together with Multiphor II Electrophoresis System (Pharmacia LKB Biotechnology, Uppsala, Sweden) for wet transfer to polyvinylidene difluoride membrane (Millipore, MA, US). Protein size was estimated by use of protein marker (ThermoFischer Scientific, MA, USA).

Together with antibodies listed in Table 2.4., for the immunofluorescence localization and nuclei staining we used 4', 6-diamidino-2-phenylindole (DAPI) (Sigma-Aldrich, Taufkirchen, Germany). Finally, prepared samples on coverslips were mounted on microscope slides using Fluoromount medium (Sigma-Aldrich, Taufkirchen, Germany).

Table 2.1. Plasmids used in the study.

Plasmid	Description	Producer
pJET 1.2	Amp ^R , blunt cloning, <i>E. coli</i> expression	Life Technologies, CA, USA
pcDNA3	Amp ^R , CMV promoter, mammalian cells expression	Life Technologies, CA, USA
pcDNA3.1-His(+)	Amp ^R , CMV promoter, mammalian cells expression	Life Technologies, CA, USA
pcDNA/LacZ	Amp ^R , CMV promoter, β -galactosidase expression	Life Technologies, CA, USA
pEGFP-N	Kan/Neo ^R , SV40 promoter, mammalian cells expression, green fluorescence	Takara, Shiga, Japan
pT7-gRNA	Amp ^R , T7 promoter, CRISPR, zebrafish expression	Addgene, MA, USA

Table 2.2. Enzymes and markers used in the study.

Enzyme/Marker	Producer
Taq DNA polymerase	Life Technologies, CA, USA
Phusion proof reading polymerase	Thermoscientific, MA, USA
Reverse transcriptase	Life Technologies, CA, USA
FastDigest restriction enzymes: KpnI, NotI, XbaI, XhoI	Life Technologies, CA, USA
Dnase I	Life Technologies, CA, USA
T4 DNA ligase	Life Technologies, CA, USA
GeneRuler DNA ladder mix	Thermoscientific, MA, USA
Precision plus protein ladder	Bio-Rad Laboratories, CA, USA

Table 2.3. Commercial kits used in the study.

Commercial kit	Producer
Rneasy Mini Kit	Qiagen, Hilden, Germany
MinElute Gel Extraction Kit	Qiagen, Hilden, Germany
QIAquick PCR Purification Kit	Qiagen, Hilden, Germany
QIAprep Spin Miniprep Kit	Qiagen, Hilden, Germany
Plasmid MIDI Kit	Qiagen, Hilden, Germany
High Capacity cDNA Reverse Transcription Kit	Life Technologies, CA, USA

Table 2.4. Antibodies used in the study.

Antibody	Host	Producer	Cat.No.
Mouse IgG _{2b} -6xHis monoclonal primary ab	mouse	Bio-Rad Laboratories, CA, USA	620-0203
Mouse IgG ₁ -Xpress monoclonal primary ab	mouse	Life Technologies, CA, USA	R910-25
Mouse IgG _{2b} -Na,K-ATPase monoclonal primary ab	mouse	SantaCruz Biotechnology, CA,USA	sc-48345
Mouse IgG-HRP secondary ab	goat	Bio-Rad Laboratories, CA, USA	170-6516
Mouse IgG-FITC secondary ab	goat	SantaCruz Biotechnology, CA,USA	sc-2010
Mouse IgG-Cy3 secondary ab	goat	SantaCruz Biotechnology, CA,USA	sc-166894

Table 2.5. Primers used for cloning of zebrafish *Oat* genes. Primers were purchased from Life Technologies (Carlsbad, CA, USA).

Protein name	Primer sequence 5' -> 3'
Oat1	F GCGGCCGCGAGCTCATGGGCTTTCGGATCTTTTG
	R TTAGGTACCTCTAGACTTGAGTTGAGGAGAACTGGATTT
Oat3	F TTAGCGGCCGCAAGCTTTCATGGCGTTCTCCGACCTGT
	R GGTACCCTCGAGAACAGACTCTTTCAGGAGGA
Oat2a	F TTAGCGGCCGCAAGCTTTCATGAGGTTTCGAGGACGTTC
	R TTAGGTACCTCTAGACTTTATGAGCCCTTCTCTTGTA
Oat2b	F TTAGCGGCCGCAAGCTTTCATGAGATTTGAAGATCTGCTCT
	R TTAGGTACCTCTAGACTAGTGTTCTGCACAATTAATTA
Oat2c	F GAATTCATGAAGTTTGAAGATCTAATTAC
	R GCGGCCGCGGTACCCTGGGGTTCATTATTGCAA

Oat2d	F	GAATTCATGAAGTTTGAAGATCTAATTAC
	R	GCGGCCGCGGTACCCTGGGGTTCATTATTGCAA
Oat2e	F	TTAGCGGCCGCAAGCTTTCATGAAGTTTGAGAACCTGTTGG
	R	TTAGGTACCTCTAGACTTCATTTGTCTCCTTGAAGGC

Table 2.6. Primers used in the quantitative Real time PCR (qPCR). Primers were purchased from Life Technologies (Carlsbad, CA, USA).

Gene name	Primer sequence 5' -> 3'	T _a	Final conc. (nM)	Efficiency (%)
<i>drOat1</i>	F TGCTGTTCTGATCTTGGACGA	62	300	92
	R TGCTATTAACCAGCGATGAC	60	300	
<i>drOat3</i>	F GGGTCAGCATTACCTCATCCA	60	300	105
	R GATGGCCGTCGTCCTAACAT	58	300	
<i>drOat2a</i>	F TCGCCATTGCAAGAACCTTAT	58	300	92
	R AAGGTGCGATGCTTAACATCTG	58	300	
<i>drOat2b</i>	F GATTGTAAGTGTCCAGCACAAGAA	58	300	101
	R TGAGCTGCTGGACGAGTTTATC	58	300	
<i>drOat2c</i>	F GCACTTTGATAACAGCACCTTCAT	58	300	95
	R GAAGAAGATGGTGGTTGTCAATTC	59	300	
<i>drOat2d</i>	F ACAGTATGGCATGGGCTGTT	60	300	100
	R AAGGTGAAGTGACAGCCACT	60	300	
<i>drOat2e</i>	F GGTGTTATGATCAGTTTGGATT	60	300	95
	R TTGGAGCAGTTACTGTGAGG	58	300	

Table 2.7. Buffers used in the study.

Buffer	Composition	pH
Phosphate-buffered saline	1.37 M NaCl, 27 mM KCl, 100 mM Na ₂ HPO ₄ , 18 mM KH ₂ PO ₄	7.4
Transport buffer	145 mM NaCl, 3 mM KCl, 1 mM CaCl ₂ , 0.5 mM MgCl ₂ , 5 mM D-glucose and 5 mM HEPES	7.4
RIPA buffer	150 mM NaCl, 1 mM EDTA, 25 mM Tris, 0.8% NP-40	-
Blocking solution	5% low fat milk, 50 mM Tris, 150 mM NaCl, 0.05% Tween 20	-

2.2. Methods

2.2.1. Phylogenetic and synteny analysis

Nucleotide and protein sequences were retrieved from the following NCBI (<http://www.ncbi.nlm.nih.gov/>) and ENSEMBL (<http://www.ensembl.org/index.html>) databases, respectively. Blastx algorithm was used. Following species were included in the phylogenetic analysis: mammals – human (*Homo sapiens*) and mouse (*Mus musculus*); bird – chicken (*Gallus gallus*); reptile – anole lizard (*Anolis carolinensis*), amphibian – frog *Xenopus laevis*; actinopterygian or ray-finned fishes – zebrafish (*Danio rerio*), pufferfishes – Japanese pufferfish (*Takifugu rubripes*) and green spotted pufferfish (*Tetraodon nigroviridis*), Atlantic cod (*Gadus morhua*), stickleback (*Gasterosteus aculeatus*) and medaka (*Oryzias latipes*) and tunicate sea squirt (*Ciona intestinalis*).

Sequences were considered to be part of the SLC22/Slc22 family if there was blastx hit with threshold value of $e = 10^{-3}$. False positive results were excluded based on the phylogenetic analysis. Sequences were aligned with MUSCLE algorithm (Edgar, 2004) and phylogenetic tree was constructed using Maximum Likelihood method in PhyML 3.0.1 software (Guindon and Gascuel, 2003). Confidence of nodes was estimated by approximate likelihood ratio test (aLRT) (Anisimova and Gascuel, 2006).

Orthology predictions using conserved synteny analysis between zebrafish and other teleost genes of interest were made using Genomicus (<http://www.genomicus.biologie.ens.fr/genomicus>), a conserved synteny browser synchronized with genomes from the Ensembl database (Louis et al., 2013).

2.2.2. Tissue-specific gene expression analysis

Adult zebrafish of both genders, strain AB, were obtained from European Zebrafish Resource Center (<https://www.ezrc.kit.edu/>) at Karlsruhe Institute for Technology (Germany), and sacrificed by immersion in ice cold water for 30 min for the collection of tissues. In order to obtain sufficient amount of material for RNA isolation, six tissues (brain, gills, liver, intestine, kidney and gonads) from five specimens of the same gender were pooled together, with one pool representing one sample. Three independent pools were collected. In the case of RNA

isolation from kidney, 14 specimens were pooled together due to small size of zebrafish kidneys. In that way, 3-5 samples for each tissue were collected to conduct tissue- and gender-specific expression analysis. After isolation, tissues were stored in RNA later for long time storage at -20°C. For RNA isolation, tissues were homogenized using a rotor-stator homogenizer at 10,000 rpm for 20 s. Total RNA isolation from each tissue was carried out with RNeasy Mini Kit (Qiagen, Hilden, Germany). RNA was quantified using Bio-Spec Nano spectrophotometer (Shimadzu Corporation, Kyoto, Japan), and the integrity of RNA was determined by gel electrophoresis. Genomic DNA digestion was carried out using RNase-free DNase Set (Qiagen, Hilden, Germany). Purified total RNA was reversely transcribed (1 µg of total RNA) using High Capacity cDNA Reverse Transcription Kit with RNase Inhibitor (Applied Biosystems, Foster City, CA, USA).

The primers (Table 2.6.) were designed using Primer express 3.0 Software (Applied Biosystems, CA, USA) and adjusted manually if necessary. Target amplicons of 90-120 bp were amplified and cloned using the pGEM-T Vector System I (Promega, Madison, WI, USA). Plasmids were purified by QIAprep Spin Miniprep Kit (Qiagen, Hilden, Germany), and amplicons were verified by sequencing at the Ruđer Bošković Institute DNA Service (Zagreb, Croatia). Primer efficiencies were determined for each gene using the recombinant plasmid as a template (Table 2.6.). Primer concentrations were optimized combining three primer concentrations: 300, 600 and 900 nM. The concentrations resulting in the highest fluorescence signal at the lowest Ct number were chosen as optimal. Quantification of the *oat* genes was performed using the qPCR relative quantification method (Qgene method) and normalized to the housekeeping gene *ef1α* (elongation factor 1α), as previously described (Muller et al., 2002; Loncar et al., 2010). The relative quantification method is described with equation (1):

$$(1) \text{ MNE} = ((E_{\text{ref}})^{\text{Ct}_{\text{ref, mean}}}) / ((E_{\text{target}})^{\text{Ct}_{\text{target, mean}}})$$

where, MNE stands for mean normalized expression; E_{ref} is housekeeping gene efficiency; E_{target} is target gene efficiency; $\text{Ct}_{\text{ref, mean}}$ is mean Ct value for the housekeeping gene; and $\text{Ct}_{\text{target, mean}}$ stands for mean Ct value of the target gene. Data are presented as gene of interest expression relative to the housekeeping gene expression multiplied by the factor of 10,000. Elongation factor ($EF1\alpha$) was chosen as the housekeeping gene given the fact that its expression was similar across all analysed tissues. Expression was considered to be high

for MNE > 600*10⁵ (Ct < 22), moderate for MNE 20*10⁵ - 600*10⁵ (Ct = 23-26) and low for MNE < 20*10⁵ (Ct >27).

qPCR was performed using the ABI PRISM 7000 Sequence Detection System using Power SYBR Green PCR Master Mix (Applied Biosystems, Foster City, CA, USA). qPCR reaction mix was prepared to a final volume of 10 µL containing: 5 µL of SYBER Green master mix, 0.5 µL of each primer (of optimal concentration), 1 µL of template (10 ng/sample) and 3 µL of Ultrapure Dnase/Rnase free distilled water (Molecular Bioproducts, San Diego, CA, USA). After the initial denaturation at 95°C for 10 min, 40 cycles of amplification were carried out with denaturation at 95°C for 15 sec, annealing and elongation at 60°C for 1 min, altogether followed by the melting curve analysis. Data were analysed with ABI PRISM Sequence Detection Software 1.4 (Applied Biosystems, Foster City, CA, USA) and GraphPad Prism Software version 5.00.

2.2.3. Cloning and heterologous expression

In order to amplify full-length zebrafish *oat* (*oat1*, *oat2a-e*, *oat3*) genes, specific primers were designed based on known sequences of zebrafish *oat* genes. Genes were amplified from zebrafish cDNA by polymerase chain reaction (PCR) using high fidelity Phusion DNA polymerase (Thermo Scientific, MA, USA), using specific forward and reverse primers, with introduced cloning sites for *NotI* and *HindIII* restriction enzymes on forward primers and *KpnI* and *XbaI* on reverse primers. Amplified DNA fragments were separated using agarose gel electrophoresis and specific gene bands were purified with commercially available kit (Table 2.3.). Afterwards, since Phusion DNA polymerase produces amplicons with blunt ends, we performed blunt-end ligation of the amplicons with previously prepared linearized pJET 2.0 vector. pJET/*oat* constructs were transformed into DH5α *E. coli* competent cells (Invitrogen, Carlsbad, CA, USA). The presence of ampicillin resistance gen in pJET vector allowed the growth of transformed DH5α cells on ampicillin-selective agar plates, overnight at 37°C. Grown bacterial colonies were screened for presence of inserted *oat* genes using PCR with Taq DNA polymerase and specific primers for each gene. To obtain sufficient amount of plasmid, transformed cells were grown in liquid cultures with ampicillin-selective Luria-Bretani medium. Recombinant plasmid with inserted gene was purified using

commercial plasmid isolation kit (Table 2.3.). Minimum of three positive clones were verified by DNA sequencing at the Ruđer Bošković Institute DNA Service (Zagreb, Croatia). Sequenced genes of each clone were compared to the reported gene sequences from the NCBI and ENSEMBL databases. If sequence of one clone differed from the sequences of two other clones in one or more base pairs, the sequences of two identical clones were considered to be valid, and one of these two clones was chosen for further investigation.

After the sequence confirmation, each gene was cloned into the pcDNA3.1 and pcDNA3.1/His vector, with gene promoter suitable for high-level heterologous expression in the mammalian cell lines. Zebrafish *oat2a-e* genes were also cloned into the vectors for expression and visualization of a protein of interest fused to the green fluorescent protein (EGFP). The cloning was performed using primer-inserted restriction sites, which allowed digestion of *oat/pJET* vector constructs with restriction enzymes and excision of inserted genes. Excised inserts were separated with agarose gel electrophoresis and purified with commercial gel extraction kit. Destination vectors, pcDNA3.1 and pcDNA3.1/His, were also digested using the same combination of restriction enzymes, and linearized vectors were purified using commercial PCR purification kit. Sticky ends of purified gene inserts and linearized vectors were ligated using T4 DNA ligase (Table 2.2.). The ligation mixtures were used for transformation of DH5 α competent cells and cultivation on ampicillin selection plates. Positive transformants were screened using PCR and multiplied by cultivation of liquid cultures. For purpose of heterologous expression, the greater volumes of liquid cultures were cultivated and plasmid purification MIDI kit was used (Table 2.3.).

2.2.3.1. Transient transfection

Transient transfection method was based on previously described method by Tom et al. (2008), with some modifications. To reach 90% confluence, HEK293 cells were seeded in the 48-well plates 48 hours prior to transfection at cell density of 2.1×10^5 cells/cm², with final volume of 0.25 mL per well. The transfection mixture consisted of recombinant plasmid with inserted gene and PEI reagent in the 1:1 ratio with the final concentration of 0.375 μ g/well for 48-well plate. PEI and plasmid solutions were prepared in phosphate buffered saline buffer (PBS) at 37°C. Solutions were mixed and briefly vortexed (3 x 3 s) and incubated at

room temperature for 15 minutes. After the incubation, 25 μ L of plasmid/PEI mixture was added to each well with 225 μ L of DMEM medium without FBS and incubated for 4 hours at 37°C and 5% CO₂. Four hours later, the medium with transfection mixture was replaced with 250 μ L DMEM-FBS per well. The transfected cells were left to grow in standard conditions for 24 hours, and after that period the cells were ready for transfection efficiency evaluation and the conduction of transport assays. To evaluate transfection efficiency, separate cells were transfected with pcDNA3.1/His/LacZ plasmid and transfection efficiency was evaluated 24 h after transfection with the LacZ staining protocol (Sambrook et al., 1989). The assay is based on the ability of enzyme β -galactosidase, coded by LacZ gene, to catalyze X-gal (5-bromo-4-chloro-3-indolyl- β -D-galactopyranoside) into the blue product 5,5'-dibromo-4,4'-dichloro-indigo. Adherent HEK293 cells transfected with pcDNA3.1/His/LacZ were washed twice with PBS, followed by fixation in 0.5% glutaraldehyde (in PBS), and 2 – 24 h incubation (at 37°C) in the X-gal solution (1 mM X-gal, 40 mM ferricyanide, 40 mM ferrocyanide, 2 mM MgCl₂ in PBS).

2.2.3.2. Stable transfection

Stable transfection was conducted using Flp-In™ System which uses pcDNA⁵/FRT expression vector. pcDNA⁵/FRT plasmid contains CMV promoter for high level expression in mammalian cells, ten unique restriction sites for easy cloning, FLP Recombination Target (FRT) site for Flp recombinase-mediated integration of the vector into the Flp-In host cell line, and hygromycin resistance gene for selection of stable cell lines. Transfection protocol is similar to that described for transient transfection as it also uses PEI reagent, but in combination with two plasmids: pcDNA⁵/FRT and pOG44 (Flp recombinase expression vector). In order to reach 90% confluence, HEK Flp-In™ cells were seeded in 6-well plates 48 h prior transfection at cell density of 3×10^5 cells/cm², with final volume of 2.5 mL per well. The transfection mixture consisted of 0.375 μ g recombinant plasmid pcDNA⁵/FRT with inserted gene, 3.375 μ g pOG44 plasmid and 3.750 μ g PEI reagent (1:1 ratio with pcDNA⁵/Frt + pOG44). PEI and plasmid solutions were prepared in PBS, solutions were mixed and briefly vortexed (3 x 3 s) and incubated at room temperature for 15 minutes. After the incubation, 250 μ L of pcDNA⁵-FRT/pOG44/PEI mixture was added to each well with 2.25 mL of DMEM medium without FBS and incubated for 4 hours at 37°C and 5% CO₂. Four hours later, the medium with

transfection mixture was replaced with 2.5 mL DMEM-FBS per well. The transfected cells were left to grow in standard conditions for 48 hours, scraped off, transferred to 25 cm² cell culture flask, and left to adhere overnight. The next morning, after the cells adhered to the flask bottom, 100 µg/mL hygromycin B was added and the cells were kept in DMEM-FBS + hygromycin B for 20-25 days with DMEM-FBS change every 3-4 days. After that period, only transfected cells (i.e. hygromycin resistant) survived and started to grow. The cells were then tested for uptake of fluorescent substrates of selected Oat(s) and later used for transport activity assays.

2.2.4. Transport activity assays

Transfected cells that showed more than 70% of transfection efficiency were used for transport activity assays. DMEM-FBS was removed from cells grown in 48-well plates and cells were preincubated in 200 µL of the transport medium for 10 min at 37°C. To assess transport and dose-responses of fluorescent substrates, 50 µL of five times concentrated fluorescent substrates was added to the preincubation medium and incubated 5 to 15 minutes at 37°C, depending on the substrate used. After the incubation, the cells were washed two times with 250 µL of pre-chilled transport medium and lysed with 250 µL of 0.1% sodium dodecyl sulphate (SDS) for 30 minutes. Lysed cells were transferred to the 96-well black plates and the fluorescence was measured using the microplate reader (Infinite M200, Tecan, Salzburg, Austria). The transport rates were determined by subtracting the measured fluorescence of transfected cells with the fluorescence of non-transfected control cells (mock cells) and by normalization of the obtained fluorescence unit calibration curves for each substrate and protein content. Calibration curves for fluorescent dyes were generated in the 0.1% SDS and in the cell matrix dissolved in the 0.1% SDS. Total protein concentration was measured using Bradford assay (Bradford, 1976). Using the calibration curves and total protein content, uptake of the fluorescent substrates was finally expressed as nM of substrates per mg of protein.

After the determination of transport kinetics for fluorescent dyes, they were used in the inhibition assays. Inhibition measurements were based on co-exposure of transfected cells and non-transfected control with determined model substrate and potential interactor. The

cells were preincubated for 10 minutes in transport medium, and for 40 seconds with test compounds, followed by 5 to 15 minutes incubation with model substrate at concentration that showed to be in the linear segment of the determined dose response curve. The initial interaction screenings were performed with one concentration of the tested compounds (100 μM) and for the interactors that showed uptake inhibition above 70%, detailed dose response experiments were performed and the respective IC50 values determined. Compounds with IC50 values in nanomolar and low micromolar range (<5 μM) were considered to be very strong interactors, compounds with K_i of 5 - 20 μM were designated as strong interactors, whereas K_i of 20 – 100 μM indicated moderate interaction and IC50 above 100 μM , weak interaction.

2.2.5. Western blot analysis

Cells were collected from 2 wells of a 6-well microplate 48 h after transfection and lysed in RIPA buffer (NaCl 150 mM, EDTA 1 mM, Tris 25 mM, NP-40 0.8%) with the AEBSF protease inhibitors cocktail (Sigma-Aldrich, Taufkirchen, Germany) for 30 min on ice. After the lysis, cells were subjected through 3 freeze/thaw cycles, briefly sonicated and centrifuged at 1,000 *g* for 10 min at 4°C. Protein concentration in total cell lysate (TCL) was measured using Bradford assay (Bradford, 1976). Twenty micrograms of protein per lane was separated by electrophoresis in 1% sodium dodecyl sulphate polyacrylamide gel. The proteins were then transferred to the polyvinylidene difluoride membrane (Millipore, MA, US) by wet blotting. Blocking was performed in blocking solution. Subsequently, membranes were washed and incubated for 1 h with anti-Xpress, or 2 h with anti-His antibody (1:5000). Goat anti-mouse IgG-HRP (1:5000) was used as secondary antibody (Bio-Rad Laboratories, CA, USA). The proteins were visualized by chemiluminescence (Abcam, Cambridge, UK). Protein size was estimated by use of protein marker (ThermoFischer Scientific, MA, USA).

2.2.6. Immunofluorescence

For immunofluorescence localization of proteins expressed by transiently transfected plasmids, HEK293T cells were grown on glass coverslips in 24-well culture plates. Fixation of

transiently transfected cells was performed with 3.7% formaldehyde in PBS during 25 min incubation. Cells were washed three times in 100 mM glycine/PBS, permeabilized with methanol for 15 min and washed 3 times in PBS. Antigen retrieval was done in 1% SDS/PBS for 5 minutes. Cells were then blocked in 5% low fat milk for 30 min with gentle agitation at room temperature. Subsequently, coverslips were transferred on microscope slides and incubated with Xpress antibody (1:100) in blocking solution for 1 h at 37°C in humidity chamber, washed and incubated with secondary FITC antibody (fluorescein isothiocyanate) (1:100) in blocking solution for 1 h at 37°C. When double staining was performed after incubation with FITC, blocking was done in 5% low fat milk for 30 min with gentle agitation, followed by incubation with Na,K-ATPase anti-mouse primary antibody for 2 hours (1:150), washing, and 1 hour incubation with Cy3-conjugated anti-mouse IgG-HRP (Cyanine3) as a secondary antibody (1:200). Nuclei were stained with 300 nM DAPI/PBS for 45 min at 37°C. After mounting the samples in Fluoromount medium, immunofluorescence was detected using confocal microscope Leica TCS SP2 AOBS (Leica Microsystems, Wetzlar, Germany).

2.2.7. Creating gene knockouts using CRISPR/Cas9 system

A search for the gene of interest was made using ENSEMBL gene/transcript annotation ("target protein-coding genes"). Targets were identified using CRISPRscan (<http://www.crisprscan.org/>), and those with high CRISPRscan score and without off-targets were chosen. Primers were designed (forward: TAGGN18, reverse: AAACN18) and the two oligos annealed using NEBuffer™ 3 (New England Biolabs, MA, USA). Two µL from each 100 µM stock in a final volume of 20 µL 1x NEBuffer™ 3 solution) were incubated at 95°C for 5 min, ramped down to 50°C at 0.1°C/sec, incubated at 50°C for 10 min, and chilled to 4°C at normal ramp speed (1°C/sec). Next step was cloning (one-step digestion/ligation), and the annealed oligos were ligated to pT7-gRNA vector (<http://www.addgene.org/46759>) by mixing the following components: 1 µL of annealed oligos, 200 ng of vector, 1 µL of 10x NEBuffer 3, 1 µL of 10x T4 ligase Buffer, 0.5 µL of BsmBI, 0.3 µL of BglII, 0.3 µL of Sall, 0.5 µL of T4 DNA ligase, and water to a total of 10 µL. Digestion and ligation were performed in a single step in a thermal cycler with the following program: 3 cycles of 20 min at 37°C/15 min at 16°C, followed by 10 min at 37°C, 15 min at 55°C, and 15 min at 80°C (optional). The ligation product was then used to transform DH5α competent cells and

grow them on LB/Amp plates overnight. Two colonies were then sequenced with M13F(-21) primer to confirm the clones.

For making gRNA, the plasmid was digested with BamHI and the linearized plasmid was gel purified. *In vitro* transcription was performed using the MEGAscript T7 kit (Ambion/Invitrogen) with 100-400 ng of purified linearized DNA following the manufacturer's instructions.

For making nls-zCas9-nls RNA, template DNA was linearized by NotI and the template was gel purified. Capped nls-zCas9-nls RNA was synthesized using mMACHINE SP6 (<https://www.thermofisher.com/order/catalog/product/AM1340>).

Finally, 1 μ L phenol red (0.05% Cf), gRNA (100 ng/ μ L Cf) and Cas9 (150 ng/ μ L Cf) were mixed, and 1 nL of the mix directly injected into the cell of the one-cell stage zebrafish embryos. After 48 h, 15 embryos were collected for DNA extraction and genotyping the F0 generation. For control, 5 WT embryos at the same developmental stage were used. DNA extraction was done in the embryo digestion buffer (Tris-Cl 10 mM, 50 mM KCl, Tween-20 30%) and proteinase K. Genotyping was performed using StepOnePlus™ Real-Time PCR System (<https://www.thermofisher.com/order/catalog/product/4376600>) and the High Resolution Melt Analysis (HRMA) software (<https://www.thermofisher.com/order/catalog/product/A30150>).

2.2.8. Data analysis

All assays were performed in 2 - 4 independent experiments run in triplicates. Data represents mean \pm standard errors of mean (SE) or standard deviations (SD). All calculations were performed using GraphPad Prism 6 for Windows as described below. The kinetic parameters, K_m and V_m values were calculated using the Michaelis-Menten equation (2):

$$(2) \quad V = \frac{V_m \times [S]}{S + K_m}$$

where, V is velocity (nanomoles of substrate per milligram of proteins per minute), V_m is maximal velocity, $[S]$ is substrate concentration and K_m is the Michaelis Menten constant. The uptake into vector-transfected HEK293 cells was subtracted to obtain transporter-

specific uptake. For the purpose of K_i calculations data were fitted to the sigmoidal four parameters dose–response model (variable slope) (3):

$$(3) \quad V = V_{\min} + \frac{(V_{\max} - V_{\min})}{1 + 10^{((\log K_i - A)h)}}$$

where V is response, V_{\min} represents minimum of response, V_{\max} represents maximum of response, h is Hill slope parameter, K_i is the concentration of inhibitor that corresponds to 50% of maximal effect and A is concentration of tested compound.

3. Results

3.1. Phylogenetic analysis

To elucidate phylogenetic relationships of zebrafish *Oat* genes within the Slc22 family, we constructed a phylogenetic tree. Among fourteen genes initially identified inside the zebrafish Slc22 family (Popovic et al., 2014), seven of them, *slc22a6*, *slc22a7a*, *slc22a7b*, *slc22a7c*, *slc22a7d*, *slc22a7e* and *slc22a8*, belong to subgroup of organic anion transporters (Oat1, Oat2a, Oat2b, Oat2c, Oat2d, Oat2e and Oat3). There are 8 organic anion transporters in human (OAT1, OAT2, OAT3, OAT4, OAT6, OAT7, OAT10 and URAT1), 8 in mouse (Oat1, Oat2, Oat3, Oat5, Oat6, Oat9, Oat10 and Urat1) and Oat8 in rat. Oat1 and Oat3 are conserved within all analyzed vertebrate groups, except birds (*oat1* and *oat3* ortholog absent in *Gallus gallus* - *Gg*) (Fig. 15). Zebrafish *oat2* includes 5 co-orthologs: *oat2a*, *oat2b*, *oat2c*, *oat2d* and *oat2e*. *oat2a* ortholog was found only in zebrafish and green spotted pufferfish (*Tetraodon nigroviridis*) and it had the closest phylogenetic relationship with human *Oat2* and other mammalian *oat2*, indicating its direct orthology with mammalian *Oat2*. *oat2b* is present only in zebrafish, stickleback (*Gasterosteus aculeatus*) and green spotted pufferfish. Out of all five zebrafish co-orthologs, the closest phylogenetic relationship was observed between *oat2c* and *oat2d*, and they were present also in green spotted pufferfish and Japanese pufferfish (*Takifugu rubripes*). *oat2e* was present only in zebrafish and medaka (*Oryzas latipes*).

Phylogenetic analysis revealed specific clustering of vertebrate *Oat/oat* genes. Zebrafish *oats* primarily clustered with other fish *oats*. Zebrafish *oat1* clustered with other fish *oat1*, but was quite distant from mammalian *Oat1/oat1*. However, fish *oat3* clustered closer together with mammalian *Oat1/oat1* comparing to fish *oat1*, indicating closer phylogenetic relationship of mammalian *Oat1/oat1* and fish *oat3* than fish *oat1*. *Oat2/oat2* was present with only one gene in reptiles, birds and mammals, while in fish there were principally more than one orthologs.

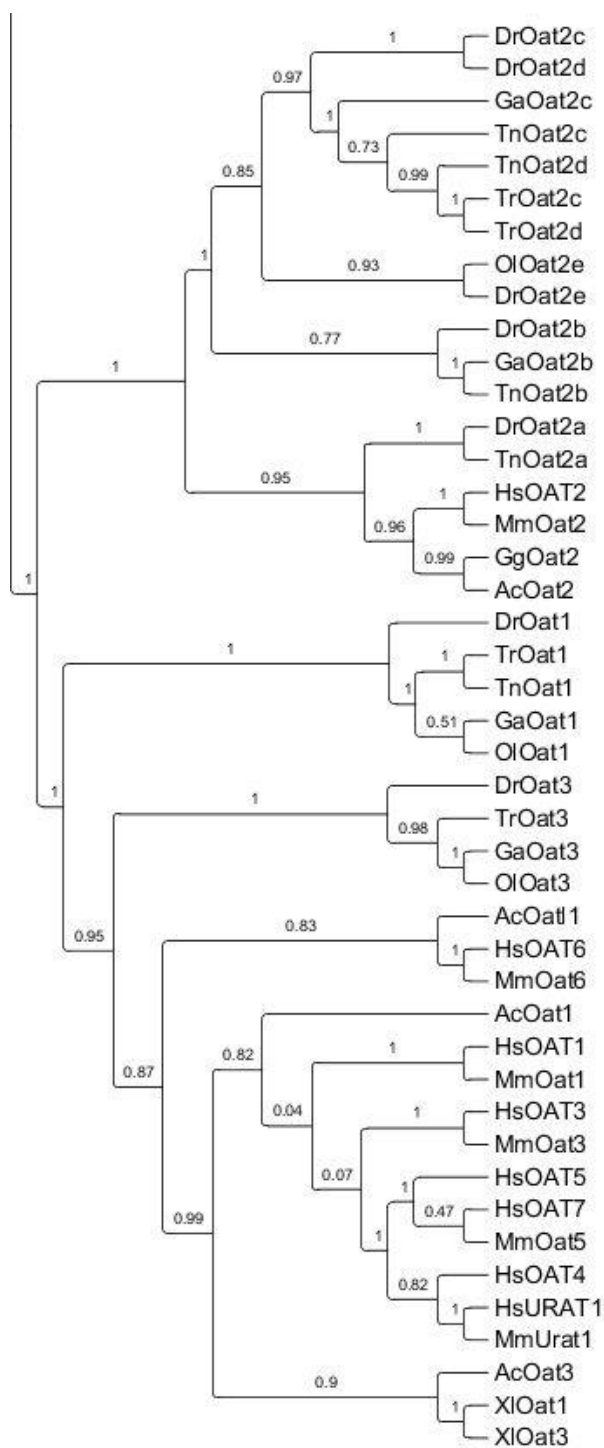


Figure 15. Phylogenetic tree of organic anion transporter genes (*OATS/Oats*) in vertebrates. Species abbreviations: human (*Homo sapiens*), mouse (*Mus musculus*), chicken (*Gallus gallus*), anole lizard (*Anolis carolinensis*), frog (*Xenopus laevis*), zebrafish (*Danio rerio*), Japanese pufferfish (*Takifugu rubripes*), green spotted pufferfish (*Tetraodon nigroviridis*), Atlantic cod (*Gadus morhua*), stickleback (*Gastrosteus aculeatus*), medaka (*Oryzias latipes*).

3.2. Synteny analysis

Zebrafish *oat2* genes are localized on two chromosomes, 11 and 17. Four *oat2* co-orthologs, *oat2b* (*slc22a7* (1 of many)), *oat2c* (*slc22a7b2*), *oat2d* (*slc22b3*), *oat2e* (*slc22b1*), are localized within the cluster with reversed orientation on chromosome 17 at 21.99 Mbp (Fig. 1). Neighboring genes near the *oat2* cluster on chromosome 17 show syntenic relationship with two *oat2* orthologs in stickleback, cave fish and tetraodon. *ryr2b*, *actn2b* and *slc16a9a* are localized upstream of *oat2b* ortholog in stickleback, and determine syntenic relationship with zebrafish ortholog. Two downstream neighboring genes, *ttbk1b* and *slc8a1b*, and an upstream neighboring gene *crip3*, showed syntenic relationship with the second *oat2* ortholog in stickleback, *oat2e*. *oat2a* (*slc22a7a*) on chromosome 11 and its neighboring genes, show syntenic relationship with *oat2a* orthologs in cave fish and tetraodon. *oat2* genes are also present in medaka and cod. However, their *oat2* ortholog does not show syntenic relationship with zebrafish orthologs. One *oat2* ortholog in medaka and cod, respectively, show synteny with *oat2* ortholog in stickleback, and with the zebrafish *oat2* cluster on chromosome 17 (Fig. 16).

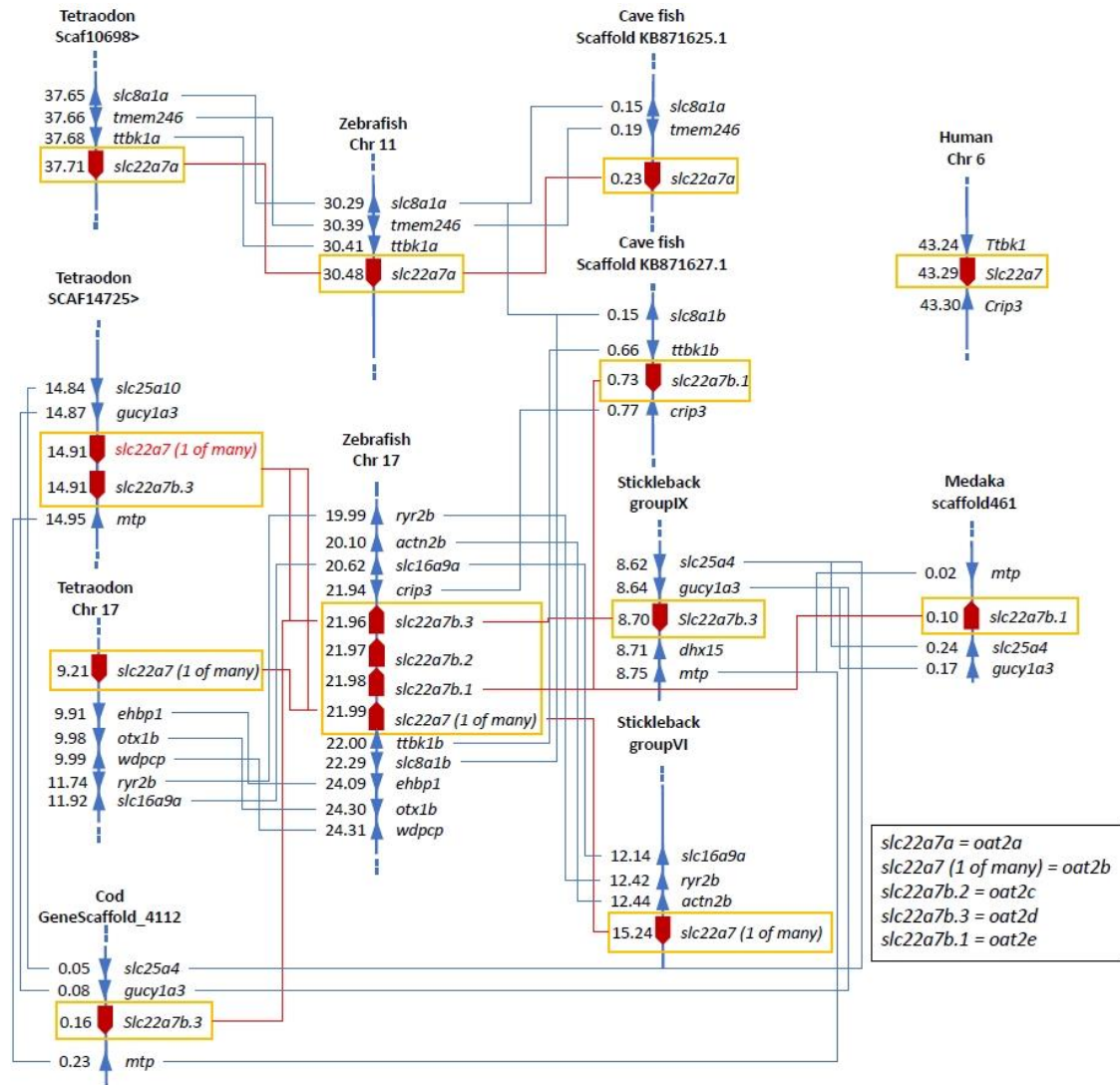


Figure 16. Conserved synteny analysis of teleost fish *slc22a7* genes. Numbers next to the gene names represent megabase pair (Mbp) of particular gene location on the chromosome. Species names: zebrafish, *Danio rerio*; green spotted puffer, *Tetraodon nigroviridis*; cod, *Gadus morhua*; cave fish, *Astyanax mexicanus*; stickleback, *Gasterosteus aculeatus*; medaka, *Oryzias latipes*; human, *Homo sapiens*.

Zebrafish *oat1* and *oat3* genes are both localized on chromosome 21. Neighboring genes near the *oat1* (*oatx*) cluster show syntenic relationship with orthologs in cave fish, medaka and tetraodon. *arsib*, *ndufa2* and *FO704810.1* are localized upstream of *oat1* ortholog in cave fish, and determine syntenic relationship with zebrafish ortholog. *ndufa2* is localized downstream of *oat1* ortholog in medaka. *nrxn2a* and *pygma* are localized upstream of *oat3* orthologs in cave fish, medaka and tetraodon and determine syntenic relationship with zebrafish ortholog. Two downstream neighboring genes, *nrg2a* and *puraa* showed syntenic relationship with *oat3* ortholog in medaka and tetraodon, while only *nrg2a* is downstream of cave fish *oat3* ortholog (Fig. 17).

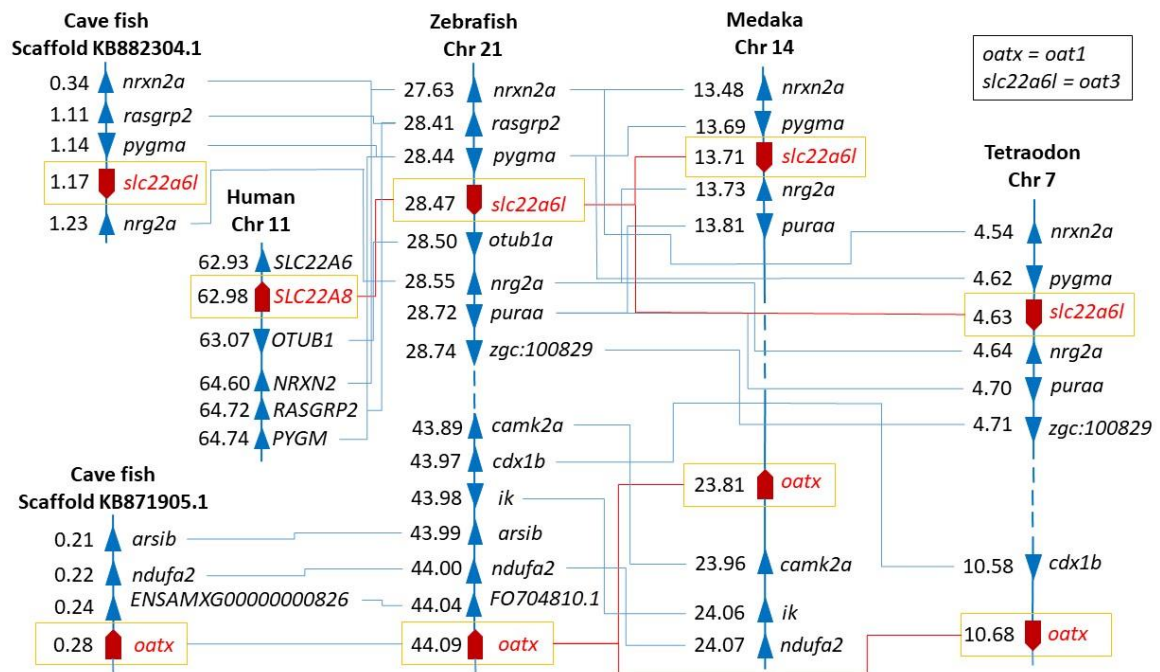


Figure 17. Conserved synteny analysis of teleost fish *oat1* and *oat3* genes. Numbers next to the gene names represent megabase pair (Mbp) of particular gene location on the chromosome. Species names: zebrafish, *Danio rerio*; green spotted puffer, *Tetraodon nigroviridis*; cod, cave fish, *Astyanax mexicanus*; medaka, *Oryzias latipes*; human, *Homo sapiens*.

3.3. Tissue expression profiles

The qPCR analysis of *Oat1* gene in adult zebrafish tissues (Fig. 18) showed the highest expression in testes in males and in brain in females. Low and very low expression was found in gills and liver in both genders.

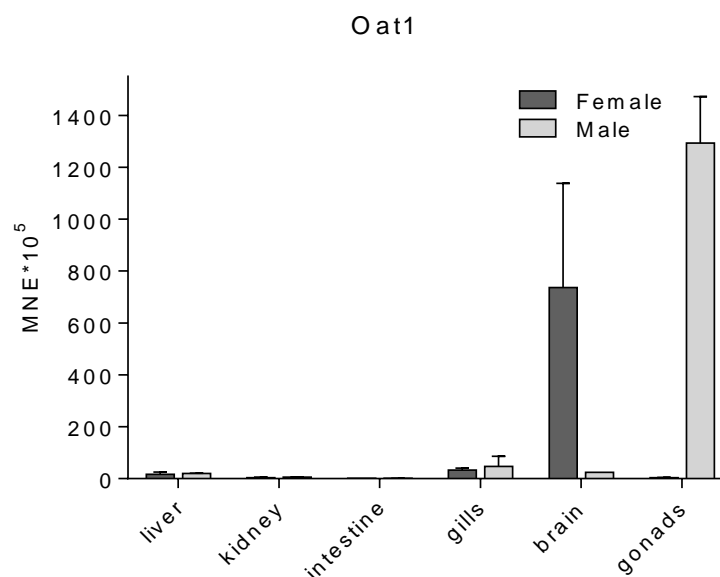


Figure 18. Tissue expression profile of *oat1* gene in adult male and female zebrafish. Results of three independent measurements (three pools) are given, except in the case of kidney (one pool of 15 individuals). Tissue expression results are presented as mean values \pm SEM from 3 to 5 pools. MNE stands for mean normalized expression normalized to the housekeeping gene *ef1 α* .

Oat2 co-orthologs showed expression in various tissues (Fig. 19). *Oat2a* had the highest expression in testes, lower in brain and very low in gills and liver. Most *Oat2b* mRNA was detected in testes, less in brain and very small amount in gills and kidney. *Oat2c* was highly expressed in kidney of females and almost twice less in males. It showed lower expression in testes, low expression in ovaries and very low in brain and gills. *Oat2d* showed the highest expression in intestine and testes, with lower expression in brain of males, and kidney of both genders. Very low expression was observed in gills and liver. *Oat2e* was highly expressed in kidney, lower in testes and brain.

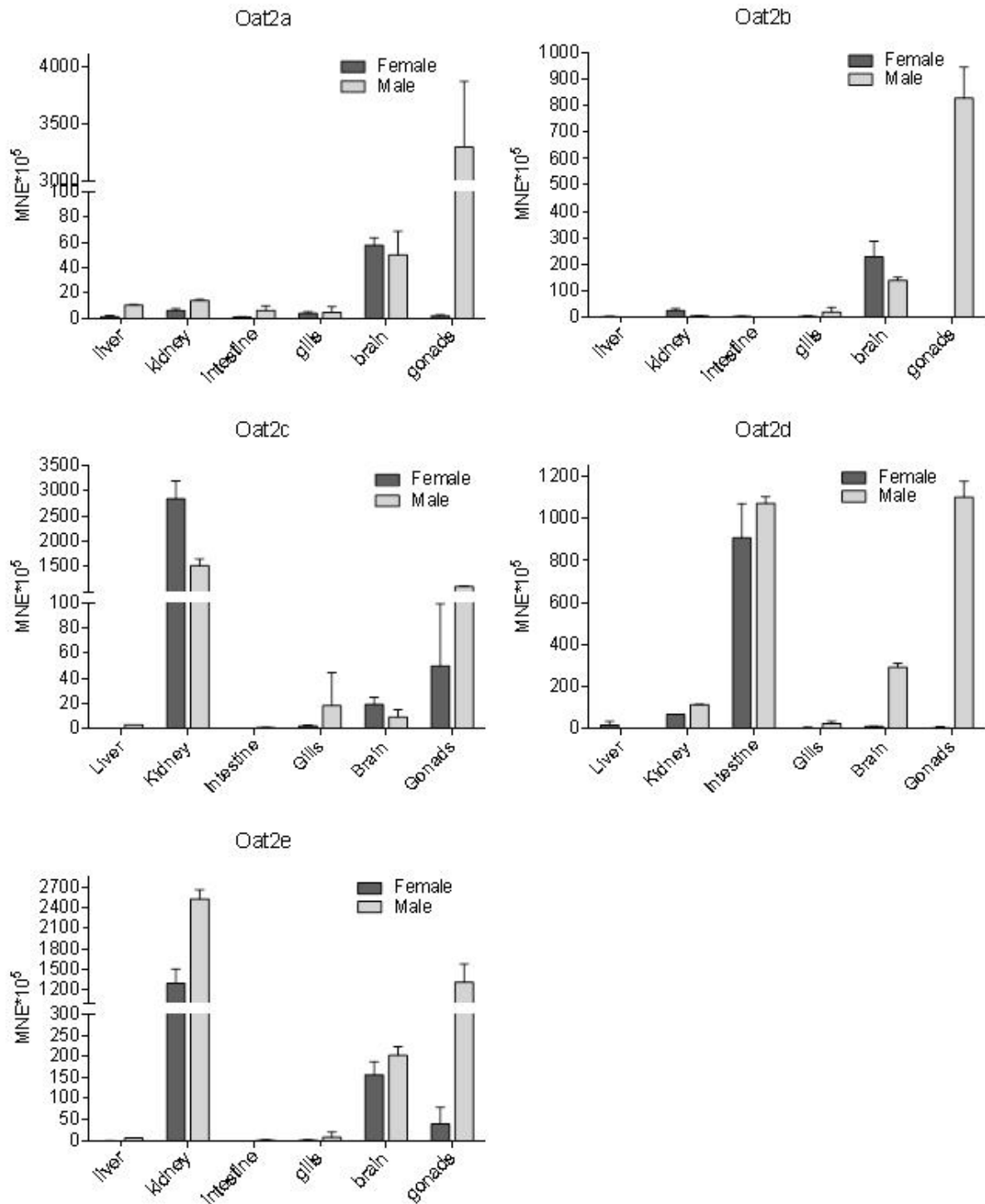


Figure 19. Tissue expression profile of *oat2* genes in adult male and female zebrafish. Results of three independent measurements (three pools) are given, except in the case of kidney (one pool of 15 individuals). Tissue expression results are presented as mean values \pm SEM from 3 to 5 pools. MNE stands for mean normalized expression normalized to the housekeeping gene *ef1a*.

Oat3 showed the highest expression of all *Oats* in zebrafish (Fig. 20), with very high expression in female kidneys. It showed lower expression in male kidneys, testes and intestine with higher prevalence in females. It also showed a very low expression in brain and gills.

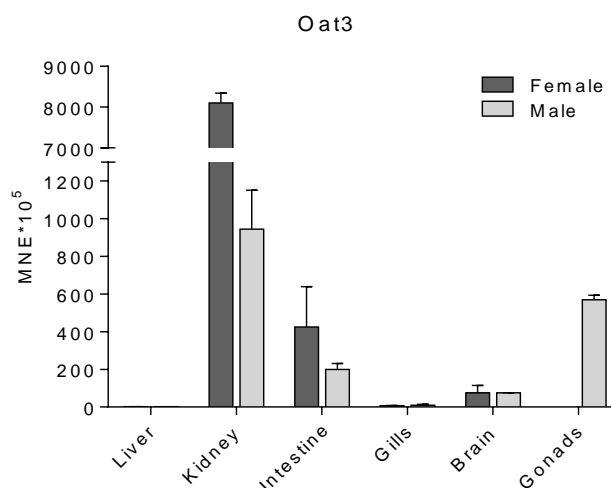


Figure 20. Tissue expression profile of *oat3* gene in adult male and female zebrafish. Results of three independent measurements (three pools) are given, except in the case of kidney (one pool of 15 individuals). Tissue expression results are presented as mean values \pm SEM from 3 to 5 pools. MNE stands for mean normalized expression normalized to the housekeeping gene *ef1 α* .

3.4. Protein identification and cell localization

To identify zebrafish Oat proteins overexpressed in transiently transfected cells, Western blot analysis was performed. The analysis was based on the expression of specific tags fused together with the Oat proteins in the heterologous expression system. Western blot analysis revealed protein bands of four zebrafish Oat2 proteins (Oat2a, b, d, and e) that correspond to the size of approximately 60 kDa, as expected (Fig. 21). However, protein band of Oat2c was not obtained. Estimated size of zebrafish Oat2 transporters are: Oat2a – 62.27 kDa, Oat2b – 61.21 kDa, Oat2c – 62.18 kDa, Oat2d – 62.92 kDa, Oat2e – 60.63 kDa.

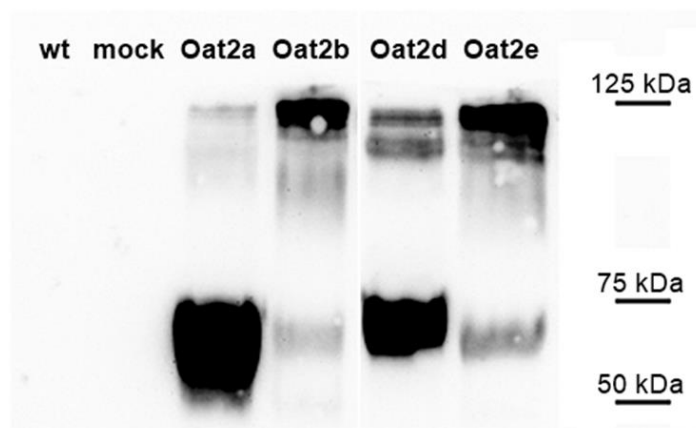


Figure 21. Western blot analysis of zebrafish Oat2a–e proteins expressed in transfected cells. Total cell lysate (TCL) of HEK293/Oat2a–e overexpressing cells shows protein bands of four Oat2s (Oat2a, b, d, and e) that correspond the size of monomeric protein (approx. 60 kDa). Oat2a is present as a monomer, whereas other Oat2 proteins show monomeric, and possible homo- or heterodimeric forms. Western blots were performed in the presence of reducing agent dithiothreitol (DTT) with anti-Xpress antibody, and visualized with chemiluminescence, as described in Materials and Methods section.

Western blot analysis revealed protein bands of zebrafish Oat1 and Oat3 (Fig. 22) that correspond the size of glycosylated monomeric protein (Oat1 ~ 90 kDa, Oat3 ~ 75 kDa). Both proteins show possible homo- or heterodimeric forms and post-translational modifications (PTMs) that can be seen as smears above the monomeric bands.

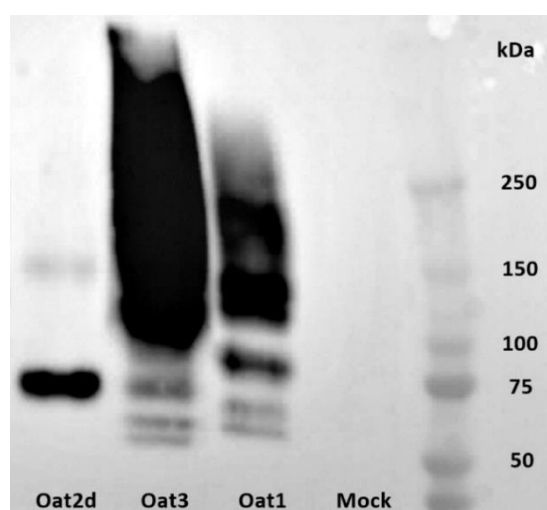


Figure 22. Western blot analysis of zebrafish Oat1 and Oat3 proteins expressed in transfected cells. Cytosolic fraction of HEK293/Oat1 and Oat3 overexpressing cells lysate

shows protein bands of Oat1 and Oat3 that correspond the size of glycosylated monomeric protein (Oat1 – 100 kDa, Oat3 - 75 kDa, possible homo- or heterodimeric forms and PTMs). Western blots were performed in the presence of reducing agent dithiothreitol (DTT) with anti-Xpress antibody, and visualized with chemiluminescence.

Immunolocalization analysis confirmed localization of all seven zebrafish Oats within the cell membranes. This was confirmed with co-localization of the green colored Oat and red colored Na/K ATPase, which is naturally localized in the cell membranes. As the result of co-localization, signals of the two dyes were combined and subsequently produced an orange signal which confirmed the localization of zebrafish Oats within the cell membrane (Figs. 23-25). These results indicate that all zebrafish Oat proteins are correctly localized and can be active in the used expression system.

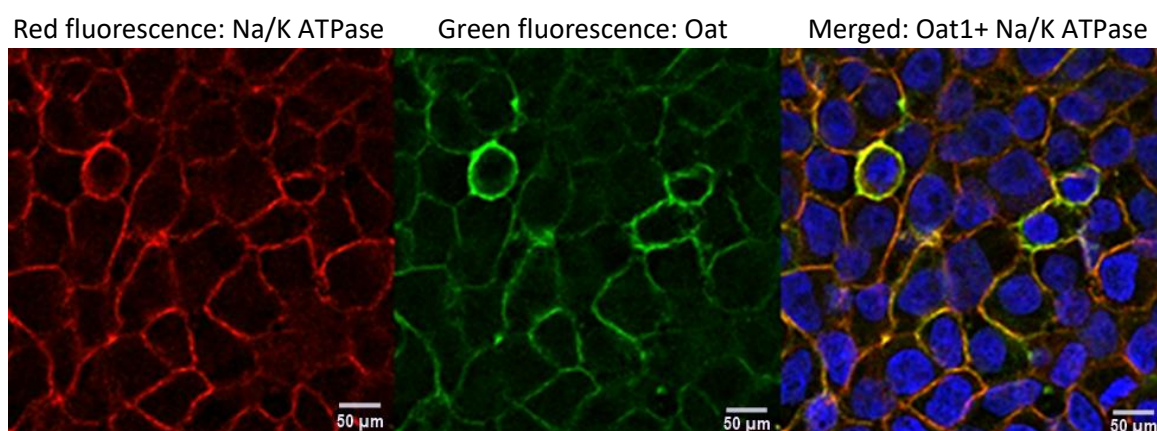


Figure 23. Immunolocalization of zebrafish Oat1 transporter by co-localization of the green colored Oat and the red colored Na/K ATPase. Signals of the two dyes were combined and subsequently produced an orange signal which confirmed the localization within the cell membrane. Nuclei are stained with DAPI (blue).

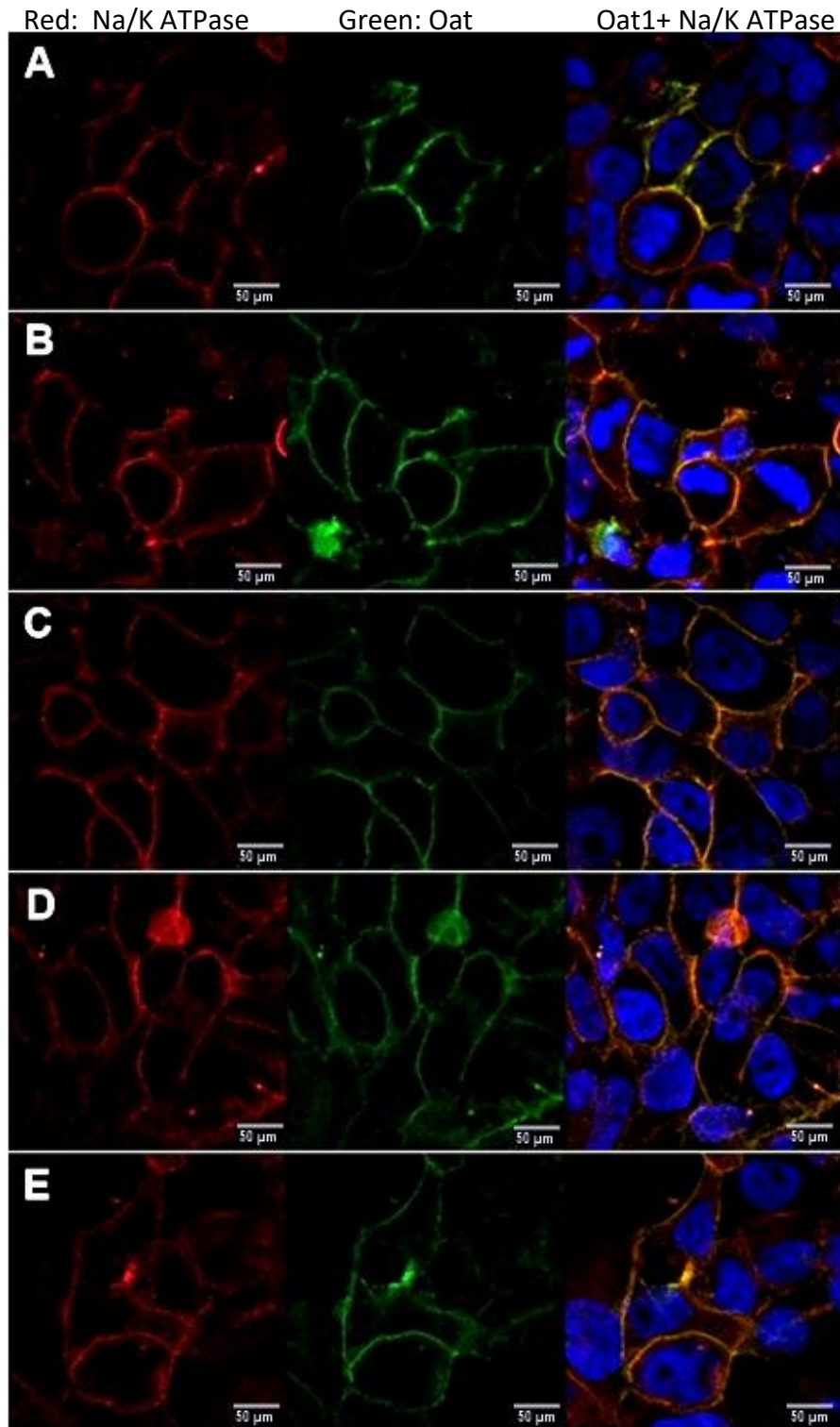


Figure 24. Immunolocalization of zebrafish Oat2 transporters by co-localization of the green colored Oat and the red colored Na/K ATPase. Signals of the two dyes were combined and subsequently produced an orange signal which confirmed the localization within the cell

membrane. A) Oat2a, B) Oat2b, C) Oat2c, D) Oat2d, E) Oat2e. Nuclei are stained with DAPI (blue).

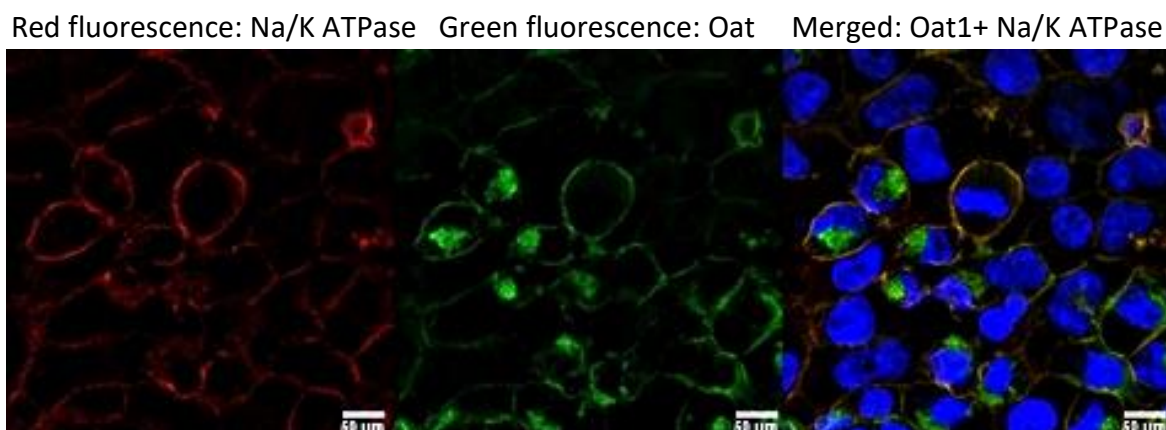


Figure 25. Immunolocalization of zebrafish Oat3 transporter by co-localization of the green colored Oat and the red colored Na/K ATPase. Signals of the two dyes were combined and subsequently produced an orange signal which confirmed the localization within the cell membrane. Nuclei are stained with DAPI (blue).

3.5. Functional characterization of zebrafish Oats

3.5.1. Fluorescent substrates

To identify suitable Oat1, Oat2a-e and Oat3 model substrates which could be used for functional characterization of zebrafish Oats, a range of commercially available anionic dyes from the group of fluoresceins was initially tested: fluorescein, 5- and 6-carboxyfluorescein (5-CF and 6-CF), 2',7'-dichlorofluorescein, 4',5'-dibromofluorescein; lucifer yellow (LY), resorufin, resazurin, calcein and eosin Y. Testing of anionic fluorescent dyes revealed two potential fluorescent substrates of the five studied Oats: Oat1, Oat2a, Oat2b, Oat2d and Oat3. However, Oat2c and Oat2e showed no transport activity with any of the fluorescent dyes tested.

LY was identified as fluorescent dye that showed high accumulation in Oat1 transfected HEK293T cells, thus revealing the interaction with Oat1 as a potential substrate. Time and dose response assays confirmed that LY is indeed an Oat1 substrate, and its transport

followed the classical Michaelis-Menten kinetics. The determined kinetic parameters of the LY transport in transfected cells resulted in V_{max} value of 5.77 nmol/mg protein/min and K_m of 11.4 μM (Fig. 26).

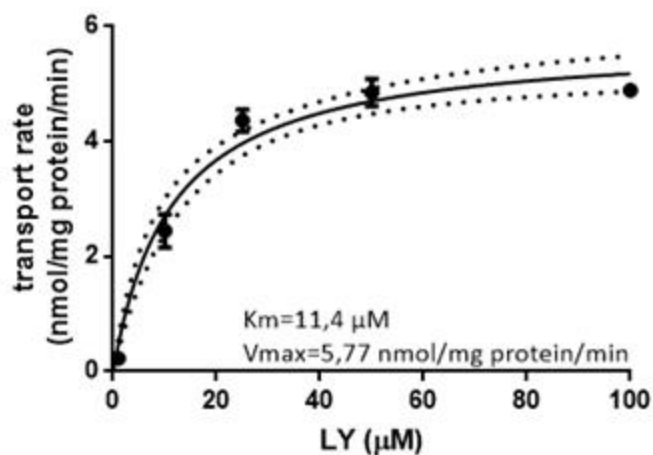


Figure 26. Dose-response of zebrafish Oat1 transport of the fluorescent model substrate LY ($K_m = 11.4 \mu\text{M}$) expressed as transport rate (nmol/mg protein/min) over LY concentration (μM) after 10 min incubation with LY. Each data point represents the mean \pm SE from triplicate determinations. Dotted lines represent confidence intervals.

LY also showed high accumulation in Oat2a transfected HEK293 cells. Time and dose response assays confirmed LY as an Oat2a substrate, and its transport followed the classical Michaelis-Menten kinetics. The determined kinetic parameters of the LY transport in transfected cells resulted in V_{max} value of 2.21 nmol/mg protein/min and K_m of 122 μM (Fig. 27).

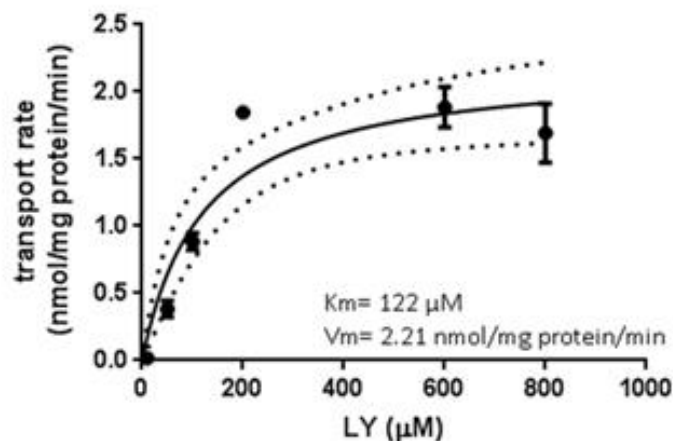


Figure 27. Dose-response of zebrafish Oat2a transport of the fluorescent model substrate LY ($K_m = 122 \mu\text{M}$) expressed as transport rate (nmol/mg protein/min) over LY concentration (μM) after 15 min incubation with LY. Each data point represents the mean \pm SE from triplicate determinations. Dotted lines represent confidence intervals.

Fluorescent dye that showed to be a potent zebrafish Oat2b substrate was 6-CF, resulting in the determined V_{max} value of 32.24 nmol/mg protein/min and K_m of 199.7 μM (Fig. 28).

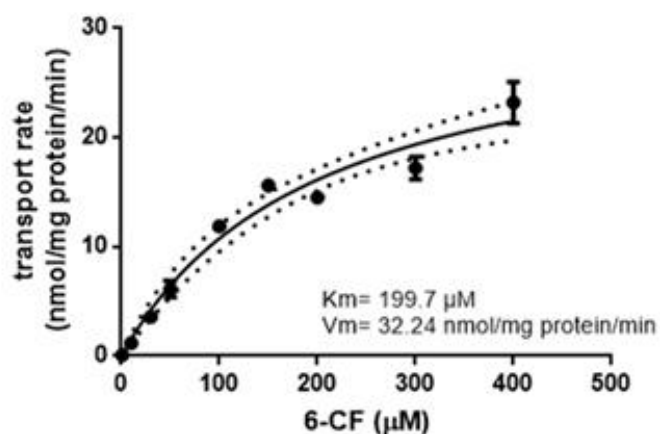


Figure 28. Dose-response curve of the Oat2b mediated transport of fluorescent substrate 6-CF ($K_m = 199.7 \mu\text{M}$) expressed as transport rate (nmol/mg protein/min) over 6-CF concentration (μM) after 15 min incubation with 6-CF. Each data point represents the mean \pm SE from triplicate determinations. Dotted lines represent confidence intervals.

Oat2d showed interaction with two fluorescent dyes – LY ($V_{max} = 36.31$ nmol/mg protein/min, $K_m = 49.68$ μM) and 6-CF ($V_{max} = 29.65$ nmol/mg protein/min, $K_m = 266.9$ μM) – with better affinity for LY where Michaelis Menten constant of 49.68 μM was actually the lowest of all tested fluorescent dyes with zebrafish Oat2a, b, and d (Fig. 29).

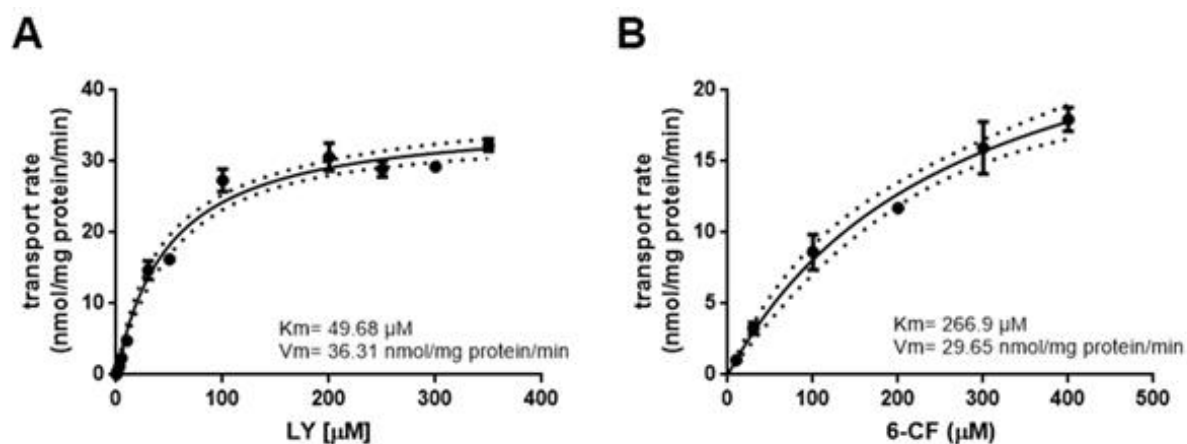


Figure 29. Dose-response curve of Oat2d mediated transport of model fluorescent substrates: A) LY ($K_m = 49.68$ μM) expressed as transport rate (nmol/mg protein/min) over LY concentration (μM) after 15 min incubation with LY; and B) 6-carboxyfluorescein ($K_m = 266.9$ μM) expressed as transport rate (nmol/mg protein/min) over 6-CF concentration (μM) after 15 min incubation with 6-CF. Each data point represents the mean \pm SE from triplicate determinations. Dotted lines represent confidence intervals.

6-CF was also identified as an Oat3 substrate, whose Michaelis Menten constant was 5.8 μM and maximum transport rate was 8.33 nmol/mg protein/min (Fig. 30).

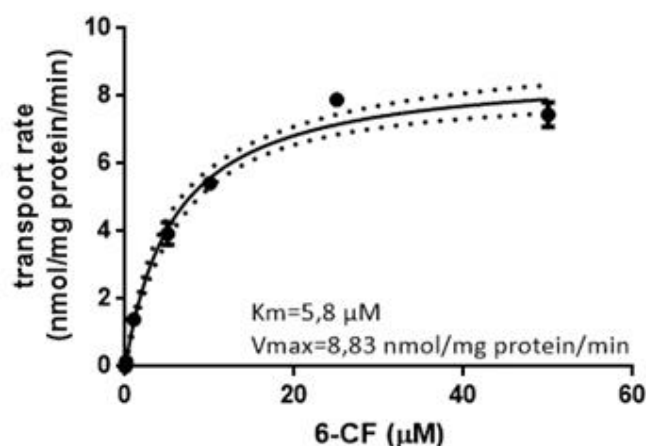


Figure 30. Dose-response of zebrafish Oat3 transport of the fluorescent model substrate 6-CF ($K_m = 5.8 \mu\text{M}$) expressed as transport rate (nmol/mg protein/min) over 6-CF concentration (μM) after 10 min incubation with LY. Each data point represents the mean \pm SE from triplicate determinations. Dotted lines represent confidence intervals.

3.5.2. Inhibition tests

3.5.2.1. The interaction screen assay

Following optimization of the transport activity assays, a series of known interactors of mammalian OATs/Oats was tested, including potential physiological interactors (cGMP, Krebs' cycle intermediates: α -KG, succinate, fumarate; creatinine and PGE2), and xenobiotic substrates (mostly pharmaceutical compounds known to be interactors of mammalian OATs/Oats, e.g., diclofenac, erythromycin and indomethacin). It is important to note that this type of transport assay does not distinguish between an interactor that is transported by the protein and one that is a non-competitive inhibitor. It reveals, however, whether a compound interferes (or not) with transport of the model fluorescence substrate.

Among the tested anionic dyes, LY was selected for further Oat1, Oat2a and Oat2d functional analysis, due to the high to very high affinity of these three Oats toward LY. For Oat2b and Oat3 functional analysis, 6-CF was used as the only anionic dye transported by Oat2b and Oat3.

As shown in Fig. 31, the most potent endogenous interactors of Oat2a were glutamate (29% LY uptake), PGE2 (44.43% LY uptake), cGMP (45.02% LY uptake), testosterone (51.47 % LY

uptake), E3S (54.16% LY uptake) and deoxycholic acid (58.19% LY uptake). Apart from endogenous interactors, the initial screening revealed numerous xenobiotic interactors. The highest inhibition (0 % LY uptake) was observed for MK571, an established cysteinyl leukotriene-based inhibitor of multidrug resistance protein (MRP; Henjakovic et al., 2015). Other potent xenobiotics identified were diclofenac, indomethacin and erythromycin, which reduced LY uptake up to 18.23, 23.39 and 48.94%, respectively.

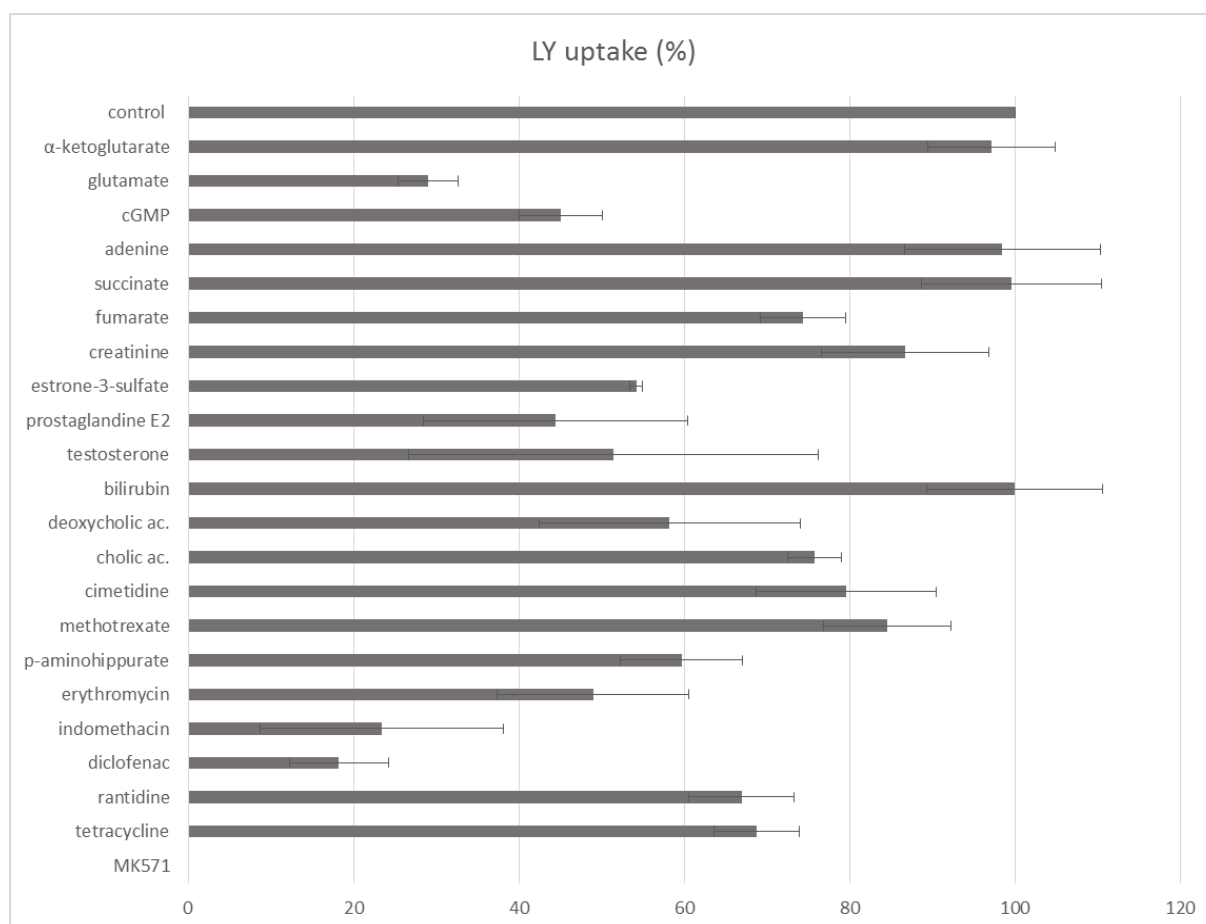


Figure 31. Interaction of zebrafish Oat2a with known substrates and inhibitors of mammalian OAT2/Oat2 subfamily members. Data are expressed as mean percentage (%) \pm SD from triplicate determinations of LY uptake after co-incubation with each interactor (100 μ M) relative to LY uptake in the absence of interactor which is set to 100%.

The most potent endogenous interactors of Oat2b were PGE2 (3.38% 6-CF uptake), E3S (24.95% 6-CF uptake), adenine (36.46% 6-CF uptake), testosterone (41.04% 6-CF uptake) and cGMP (41.55% 6-CF uptake). Xenobiotics that showed the highest inhibition rate were

diclofenac, indomethacin, tetracycline and erythromycin, which reduced LY uptake up to 7.52, 17.15, 30.45 and 41.71%, respectively (Fig. 32).

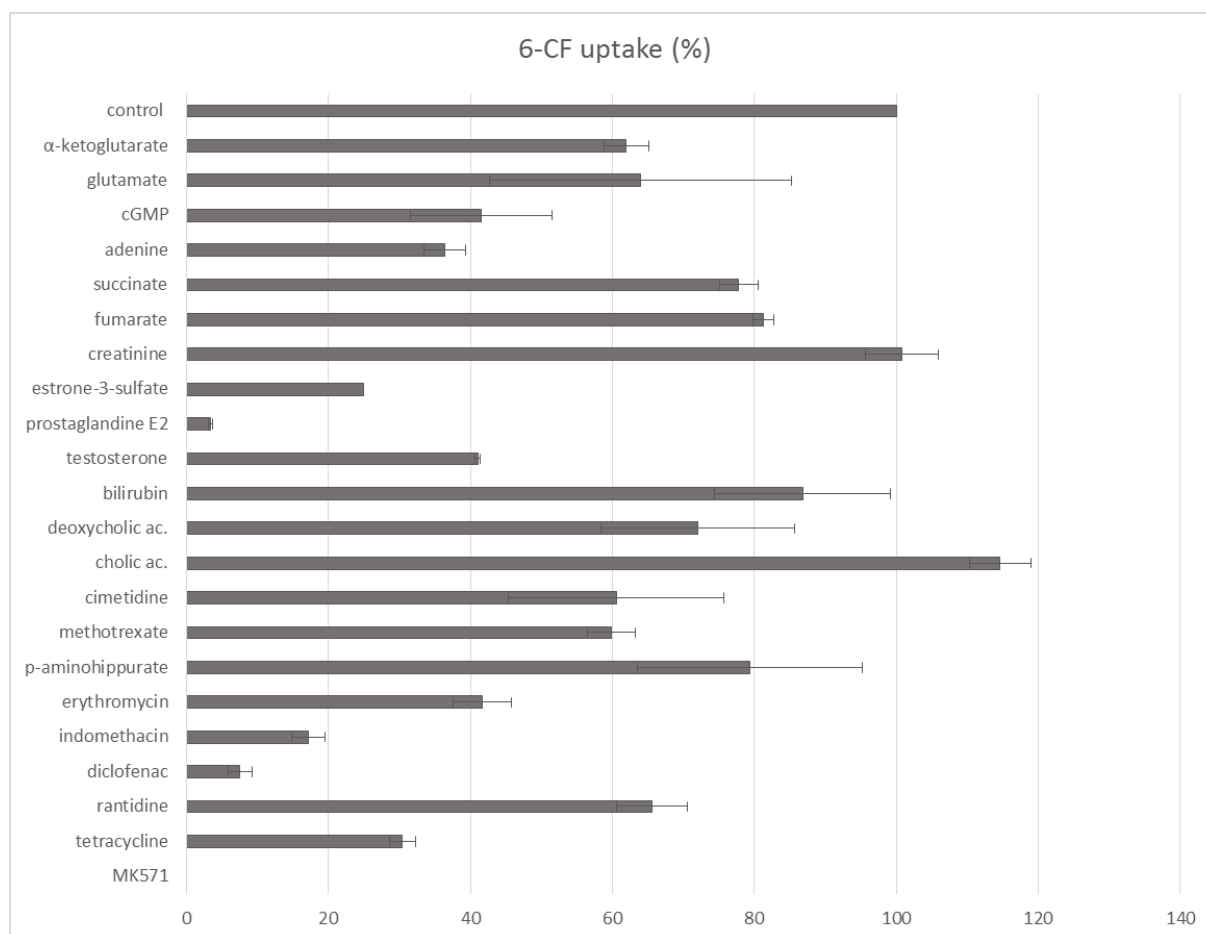


Figure 32. Interaction of zebrafish Oat2b with known substrates and inhibitors of mammalian OAT2/Oat2 subfamily members. Data are expressed as mean percentage (%) \pm SD from triplicate determinations of 6-CF uptake after co-incubation with each interactor (100 μ M) relative to 6-CF uptake in the absence of interactor which is set to 100%.

Oat2d has also shown interaction with numerous endo- and xenobiotics. Endogenous compounds that showed the highest inhibition rate were α -KG (21.20% LY uptake), deoxycholic acid (29.04% LY uptake) and bilirubin (48.81% LY uptake). Xenobiotic that has shown the highest inhibition of Oat2d transport (0% LY uptake) was MK571, followed by tetracycline (10.90% LY uptake), diclofenac (33.34 % LY uptake), PAH (35.78% LY uptake) and indomethacin (43.07% LY uptake) (Fig. 33).

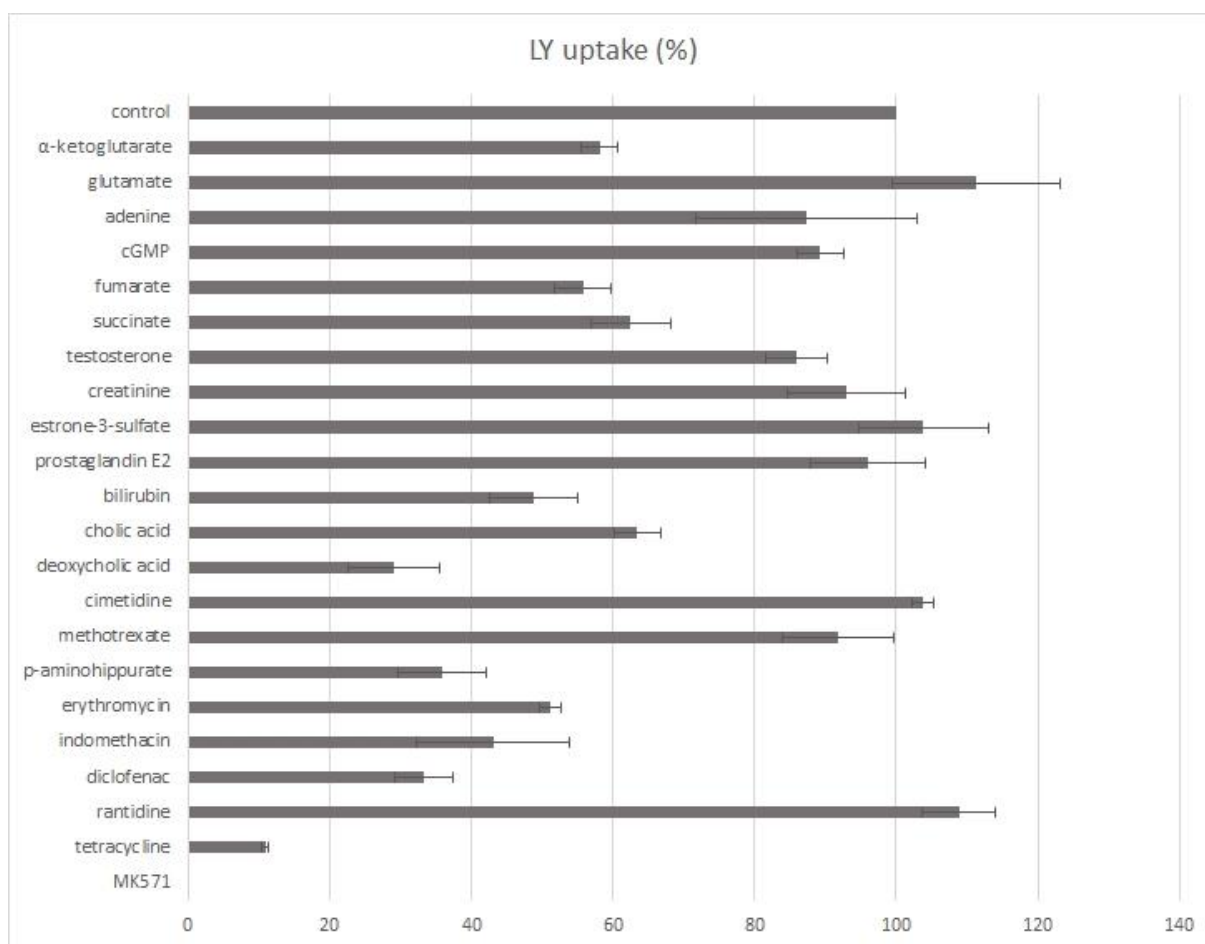


Figure 33. Interaction of zebrafish Oat2d with known substrates and inhibitors of mammalian OAT2/Oat2 subfamily members. Data are expressed as mean percentage (%) \pm SD from triplicate determinations of LY uptake after co-incubation with each interactor (100 μ M) relative to LY uptake in the absence of interactor which is set to 100%.

Oat1 and Oat3 also showed interaction with a wide range of physiological (Fig. 34) and xenobiotic (Fig. 35) compounds, with high level of overlapping interactors. The most potent endogenous interactors of Oat1 were: bilirubin (0.81% LY uptake), deoxycholic acid (1.71% LY uptake), progesterone (2.92% LY uptake), pregnenolone sulfate (9.89% LY uptake), E3S (11.37% LY uptake), β -estradiol 17-(β -D-glucuronide) (19.02% LY uptake), corticosterone (29.32% LY uptake) and α -KG (29.77% LY uptake).

Physiological compounds that showed the strongest interaction with Oat3 were: bilirubin (0.34% 6-CF uptake), deoxycholic acid (1.31% 6-CF uptake), DHEAS (1.62% 6-CF uptake), pregnenolone sulfate (1.89% 6-CF uptake), androstenedione (4.87% 6-CF uptake),

progesterone (5.05% 6-CF uptake), testosterone (5.63% 6-CF uptake), E3S (5.86% 6-CF uptake), β -estradiol 17-(β -D-glucuronide) (9.2% 6-CF uptake), 17α -ethynylestradiol (10.83% 6-CF uptake), dihydrotestosterone (DHT) (11.59% 6-CF uptake), corticosterone (18.98% 6-CF uptake), ethynyltestosterone (19.45% 6-CF uptake) and estrone (26.12% 6-CF uptake).

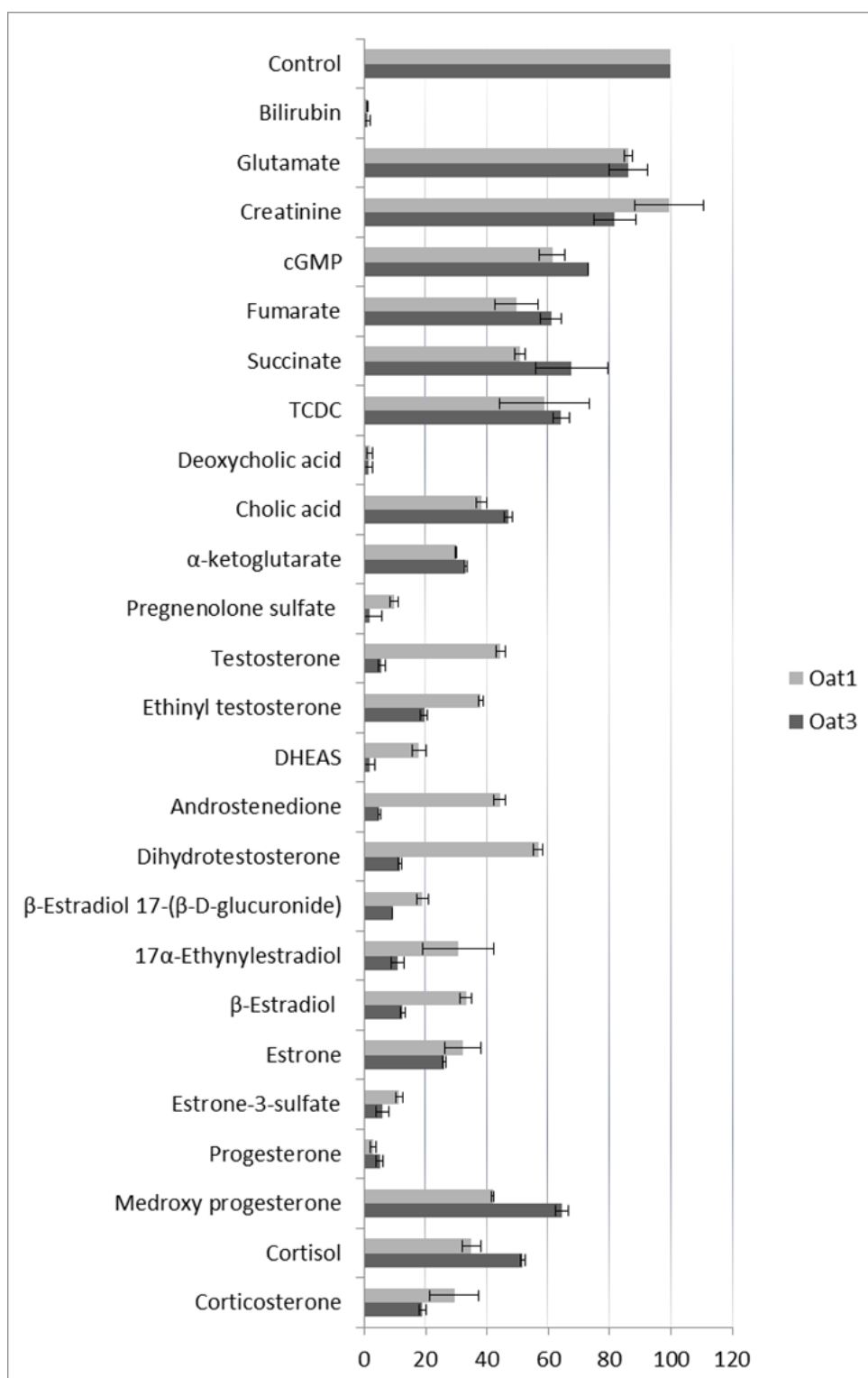


Figure 34. Interaction of zebrafish Oat1 and Oat3 with physiological compounds that are known substrates or inhibitors of mammalian OAT1/Oat1 and OAT3/Oat3 subfamily members. Data are expressed as mean percentage (%) \pm SD from triplicate determinations of LY or 6-CF uptake after co-incubation with each interactor (100 μ M) relative to LY/6-CF uptake in the absence of interactor which is set to 100%.

Xenobiotics that showed the strongest interaction with Oat1 were: indomethacin (0.23% LY uptake), furosemide (2.32% LY uptake), tributyltin (TBT) (5.7% LY uptake), ibuprofen (6.57% LY uptake), methotrexate (15.2% LY uptake), perfluorooctanoic acid (PFOA) (16.63% LY uptake), perfluorooctanesulfonic acid (PFOS) (16.63% LY uptake) and tripropyltin (TPrT) (19.73% LY uptake) (Fig. 34).

The most potent Oat3 interactors from the group of xenobiotics were: indomethacin (3.22% 6-CF uptake), TBT (4.36% 6-CF uptake), tripropyltin (TPrT) (4.92% 6-CF uptake), trimethyltin (TMT) (5.44% 6-CF uptake), MTX (5.65% 6-CF uptake), triethyltin (TET) (7.56% 6-CF uptake), ibuprofen (10.6% 6-CF uptake), PFOA (15.4% 6-CF uptake), triphenyltin (TpheT) (15.94% 6-CF uptake), furosemide (26.37% 6-CF uptake), PFOS (28.84% 6-CF uptake) and PAH (29.07% 6-CF uptake).

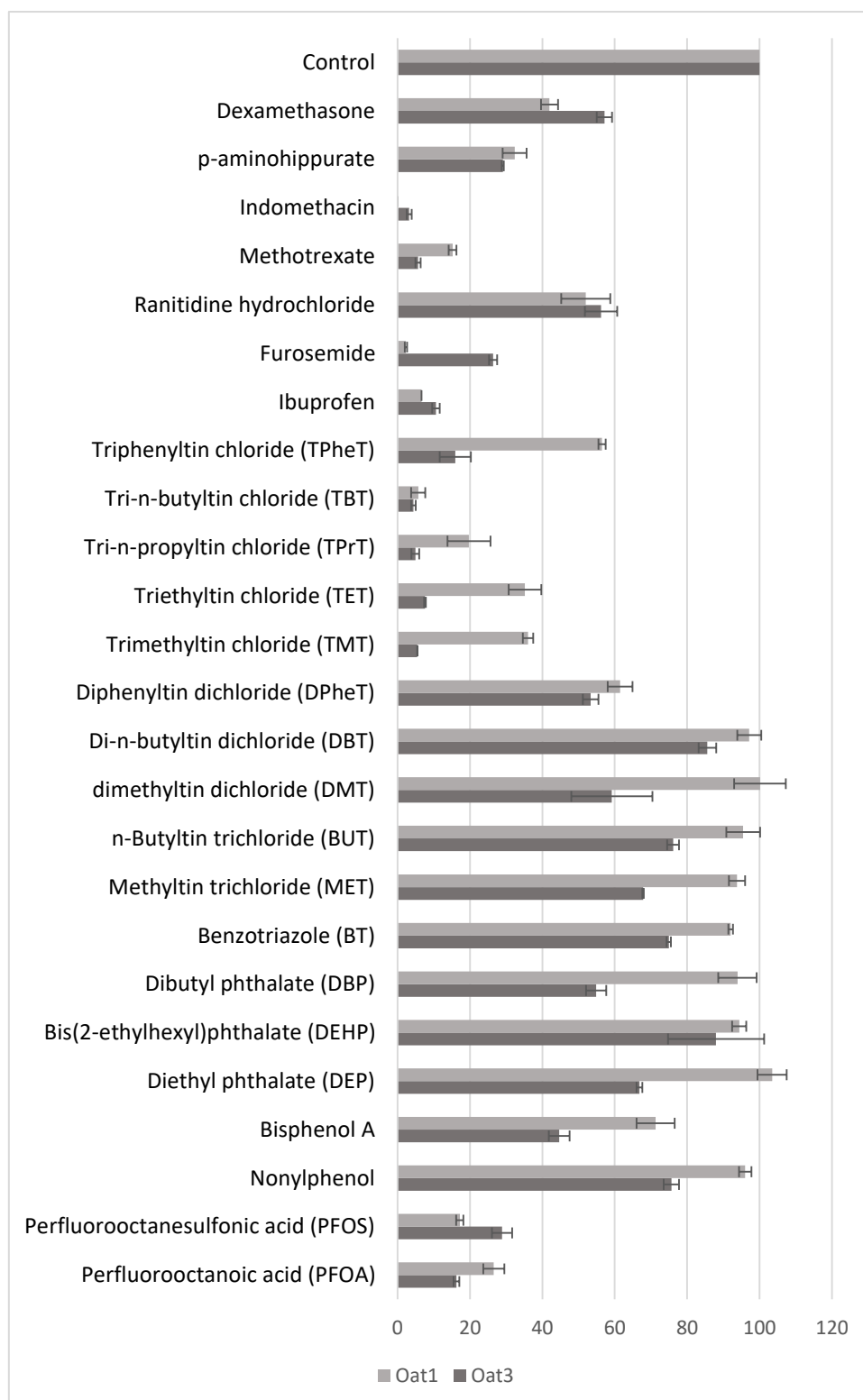


Figure 35. Interaction of zebrafish Oat1 and Oat3 with xenobiotic compounds that are known interactors of mammalian OAT1/Oat1 and OAT3/Oat3 subfamily members. Data are expressed as mean percentage (%) \pm SD from triplicate determinations of LY or 6-CF uptake after co-incubation with each interactor (100 μ M) relative to LY/6-CF uptake in the absence of interactor which is set to 100%.

3.5.2.2. Dose-response assays

After screening the described series of endogenous and xenobiotic compounds, the most potent interactors were selected for detailed dose-response analyses and determination of IC₅₀ values for each of the five functional Oats (Oat1, Oat2a, Oat2b, Oat2d and Oat3).

Among physiological compounds, Oat1 showed the strongest interaction with bilirubin (IC₅₀ = 1.08 μ M), pregnenolone sulfate (IC₅₀ = 7.05 μ M), α -KG (IC₅₀ = 24.61 μ M) and corticosterone (IC₅₀ = 64.90 μ M) (Fig. 36). Dose-response curves of other strong physiological interactors can be found in supplemental data (Fig. S2).

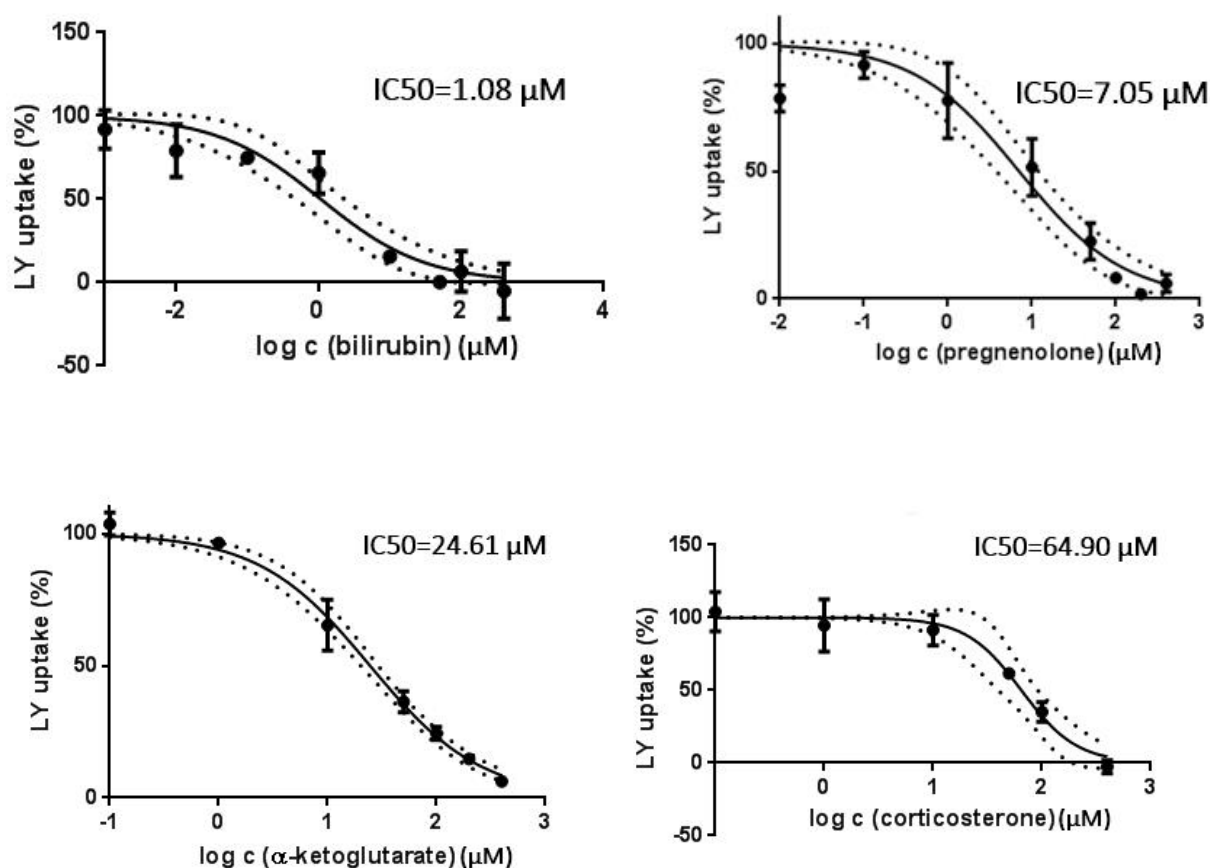


Figure 36. Concentration dependent inhibition of Oat1 mediated LY uptake by bilirubin, pregnenolone sulfate, α -KG and corticosterone. Values on X-axis were transformed to logarithmic scale ($\log X$). Each data point represents the mean \pm SD from triplicate determinations. Dotted lines represent confidence intervals.

Among xenobiotic compounds, Oat1 showed strongest interaction with ibuprofen and indomethacin, which showed concentration dependent inhibition of Oat1 mediated LY transport ($IC_{50} = 1 \mu\text{M}$ and $0.05 \mu\text{M}$, respectively) (Fig. 37). Dose-response curves of other strong xenobiotic interactors can be found in supplemental data (Fig. S3).

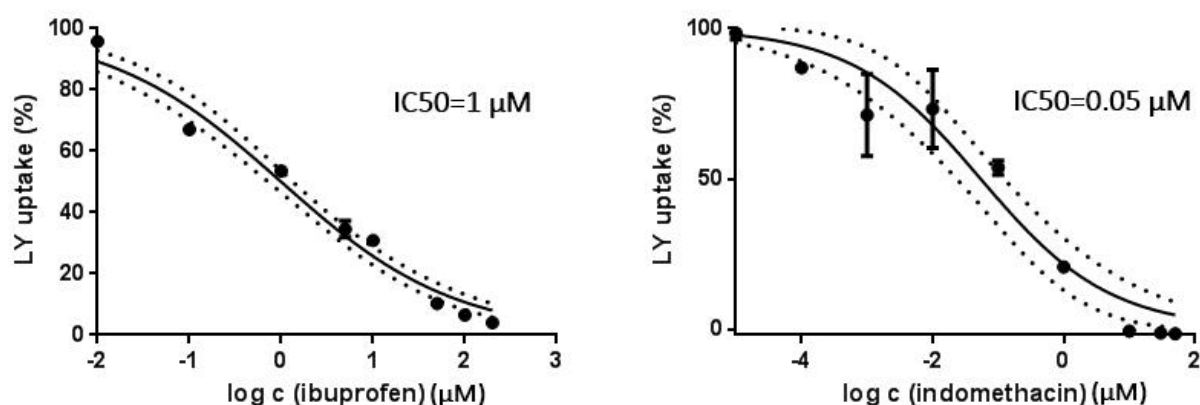


Figure 37. Concentration dependent inhibition of Oat1 mediated LY uptake by ibuprofen and indomethacin. Values on X-axis were transformed to logarithmic scale ($\log X$). Each data point represents the mean \pm SD from triplicate determinations. Dotted lines represent confidence intervals.

cGMP and diclofenac both showed concentration dependent inhibition of Oat2a mediated LY transport ($IC_{50} = 27.74 \mu\text{M}$ and $19.14 \mu\text{M}$, respectively) (Fig. 38).

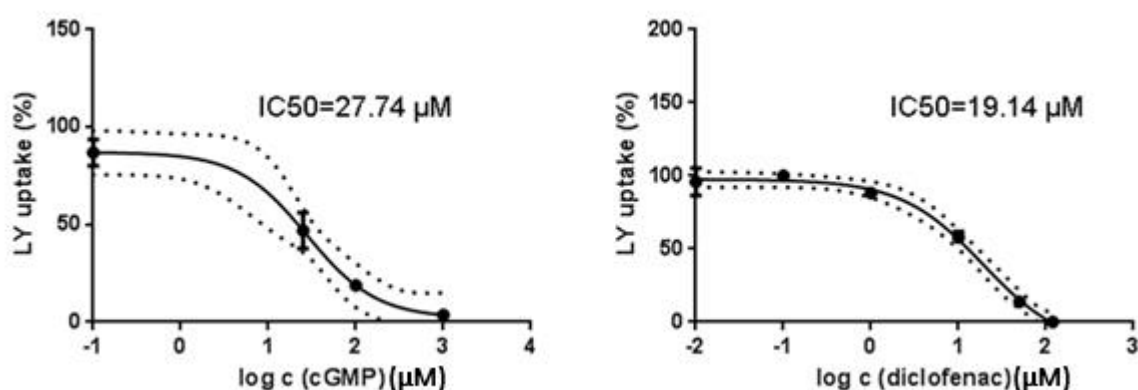


Figure 38. Concentration dependent inhibition of Oat2a mediated LY uptake by cGMP and diclofenac. Values on X-axis were transformed to logarithmic scale ($\log X$). Each data point

represents the mean \pm SD from triplicate determinations. Dotted lines represent confidence intervals.

Two of the most potent Oat2b interactors, E3S and diclofenac, clearly showed dose dependent inhibition of Oat2b mediated 6-CF uptake ($IC_{50} = 30.96 \mu\text{M}$ and $12.6 \mu\text{M}$, respectively) (Fig. 39).

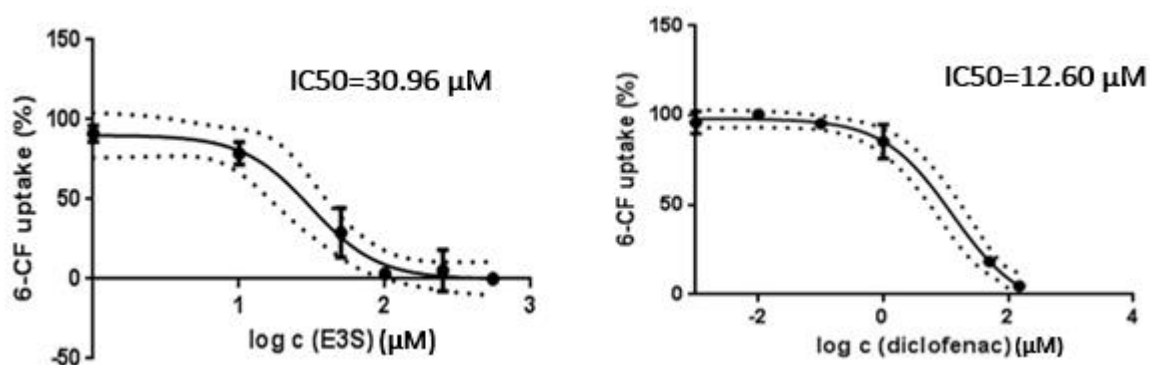


Figure 39. Concentration dependent inhibition of Oat2b mediated 6-CF uptake by E3S and diclofenac. Values on X-axis were transformed to logarithmic scale ($\log X$). Each data point represents the mean \pm SD from triplicate determinations. Dotted lines represent confidence intervals.

Finally, both of the most potent tested Oat2d interactors, fumarate and indomethacin, showed inhibition of Oat2d mediated LY uptake ($IC_{50} = 68.24 \mu\text{M}$ and $20.41 \mu\text{M}$, respectively) (Fig. 40).

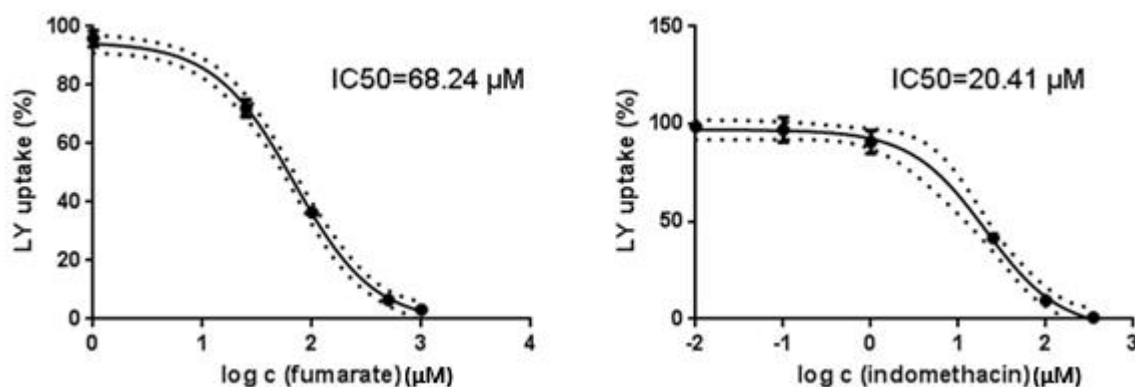


Figure 40. Concentration dependent inhibition of Oat2d mediated LY uptake by fumarate

and indomethacin. Values on X-axis were transformed to logarithmic scale ($\log X$). Each data point represents the mean \pm SD from triplicate determinations. Dotted lines represent confidence intervals.

Among physiological compounds, Oat3 showed the strongest interaction with DHEAS ($IC_{50} = 0.90 \mu M$), β -estradiol 17-(β -D-glucuronide) ($IC_{50} = 6.31 \mu M$), ethynyltestosterone ($IC_{50} = 5.38 \mu M$), and pregnenolone sulfate ($IC_{50} = 6.80 \mu M$) (Fig. 41). Dose-response curves of other strong physiological interactors can be found in supplemental data (Fig. S4).

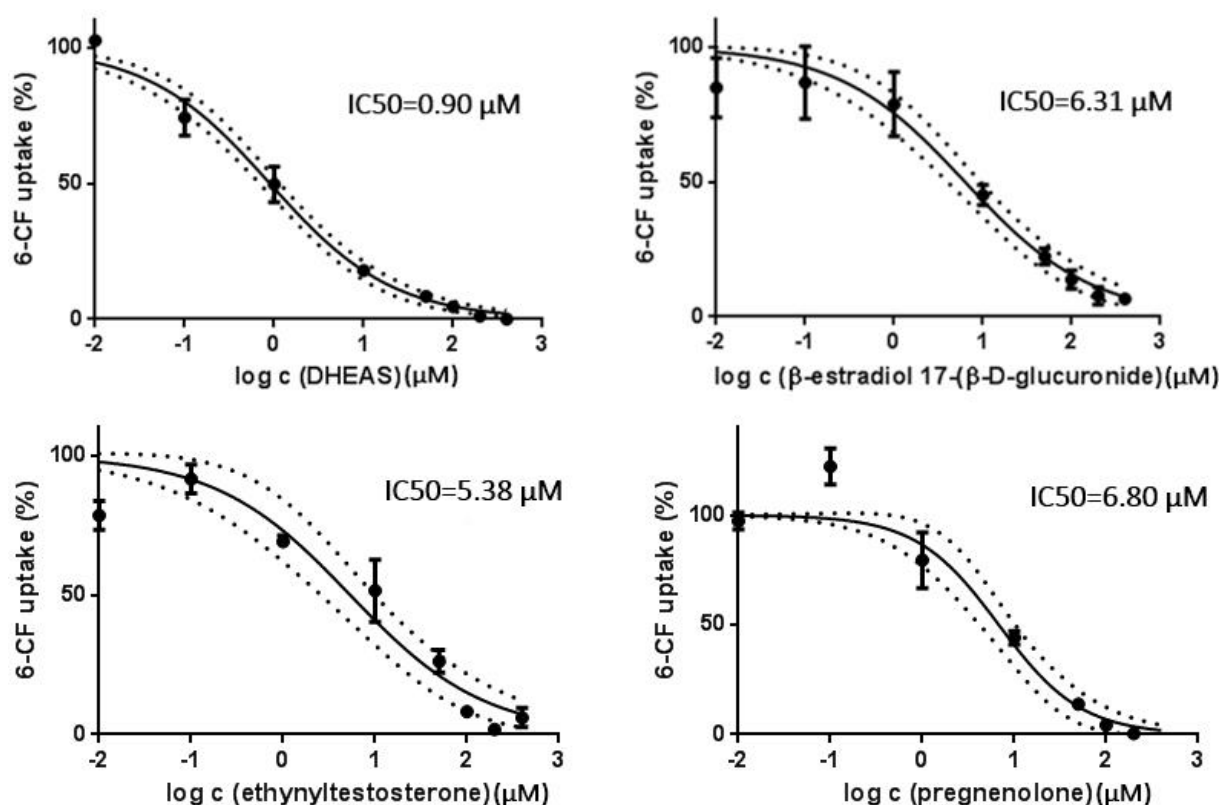


Figure 41. Concentration dependent inhibition of Oat3 mediated 6-CF uptake by DHEAS, β -estradiol 17-(β -D-glucuronide), ethynyltestosterone and indomethacin. Values on X-axis were transformed to logarithmic scale ($\log X$). Each data point represents the mean \pm SD from triplicate determinations. Dotted lines represent confidence intervals.

Among xenobiotic compounds, Oat3 showed the strongest dose-response with ibuprofen, indomethacin, MTX and TPRT ($IC_{50} = 5.98 \mu M$, $0.03 \mu M$, $9.92 \mu M$ and $0.05 \mu M$, respectively) (Fig. 42). Dose-response curves of other strong xenobiotic interactors can be found in supplemental data (Fig. S5).

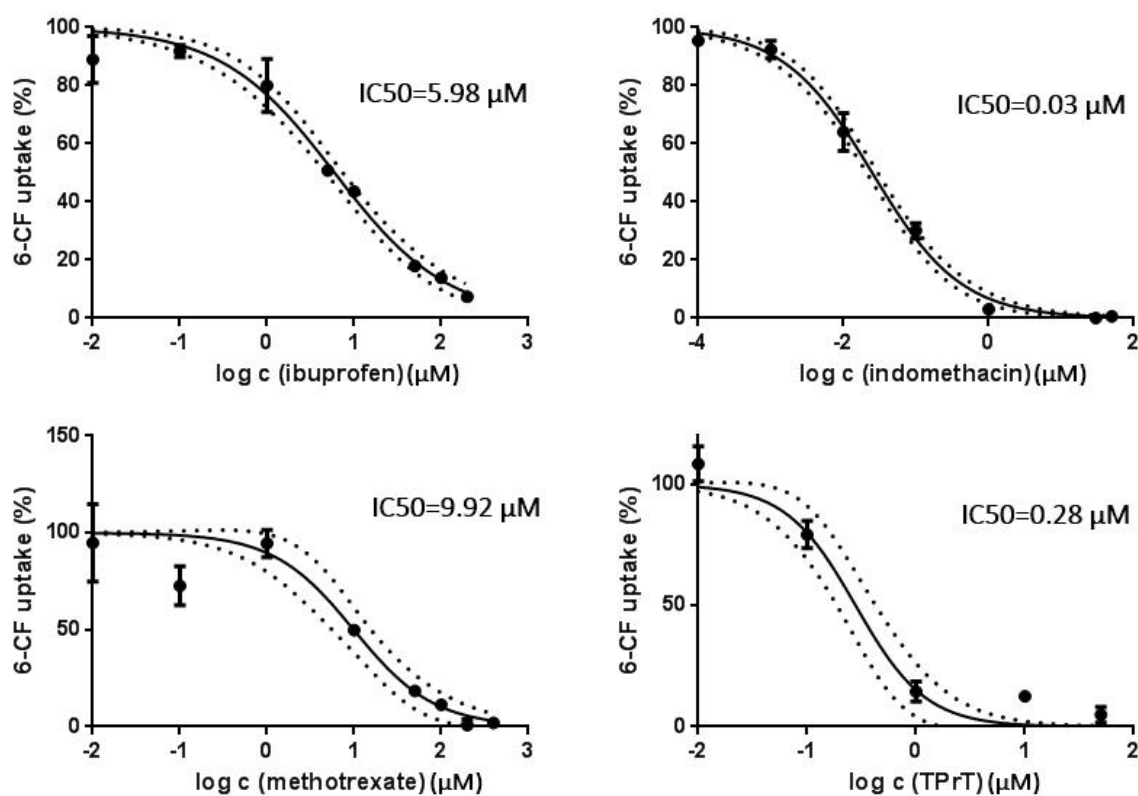


Figure 42. Concentration dependent inhibition of Oat3 mediated 6-CF uptake by ibuprofen, indomethacin, MTX and TPRT. Values on X-axis were transformed to logarithmic scale ($\log X$). Each data point represents the mean \pm SD from triplicate determinations. Dotted lines represent confidence intervals.

3.5.3. Determining the type of interaction

After determination of the IC₅₀ values, the type of interaction for the strongest physiological and xenobiotic compounds with Oat1 and Oat3 was determined (Table 3.1 and 3.2). It was done by comparing kinetic parameters of LY or 6-CF uptake in the presence and in the absence of different interacting compounds, where their concentrations were equal to their previously calculated IC₅₀ values. Namely, if an interacting compound is a competitive inhibitor (i.e. substrate) of uptake of fluorescent model substrate, it will cause an increase in K_m of the enzyme, but leave V_{max} unaffected. In that case it is correct to assume that it is being transported by Oat, in which case the IC₅₀ value of the interacting compound will actually represent its K_m value. However, if a compound is a noncompetitive inhibitor, its presence will decrease V_{max} and will not affect K_m. Noncompetitive inhibitors have a separate binding site on the enzyme and can bind the enzyme-substrate complex. However, they can also bind the enzyme when substrate is not bound. Finally, third type of interaction is an uncompetitive inhibition, where both V_{max} and K_m are decreased. Uncompetitive inhibitors are similar to noncompetitive inhibitors, as they have a separate binding site on the enzyme, but they only bind to the enzyme when substrate is bound to the enzyme.

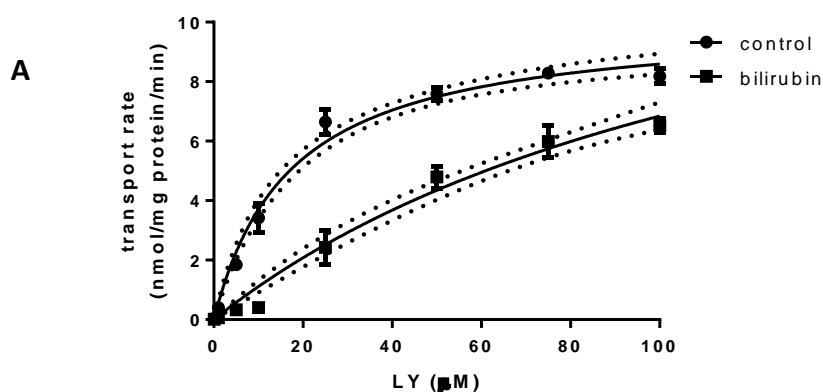
Table 3.1. Determination of type of interaction for set of zebrafish Oat1 interactors. Kinetic parameters of 6-CF uptake are given as K_m (μM), V_{max} (nmol LY/mg protein/min), and 95% confidence intervals (c.i.) for each. The mark “S” denotes Oat1 substrates, and the “I” denotes inhibitors. Data are mean ± SD from triplicate determinations.

Interactor	K_m (LY)	c.i.	V_{max} (LY)	c.i.	type of interaction
Control (LY)	17,2	13.48 - 20.92	10,07	9.42 - 10.72	
bilirubin	134.50	51.95 - 217.0	16.05	9.65 - 22.44	S
deoxycholic acid	28.26	19.22 - 37.29	7.26	6.43 - 8.09	M
α-ketoglutarate	44.37	27.91 - 60.83	10.56	8.87 - 12.25	S
pregnenolone	130.80	83.52 - 178.1	14.94	10.46 - 18.41	S
estrone-3-sulfate	24.53	18.29 - 30.76	10.72	9.79 - 11.64	S
corticosterone	35.51	26.23 - 44.78	10.36	9.29 - 11.42	S
PFOA	36.44	29.20 – 43.67	11.69	10.67 - 12.51	S
indomethacin	25.09	20.82 - 30.97	10.25	9.55 - 10.94	S
methotrexate	29.89	16.62 - 43.17	11.31	9.39 – 13.24	S
ibuprofen	14.66	11.90 - 17.41	9.21	8,64 - 9,37	I

Table 3.2. Determination of type of interaction for set of zebrafish Oat3 interactors. Kinetic parameters of 6-CF uptake are given as K_m (μM), V_{max} (nmol 6-CF/mg protein/min), and 95% confidence intervals (c.i.) for each. The mark “S” denotes Oat3 substrates, and the “I” denotes inhibitors. Data are mean \pm SD from triplicate determinations.

Interactor	K_m (6-CF)	c.i.	V_{max} (6-CF)	c.i.	type of interaction
Control (6-CF)	18.65	12.56-24.74	22.53	19.26 - 25.79	
bilirubin	32.49	25.67 – 39.31	29.9	26.53 - 33.27	S
deoxycholic acid	42.55	31.05 - 54.05	17,20	14.48 - 19.92	S
pregnenolone sulfate	14.39	11.9 - 16.87	18.37	17.08 - 19.65	I
testosterone	7.04	3.59 - 10.49	9.21	7.84 - 10.58	I
DHEAS	7.74	5.33 - 10.16	4.58	4.13 - 5.03	I
progesterone	12.70	8.99 – 16.4	11.54	7.04 - 16.04	I
indomethacin	28.04	25.74 – 30.34	22.56	18.76 - 26.36	S
methotrexate	64.38	50.40 - 78.36	24.45	20.95 - 27.95	S
ibuprofen	18.33	14.64 - 22.02	19.10	17.40 - 20.79	I
trimethyltin	12.21	1.84 - 22.57	14.94	10.67 - 19.24	I
tripropyltin	38.56	26.26 - 50.86	10.93	1.33 - 20.53	S

Example of dose-response curves used to determine type of interaction with Oats are shown in Figure 43 (A, B, C). Aside from competitive and noncompetitive inhibition (S and I), mixed type of inhibition was also observed for Oat1 and deoxycholic acid, which resulted in changes in both K_m and V_m values of the LY kinetics (Fig. 43, C).



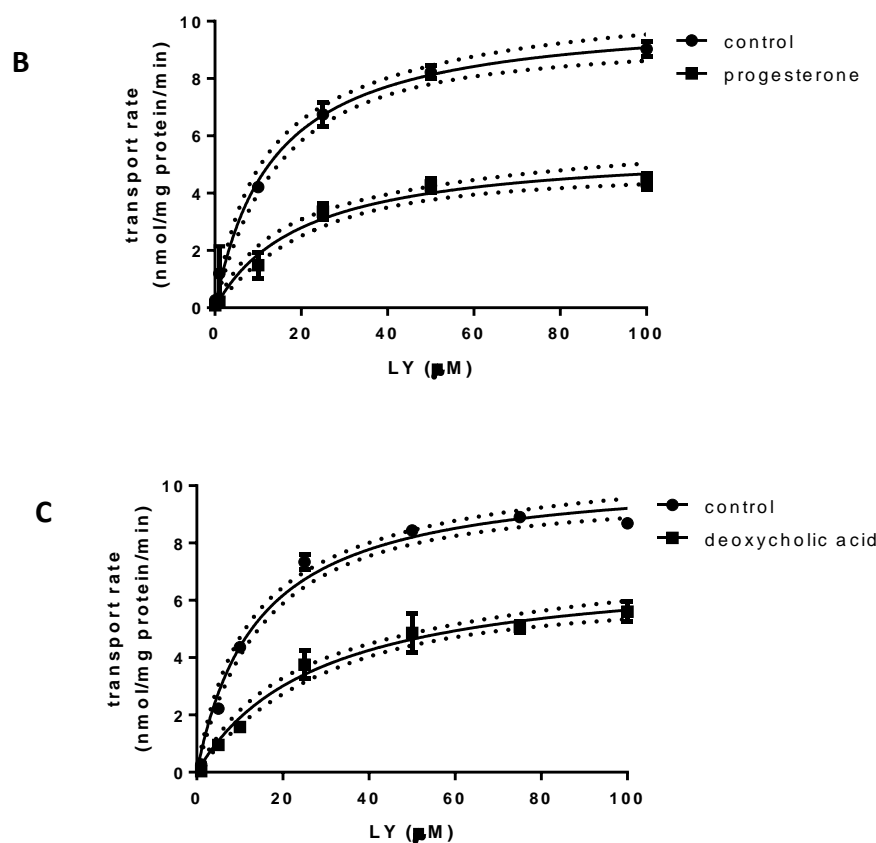


Figure 43. Example of dose-response curves used to determine type of interaction with Oat1. A) bilirubin as competitive inhibitor, B) progesterone as noncompetitive inhibitor, C) deoxycholic acid showing mixed type of inhibition.

3.6. Creating gene knockouts using CRISPR/Cas9 system

As Oatp1d1 is the best characterized transporter of organic anions in zebrafish *in vitro*, and it has the highest expression in zebrafish tissues (especially in the liver), we proceeded to its characterization *in vivo* by creating zebrafish knockouts for the purpose of verification of Oatp1d1 function in living organism. For the purpose of generating the *Oatp1d1* knockout zebrafish we used pT7-gRNA vector with annealed oligos (Table 3.3). 48 hours after microinjection, we collected 15 of the injected embryos (F0) and 5 wild type embryos (WT) and performed genotyping using the HRM analysis. Primers used for genotyping are listed in the Table 3.3.

Table 3.3. Oligos and primers used for creating *Oatp1d1* zebrafish gene knockouts

Gene	Target sequence	Start (cDNA)	Ordered oligos	Forward Genotyping primer	Reverse Genotyping primer
Oatp1d1	GGGAGGTCTGGCAGCCAGCG	1200	taGGGAGGTCTGGC AGCCAGCG	AGACGGAAAC GCTCATCTCT	CAACACAATTG GTTTGAGGTCT
			aaacCGCTGGCTGCC AGACCTC		

Genotyping using HRM analysis software (Fig. 44) has revealed the mutation efficiency of 40%.

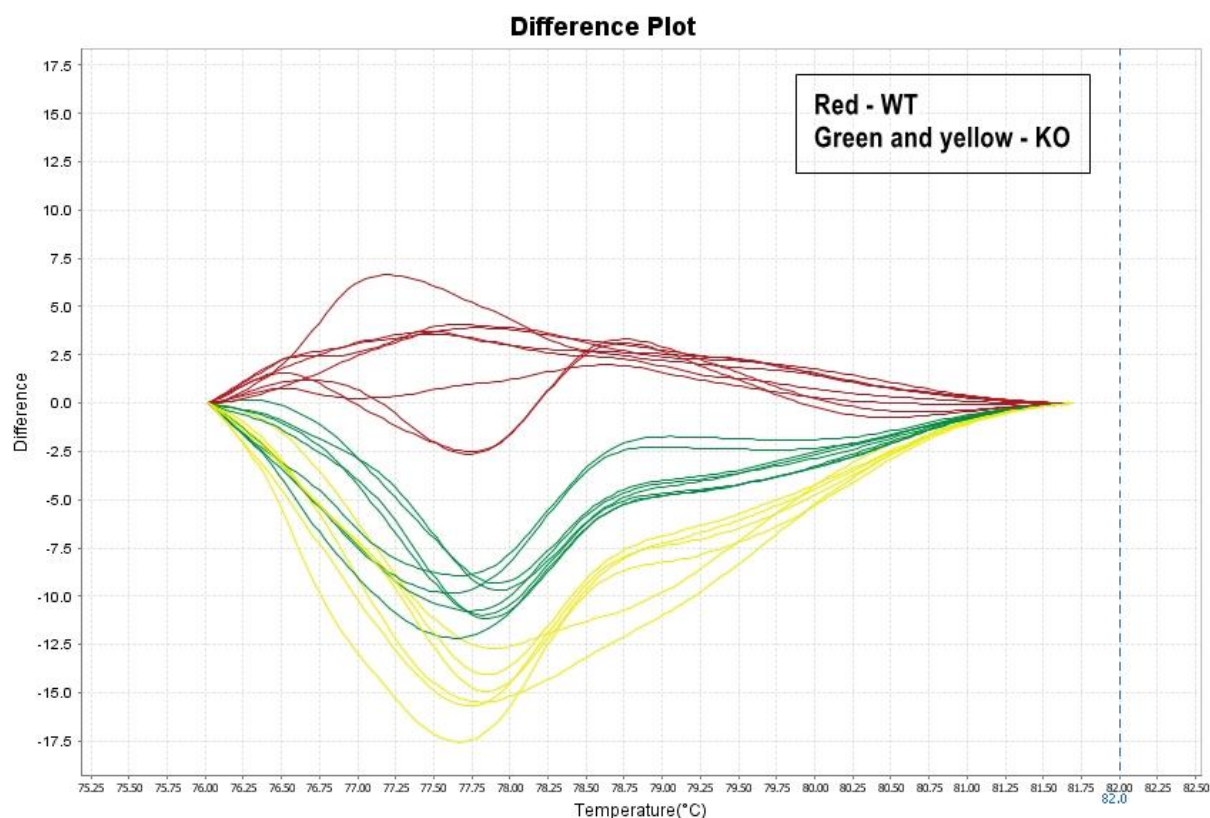


Figure 44. High resolution melting curve of *Oatp1d1* FO embryos generated using HRM software as described in Material and methods section. Red curves present WT embryos, while green and yellow curves indicate mutations (KO).

The remaining embryos were reared to reach sexual maturity, which usually takes about 5-6 months in standard conditions. Mature F0 males and females were then crossed with WT zebrafish of opposite gender in 1 individual F0 : 1 individual WT ratio to produce progeny and to screen the potential founders (males and females that carry the mutation). All the steps in creating Oatp1d1 gene knockouts are depicted in Fig. 45.

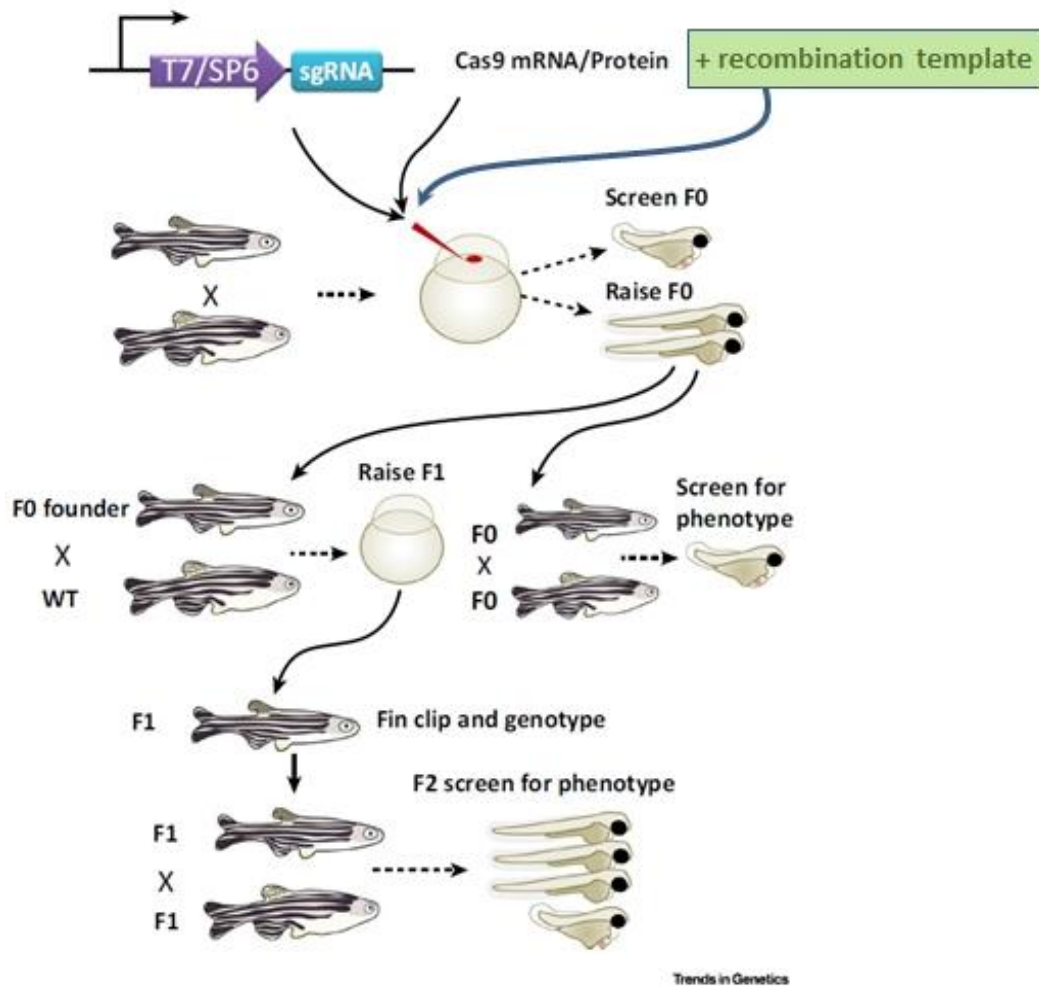


Figure 45. *In vivo* implementing the CRISPR/Cas9 gene editing approach.

After the identification of “founders”, they were crossed again with WT fish to produce first filial generation of offspring (F1). After the F1 generation reached sexual maturity, they were inter-crossed: one F1 male to one F1 female fish and their progeny presented the second filial generation of offspring (F2). F2 individuals will then be fin-clipped for genotyping and

homozygotes will be used for experiments that follow. In F2 generation we can expect the proportion of homozygotes from 25%-100%, depending on genotype of F1 parents. F2 homozygotes will be used for tracking eventual changes in phenotype, and ultimately for exposure experiments with model compounds for the purpose of *in vivo* verification of the function of the investigated proteins.

4. Discussion

Membrane transporters are one of the crucial determinants of absorption, distribution, metabolism and excretion (ADME) both of physiological compounds and xenobiotic substances (Klaassen and Lu, 2008). Despite being an integral element of the ADME processes, organic anion transporters have not been thoroughly investigated in non-mammalian species. Therefore, using the zebrafish model in this study we present the first detailed characterization of fish organic anion transporters. Our major goal was to obtain knowledge that can provide first insights into potential roles of Oats in relation to their physiological and/or defensive functions in zebrafish which could be further correlated with OAT/Oat functions recognized in higher vertebrates and human.

Zebrafish *Slc22* transporters share structural similarity with mammalian SLC22: they possess 12 α -helical TMDs, large extracellular LP1 and intracellular LP6, and intracellular orientation of C and N termini (Burckhardt and Wolff, 2000; Koepsell, 2011), indicating high degree of conservation of their secondary structure in vertebrates. Based on structural models of rat Oct1 and rabbit Oct2, developed using the structural template of LacY and GlpT, TMDs 1, 2, 4, 5, 7, 8, 10, and 11 form a large hydrophilic cleft for substrate binding (Zhou et al., 2006).

Through extensive genome search and phylogenetic analysis of *Slc22* genes, we recently identified seven organic anion transporters in zebrafish: Oat1, Oat2a, Oat2b, Oat2c, Oat2d, Oat2e and Oat3 (Mihaljevic et al., 2016). Phylogenetic tree (Fig. 15) clearly showed distinct clusters of three subfamilies: OAT1/Oat1, OAT2/Oat2 and OAT3/Oat3. *Oat1/oat1* and *Oat3/oat3* genes were present with only one gene (one-to-one orthology) in all analyzed vertebrate groups, including zebrafish, which indicates high degree of conservation of OAT1 and OAT3 function in the physiology of vertebrates. This is not surprising, considering crucial physiological role of these transporters in the uptake of endogenous compounds including medium chain fatty acids cAMP and cGMP, prostaglandins, urate and neurotransmitter metabolites (Rizwan and Burckhardt, 2007; Cropp et al., 2008; Nakakariya et al., 2009). However, *oat2* was present in more than one orthologs in most fish species analyzed and thus showed one-to-many orthology, meaning that one gene in one species is orthologous to multiple genes in another species, contrary to higher vertebrates where it was represented with one gene only. Occurrence of more than one *oat2* ortholog in fish is most likely a result of the whole genome duplication (WGD) event that occurred at the root of the teleost lineage and after the divergence of tetrapods.

oat2c and *oat2d* orthologs were found only in teleost fish and clustered closely together in phylogenetic tree. Since *oat2c* and *oat2d* are so closely related, and since they are both present in three teleost species (zebrafish, green spotted pufferfish and Japanese pufferfish), while in stickleback only *oat2c* was present, it can be suggested that *oat2d* probably originated by duplication of *oat2c*. *oat2e* was only present in zebrafish and medaka and it is likely also a product of duplication of *oat2c* or *oat2d*, with whom it shows the closest phylogenetic relationship. Since *oat2a* was positioned closest to human and mammalian *OAT2/Oat2* in the phylogenetic tree, they are probably direct orthologs, and all other *oat2* fish co-orthologs (*oat2b-e*) are presumably products of *oat2a* duplication. It is likely that *oat1* and *oat3* were also present in more copies after the WGD event, but their duplicates were eventually lost. The loss of one duplicate is the most common fate after WGD, with a probability of approximately 80%. After WGD, both duplicated gene copies initially encode proteins with identical sequences and expression patterns, but over time some gene pairs revert to single copy (loss of one of the duplicated copies). Other pairs either evolve new functions (neofunctionalization), including different tissue-specific expression domains, or share between the two duplicates the functions of the ancestral single copy gene (subfunctionalization), or both (Holtzman et al., 2016; Pasquier et al., 2017).

Conserved synteny analysis performed in this study confirmed multiple duplications of zebrafish *oat2* genes (Fig. 16). It showed double conserved synteny of five zebrafish *oat2* genes on chromosomes 11 (*oat2a*) and 17 (*oat2b-e*) with human *OAT2* on chromosome 6. Zebrafish has five *oat2* co-orthologs, while other fish species have less (green spotted pufferfish – 4, cave fish – 2, stickleback – 2, cod – 1 and medaka – 1). Zebrafish *oat2a* has direct orthology with green spotted pufferfish and cave fish *slc22a7a* genes. Therefore, gene environment of the fish *oat2* ortholog cluster is relatively conserved. Conserved synteny of zebrafish *oat1* and *oat3* (Fig. 17) revealed the location of both genes on the same zebrafish chromosome 21. Similar syntenic relationship is present in medaka (chromosome 14), tetraodon (chromosome 7), as well as in humans (chromosome 11).

Considering tissue expression pattern of zebrafish *Oat* transcripts, *Oat1* has shown the highest expression in testes of males and brain of female zebrafish (Fig. 18), while expression in kidney, where human and rodent *OAT1/Oat1* is highly expressed, was not obtained. However, expression in brain was also observed in human and rodents (Sekine et al, 1997).

Oat2a-e have shown expression in various zebrafish tissues, with the highest levels determined in testes, kidney and intestine (Fig. 19), while human OAT2 is highly expressed in liver, moderately in kidney and low in testes, intestine and uterus (Simonson et al., 1994). However, considering high expression of human OAT2 in liver, it is surprising that none of the zebrafish Oat2s is significantly expressed in liver. In kidney, Oat2c and Oat2e are found at moderate expression levels which resemble the pattern of human OAT2 and rat Oat2 (Simonson et al., 1994; Rizwan and Burckhardt, 2007). Zebrafish Oat2b, Oat2d and Oat2e are moderately expressed in brain, as opposed to the lack of expression of OAT2/Oat2 in the mammalian brain (Rizwan and Burckhardt, 2007). Therefore, we suggest that Oat2 transporters in zebrafish have distinct function from mammalian OAT2/Oat2 transporters, with the only overlap in respect to the renal expression of Oat2c and Oat2e.

Considering that zebrafish Oat3 is expressed predominantly in kidney (Fig. 20), it resembles both human OAT1 and OAT3 which are dominant in mammalian kidney (Motohashi et al., 2002). Moderate expression in intestine and brain also resembles the expressions of human OAT1 (brain) and OAT3 (intestine and brain) (Motohashi et al., 2002), thus indicating possible involvement of zebrafish Oat3 in the renal elimination of drugs similar to the function of mammalian OAT1 and 3 (Koepsell, 2013). Additionally, zebrafish Oat3 was expressed in testes, which is similar to human OAT3 that was also detected in testes (Nigam et al., 2015), where human OAT1 was absent.

Oat1 protein obtained by Western blot analysis was about 90 kDa in size (Fig. 22), similar to the size of human OAT1 which varies from 60 to 90 kDa, depending upon glycosylation status (Robertson and Rankin, 2006). Molecular weights of Oat1 transporters from other species are in the same range, e.g., rat Oat1 57–77 kDa (Robertson and Rankin 2006), flounder Oat1 62 kDa (Wolff et al. 1997), and monkey Oat1 70 kDa (Tahara et al. 2005). Tanaka et al. (2004a) showed that mouse OAT1 and human OAT1 are glycosylated in HeLa cells. Immunoblot analysis of mouse OAT1 and human OAT1 revealed single bands with an apparent molecular mass of approximately 90 kDa. When these proteins were treated with PNGase F, an enzyme removing the N-linked carbohydrate groups from glycoproteins, the molecular mass shifted to a smaller size of approx. 55 kDa, consistent with the predicted (unglycosylated) sizes for mouse OAT1 and human OAT1 (Tanaka et al., 2004a). Based on nucleotide sequence of zebrafish Oat1, predicted molecular mass is 60 kDa. The obtained 90

kDa protein clearly suggests that the zebrafish Oat1 protein is also glycosylated. Predicted structure of OATs/Oats comprises a large hydrophilic loop between TMD 1 and 2, which contains several (2-5) potential N-glycosylation sites. N-glycosylation of proteins has been demonstrated to play a variety of roles including modulation of biological activity, regulation of intracellular targeting, protein folding, and maintenance of protein stability (Tanaka et al., 2004a). Zebrafish Oat1 showed possible homo- or heterodimeric forms and post-translational modifications (PTMs) that can be seen as smears above the monomeric bands. Among OATs/Oats, oligomerization has only been demonstrated in human OAT1, where it may depend on interactions of the TMD6 of two monomers (Duan et al., 2011). As oligomerization may be important for membrane trafficking (Keller et al., 2011; Brast et al., 2012), this topic remains to be addressed in more detail in follow up studies.

The molecular weight of zebrafish Oat2a-e is approximately 60 kDa, as shown by the Western blot analysis (Fig. 21), which corresponds to the molecular weight predicted from the amino acid sequences of each protein. Zebrafish Oat2a-e are similar in size to Oat2 proteins found in other animal species: mouse and rat Oat2s are 52–66 kDa in size, whereas the molecular weight of human OAT2 is 59.8 kDa (Simonson et al. 1994; Ljubojevic et al. 2007). Furthermore, it appears that Oat2b, d, and e, may be present in monomeric and dimeric forms (Fig. 21). Based on molecular masses of Oat2s, we conclude that zebrafish Oat2s are less glycosylated than zebrafish Oat1 in HEK293T expression system. At protein level we identified four out of five Oat2 co-orthologs by Western blot analysis: Oat2a, Oat2b, Oat2d and Oat2e. The reason why we were unable to obtain Oat2c protein was probably caused by the structure of the protein, as it is possible that the tag for antibodies (His and Xpress tag were aimed) was somehow hidden inside the protein molecule due to protein folding, and was unreachable for the antibodies.

Zebrafish Oat3 showed a protein band of approximately 75 kDa (Fig. 22). Human OAT3 is 62-80 kDa, also depending upon glycosylation status, while rat Oat3 weights from from 50 to 130 kDa, perhaps indicating dimerization or additional protein partners (Srimaroeng et al., 2008). Monkey Oat3 is 70 kDa (Robertson and Rankin, 2006). As observed for zebrafish Oat1, the obtained size of Oat3 indicates a glycosylated protein, as well as possible dimeric and higher level oligomeric forms.

HEK293 cells are not polarized and lack well defined apical and basolateral membranes, while mammalian OATs/Oats are in the expressing tissues mostly localized on basolateral membranes (Nies et al., 2011). That fact could present a problem for a correct localization in the cell membrane. Nevertheless, all seven zebrafish Oats showed localization within plasma membranes of the transiently transfected HEK293T cells (Fig. 23-25), indicating that all transfected proteins could be functionally active in transporting compounds across plasma membranes. This result confirmed the used heterologous expression system as a suitable *in vitro* tool for initial characterization of zebrafish Oat transporters. Nevertheless, the performed live cell imaging has shown that Oat2a, Oat2c, Oat2e and Oat3 remain inside the cell at a higher proportion when compared to Oat1, Oat2b and Oat2d, probably as a result of either protein processing in the cytosol or in the ER/Golgi system. Alternatively, the proteins could be partly retained in intracellular membranous compartments where they could be transporting their substrates (Hotchkiss et al., 2015).

In the next step of our study we aimed at identifying model fluorescent substrate(s) of zebrafish Oats that would enable development of high-throughput screening protocols, identification of interactors, and a detailed *in vitro* characterization of substrate preferences of these transporters. We tested a range of commercially available anionic dyes: fluorescein, 5-CF and 6CF, 2',7'-dichlorofluorescein, 4',5'-dibromofluorescein, LY, resorufin, resazurin, calcein and eosin Y. Two of the tested fluorescent dyes were shown to be substrates for five organic anion transporters in zebrafish: LY uptake was mediated by Oat1, Oat2a and Oat2d, whereas 6-CF was transported by Oat2b, Oat2d and Oat3. Oat1 and Oat3 showed higher substrate affinities ($K_m = 11.4 \mu\text{M}$ and $5.8 \mu\text{M}$, Fig. 26 and 30, respectively) than Oat2 members ($K_m = 122 \mu\text{M}$, $199.7 \mu\text{M}$ and $49.7 \mu\text{M}$ (LY) and $266.9 \mu\text{M}$ (6-CF), Fig. 27-29, respectively). After the determination of transport kinetics for fluorescent dyes, these model fluorescent substrates were used in the inhibition assays based on co-exposure of transfected cells and non-transfected or mock-transfected control with determined model substrate and potential interactor.

Our initial screening assay revealed interaction of Oat1, Oat2a, 2b, 2d and Oat3 with numerous endo- and xenobiotics, confirming polyspecific properties of related transporters (Figs. 31-35). Herewith, the results of interaction screening for Oat2 members will be

discussed first, while the results for Oat1 and Oat3 will be depicted together so they could be easily compared due to high level of overlapping of their interactors.

Among potential physiological substrates, Oat2a and Oat2b showed strong interaction with PGE2 (44.43% and 3.38% uptake of the model substrate, respectively). PGE2 was identified as a substrate for human OAT2 with K_m value of 0.71 μM (Enomoto et al., 2002; Kimura et al., 2002). Furthermore, HEK-293T cells possess endogenous multidrug resistance proteins MRP2 and MRP4 (Cheung et al., 2014) which may extrude the prostaglandins accumulated by Oats. Therefore, MK571, an established cysteinyl leukotriene-based inhibitor of MRPs, was used as a model MRP inhibitor by Henjakovic et al. (2015), but it turned out to be a potent inhibitor of human OAT2 as well. Similarly, in our study MK571 has shown the highest inhibition potency towards all three zebrafish Oat2s among all tested xenobiotics, resulting in complete inhibition of the LY transport (i.e. 0 % uptake).

Previous reports have identified cGMP as a possible physiological substrate for human OAT1, OAT2, and OAT3 (Cheng et al., 2012; Cropp et al., 2008). Importantly, interaction with cGMP was confirmed for all three zebrafish Oat2s (Oat2a = 45.02%, Oat2b = 41.55% and Oat2d = 89.27% uptake of the model substrate). The determined uptake of cGMP via Oats could prevent loss of this intracellular second messenger and prolong its action. Additionally, Oats may also clear blood from cGMP by uptake into cells and subsequent release into the tubular lumen via MRP2 and MRP4 (Henjakovic et al., 2015). It has also been discussed that increased renal cGMP levels may have an antifibrotic benefit (Schinner et al., 2015).

Testosterone, a 19-carbon androgen, has shown interaction with zebrafish Oats with percentage of the model substrate uptake of 41.04, 51.47 and 85.93 for Oat2b, Oat2a and Oat2d, respectively. Oat2a, b, and d are all expressed in zebrafish testes, and this result may suggest their possible role in transporting this steroid hormone in male zebrafish. Additionally, it was observed that testosterone treatment can cause a remarkable decrease of Oat2 protein expression in castrated male rats (Ljubojevic et al., 2007) and mice (Buist and Klaassen, 2004, Cheng et al., 2008).

Pregnenolone and its 3 β -sulfate, pregnenolone sulfate, like DHEA, DHEA sulfate, and progesterone, belong to the group of neurosteroids that are found in high concentrations in

certain areas of the brain. It has been shown they are synthesized there, affect synaptic functioning, are neuroprotective, and enhance myelination (Vallée et al., 2001).

Among xenobiotic compounds, besides MK571 which caused a complete inhibition of zebrafish Oats mediated transport, the strongest interaction was observed with NSAIDs diclofenac and indomethacin, and antibiotics tetracycline and erythromycin. Human OAT2 was shown to transport a number of pharmacologically active agents, and has been increasingly recognized in terms of its role in drug disposition (Shen et al., 2016). Out of these four pharmaceuticals, three have been well characterized as substrates of human OAT2: erythromycin and tetracycline (Babu et al., 2002, Kobayashi et al., 2005b, Yee et al., 2013), and diclofenac (Zhang et al., 2016). Indomethacin has been identified as a potent inhibitor of human OAT2 (IC₅₀ values 2.1 to 6.5 μ M) (Shen et al., 2015, Zhang et al., 2015), OAT1 (IC₅₀ values 3 to 10 μ M), and OAT3 (IC₅₀ values 0.61 to 5.95 μ M) (Khamdang et al., 2002). H-2 receptor antagonist cimetidine (CMD) has been described as a human OAT2 substrate by Tahara et al. (2005). In this study, CMD only inhibited Oat2b transport (60.55% of 6-CF uptake), while it had no effect on Oat2a and Oat2d transport (Figs. 31-33).

Although the *in vitro* functional assay for Oat2c and Oat2e was not developed in this study, considering that all 5 zebrafish Oat2 co-orthologs were expressed at the mRNA level across zebrafish tissues, we suppose these are not pseudogenes and are probably functional *in vitro* (and *in vivo*). However, their fluorescent model substrates were not identified in this study, and additional tests with other fluorescent anionic dyes or fluorescently (or radioactively) labeled compounds should be performed.

Zebrafish Oat1 and Oat3 showed interaction with various endogenous compounds including second messengers (cGMP), Krebs's cycle intermediates (α -KG, succinate, fumarate), bile pigments (bilirubin), bile salts (cholic and deoxycholic acid, TCDC), steroid hormones and hormone conjugates (estradiol, ethynylestradiol, estradiol glucuronide, estrone, E3S, progesterone, medroxy progesterone, pregnenolone sulfate, androstenedione, corticosterone, cortisol, testosterone, ethynyltestosterone, DHT, DHEAS).

Interaction with cGMP, a possible physiological substrate for human OAT1, OAT2, and OAT3 (Cheng et al., 2012; Cropp et al., 2008) and Rat Oat1 (Burckhardt and Burckhardt, 2010), was also observed for zebrafish Oat1 and Oat3, together with Oat2a, 2b and 2d.

Out of Kreb's cycle intermediates, α -KG showed the strongest and similar interaction with zebrafish Oat1 and Oat3 and was determined in this study as substrate for zebrafish Oat1 (Table 3.1). α -KG was shown to be an interactor of human, rat and monkey OAT1/Oat1 (reviewed in Srimaroeng et al., 2008). It was confirmed that rOat1 in fact translocates α -KG (Sekine et al., 1998).

Bilirubin, a bile pigment and degradation product of heme was shown to be a substrate for both, zebrafish Oat1 and Oat3 (Table 3.1 and 3.2). Interaction of bilirubin with mammalian Oats has not been observed. Data obtained in this study imply that Oat1 and Oat3 participate in excretion of bilirubin, which is normally excreted through bile and subsequently by intestine.

Among bile salts, the strongest interaction was observed with deoxycholic acid, which was determined as substrate for zebrafish Oat1, while with Oat3 it showed a mixed type of interaction. Chen et al. (2008) showed that deoxycholic acid inhibits rat Oat1.

Zebrafish Oat1 and Oat3 showed strong interaction with numerous steroid hormones, with Oat3 showing slightly stronger interaction. Here it is shown that E3S and corticosterone were substrates of Oat1, while pregnenolone sulfate was substrate of both Oat1 and Oat3. On the other hand, progesterone, testosterone and DHEAS were shown to be Oat3 inhibitors. These results indicate that both Oat1 and Oat3 most likely participate in maintenance of homeostasis of steroid hormones in zebrafish, which is similar to function proposed for Oatp1d1 transporter (Popovic et al., 2013). Flounder Oat1 also effectively transports E3S (Eraly et al., 2003; Aslamkhan et al., 2006).

Among xenobiotics, the strongest interaction with Oat1 and Oat3 was observed with NSAIDs indomethacin and ibuprofen, antineoplastic MTX, diuretic furosemide, and by industrials PFOA, PFOS, and organotin compounds (TMT, TET, TPrT, TBT).

Results of this study showed that indomethacin is a substrate, while ibuprofen is an inhibitor of both zebrafish Oat1 and Oat3 (Table 3.1 and 3.2). Numerous NSAIDs have been tested as inhibitors of human and rOAT1. Among others, high affinities were reported for ibuprofen and indomethacin. Rat Oat1 showed comparable IC₅₀ values (for IC₅₀ values for human and rat OAT1 see Burckhardt and Burckhardt, 2011; Van Wert et al., 2010). Indomethacin was shown to be taken up by human OAT1, while for ibuprofen equivocal results were reported

(Burckhardt, 2012). Taken together, NSAIDs inhibit OAT1/Oat1, but transport of these compounds may be low. By inhibiting OAT1/Oat1, NSAIDs could impair secretion of other anionic compounds, if their free plasma concentration (c_{free}) is in the range of the *in vitro* IC50 values.

It has been shown that antineoplastic MTX is a substrate of both zebrafish Oat1 and Oat3 (Table 3.1 and 3.2). Human OAT3 also mediates the high-affinity transport MTX (K_m 5-10.9 mM). MTX is an antineoplastic agent used in the treatment of acute lymphoblastic leukemia (Balis et al., 1998) and choriocarcinomas (Ohno et al., 1993) and some nonneoplastic diseases, such as psoriasis (Zonneveld et al., 1996), rheumatoid arthritis (Zonneveld et al., 1996), systemic lupus erythematosus (Ravelli et al., 1998) and dermatomyositis (Itoh et al., 1999). Because MTX manifests potentially toxic effects, such as suppression of bone marrow (Iqbal and Ali, 1993) and intestinal epithelial damage (Nakamaru et al., 1998) under high plasma concentration, understanding of the pharmacokinetics of MTX is required. In humans, MTX is mainly excreted in the urine in the unchanged form via both glomerular filtration and tubular secretion. It has been reported that concomitant use of MTX with acidic drugs, such as NSAIDs and β -lactam antibiotics, causes severe suppression of bone marrow. This seems to be the result of competitive inhibition of the process of the renal organic anion transport system (Cha et al., 2001).

A strong interaction with zebrafish Oat1 and Oat3 was observed for loop diuretic furosemide. Furosemide was shown to be a substrate of hOAT1 and hOAT3, while it was inhibitor of hOAT2. Loop diuretics have to reach their downstream target salt transporters from the lumen and thus must be secreted in the proximal tubules (Burckhardt and Burckhardt, 2011). Zebrafish Oat1 and Oat3, just like human OAT1 and OAT3, may be involved in the secretion, because furosemide interacted with very strong affinity with zebrafish Oat1 (IC50 = 2.5 μ M) and strong affinity with zebrafish Oat3 (IC50 = 26.4 μ M), while it showed intermediate affinity towards hOAT1 (IC50 between 10 and 100 mM) and very strong affinity for hOAT3 (IC50 1.7-7.3 μ M).

Xenobiotics from the group of industrials also showed strong affinity towards zebrafish Oat1 and Oat3. PFOA, a toxic environmental contaminant showed very strong interaction with zebrafish Oat1 and Oat3 and was confirmed as a substrate of zebrafish Oat1 (Table 3.1). PFOA is also a substrate of hOAT1 and hOAT3 (Nikagawa et al., 2008). Organotin are widely

used industrial chemicals present in environment in nanomolar concentrations and their yearly consumption reaches 40,000-80,000 t, which makes this group of compounds the most extensively used organometallic chemicals in the world (Cole et al., 2015). Mihaljević et al. (2017) found organotin compounds to be strong interactors of zebrafish Oct1 uptake transporter with IC50 values for DBT, TPrT and TBT in low μM range. TPheT, TBT, TPrT, TET, TMT all showed very strong interaction with zebrafish Oat1 and Oat3 (Fig. 35). TPrT was identified as a substrate (IC50 = 0.3 μM , Fig. 42, Table 3.2), while TMT was inhibitor of zebrafish Oat3 (Table 3.2).

OAT1/Oat1 and OAT3/Oat3 are well characterized in mammalian species. OAT2/Oat2 is less characterized, but the literature describing OAT2/Oat2 is rapidly evolving, with numerous contradicting publications regarding the transport mechanism, tissue distribution, and substrate preference. These differences can be partly attributed to various experimental systems and protocols used as well as to more than one transcript variants used in studies with this transporter (e.g., there are 3 transcript variants for hOAT2).

Finally, to foster *in vivo* studies on ecotoxicological relevance of zebrafish uptake transporters, a goal to generate the first zebrafish Oatp1d1 gene knockout by implementing CRISPR/Cas9 gene editing approach was set for this study. As for now, the first Oatp1d1 CRISPR/Cas9 knockouts were successfully generated in our group, and initial genotyping was performed on F1 generation embryos. Yet, more work has to be done before reaching F2 generation homozygotes ready for exposure experiments. Zebrafish typically take up to 3-4 months to reach fertility, so up to a year is needed in ideal conditions to get a homozygous F2 generation. Which is a generation that should be optimally used for tracking eventual changes in phenotype, and ultimately for exposure experiments with model compounds for the purpose of *in vivo* verification of the function of the investigated protein(s). Therefore, based on the valuable initial knowledge and experience on zebrafish functional genomics obtained during this study I do hope and believe more CRISPR/Cas9 knockouts will be available for my postdoctoral studies on uptake transporters in zebrafish.

5. Conclusions

This study provides the first comprehensive data set on Oat transporters in zebrafish (*Danio rerio*) as an important vertebrate model species. It revealed similarities and differences in comparison to human and mammalian orthologs, confirmed their broad ligand selectivity, identified potent interactors among both physiological and xenobiotic substances, and offered the first indications of their potential physiological and/or defensive relevance. The most important conclusions of this study are:

1. Seven organic anion transporters are present in zebrafish: Oat1, Oat2a, 2b, 2c, 2d, 2e and Oat3, encoded by genes *slc22a6*, *slc22a7(a-e)* and *slc22a8*, respectively. Zebrafish Oat1 and Oat3 showed one-to-one orthology, while Oat2s showed one-to-many orthologies;
2. New model substrates were identified for five zebrafish Oat proteins, and high throughput *in vitro* assays for identification of their interactors were developed and standardised;
3. Zebrafish Oats showed interaction with a variety of endogenous compounds including signaling molecules, Krebs's cycle intermediates, bile pigments, bile salts, steroid hormones and their conjugates; and various xenobiotics including NSAIDs antineoplastics, diuretics and industrials;
4. Zebrafish Oat1 and Oat3, just as human OAT1 and OAT3, show overlapping substrate selectivity. Phylogenetic analysis reveals that OAT3/Oat3 is located closest to OAT1/Oat1 in human, as well as in zebrafish, which may underlie the similar substrate selectivity;
5. Considering that Oat3 is the only OAT1/3 co-ortholog in zebrafish kidney, we propose that it plays a role in the elimination of endogenous anions and xenobiotics in zebrafish kidney, similar to the mammalian co-orthologs OAT1/Oat1 and OAT3/Oat3;
6. Creation of the first zebrafish knockouts for organic anion transporting polypeptide 1d1 by implementing CRISPR/Cas9 gene editing technology will enable *in vivo* verification of the proposed Oatp1d1 function;

7. Based on these initial insights and the assays developed, the putative physiological and/or defensive role of zebrafish Oats can be more specifically addressed in follow-up studies through detailed functional characterization of single transporter(s) in suitable expression systems, and by zebrafish functional genomics studies using targeted gene knockouts.

6. References

- Arunachalam, M., Raja, M., Vijayakumar, C., Malaiammal, P., Mayden, R. L., 2013. Natural history of zebrafish (*Danio rerio*) in India. *Zebrafish* 10, 1–14.
- Barrangou, R., 2015. The roles of CRISPR-Cas systems in adaptive immunity and beyond. *Current Opinion in Immunology* 32, 36–41.
- Barrangou, R., Fremaux, C., Deveau, H., Richards, M., Boyaval, P., Moineau, S., Romero, D. A., Horvath, P., 2007. CRISPR provides acquired resistance against viruses in prokaryotes. *Science*, 315, 1709–1712.
- Bradford, M. M., 1976. A rapid and sensitive method for the quantitation of microgram quantities of protein utilizing the principle of protein-dye binding. *Anal. Biochem.* 72, 248–254.
- Brast, S., Grabner, A., Sucic, S., Sitte, H.H., Hermann, E., Pavenstädt, H., Schlatter, E., Ciarimboli, G., 2012. The cysteines of the extracellular loop are crucial for trafficking of human organic cation transporter 2 to the plasma membrane and are involved in oligomerization. *FASEB J.* 26, 976–986.
- Breljak, D., Brzica, H., Sweet, D. H., Anzai, N., Sabolic, I., 2013. Sex-dependent expression of Oat3 (Slc22a8) and Oat1 (Slc22a6) proteins in murine kidneys. *Am J Physiol Renal Physiol* 304,, F1114–F1126
- Buist, S. C., Cherrington, N.J., Choudhuri, S., Hartley, D. P., Klaassen, C. D., 2002. Gender-specific and developmental influences on the expression of rat organic anion transporters. *Journal of Pharmacology and Experimental Therapeutics* 301, 145–151.
- Burckhardt, B. C., Burckhardt, G., 2003. Transport of organic anions across the basolateral membrane of proximal tubule cells. *Reviews of Physiology, Biochemistry and Pharmacology* 146, 95–158.
- Burckhardt, G., 2012. Drug transport by Organic Anion Transporters (OATs). *Pharmacol. Ther.* 136, 106–130.
- Burckhardt, G., Burckhardt, B. C., 2011. In vitro and in vivo evidence of the importance of organic anion transporters (OATs) in drug therapy. In: *Drug Transporters*, edited by Fromm, M. F. and Kim, R. B., Berlin: Springer, 2011, 29–104.
- Cerrutti, J. A., Brandoni, A., Quaglia, N. B., Torres, A. M., 2002a. Sex differences in p-aminohippuric acid transport in rat kidney: Role of membrane fluidity and expression of OAT1. *Molecular and Cellular Biochemistry* 233, 175–179.
- Cerrutti, J. A., Quaglia, N. B., Brandoni, A., Torres, A. M., 2002b. Effects of gender on the pharmacokinetics of drugs secreted by the renal organic anions transport systems in the rat. *Pharmacological Research* 45,107–112.
- Cerrutti, J. A., Quaglia, N. B., Torres, A. M., 2001. Characterization of the mechanisms involved in the gender differences in p-aminohippurate renal elimination in rats. *Canadian Journal of Physiology and Pharmacology* 79, 805–813.

- Cha, S.H., Sekine, T., Fukushima, J.I., Kanai, Y., Kobayashi, Y., Goya, T., Endou, H., 2001. Identification and characterization of human organic anion transporter 3 expressing predominantly in the kidney. *Molecular Pharmacology* 59:1277–1286.
- Chang, N., Sun, C., Gao, L., Zhu, D., Xu, X., Zhu, X., Xiong, J-W., Xi, J. J., 2013. Genome editing with RNA-guided Cas9 nuclease in Zebrafish embryos. *Cell Research* 23, 465-472.
- Chen, J., Terada, T., Ogasawara, K. et al., 2008. Adaptive responses of renal organic anion transporter 3 (OAT3). *Am J Physiol Renal Physiol* 295, F247-F252.
- Cole, R. F., Mills, G. A., Parker, R., Bolam, T., Birchenough, A., Kröger, S., Fones, G. R., 2015. Trends in the analysis and monitoring of organotin in the aquatic environment. *Trends in Environmental Analytical Chemistry* 8, 1–11.
- Cong, L., Ran, F. A., Cox, D., et al., 2013. Multiplex genome engineering using CRISPR/Cas systems. *Science* 339, 819-823.
- Cropp, C. D., Komori, T., Shima, J. E., Urban, T. J., Yee, S. W., More, S. S., Giacomini, K. M., 2008. Organic Anion Transporter 2 (SLC22A7) is a facilitative transporter of cGMP. *Mol. Pharmacol.* 73, 1151–58.
- Dantzler, W. H., Wright, S. H., 2003. The molecular and cellular physiology of basolateral organic anion transport in mammalian renal tubules. *Biochimica et Biophysica Acta: Biomembranes* 1618, 185–193.
- Deltcheva, E., Chylinski, K., Sharma, C. M. et al., 2011. CRISPR RNA maturation by trans-encoded small RNA and host factor Rnase III. *Nature* 471, 02-607.
- Doring, B. and Petzinger, E., 2014. Phase 0 and phase III transport in various organs: Combined concept of phases in xenobiotic transport and metabolism. *Drug Metab Rev* 46(3), 261-282.
- Duan, P., Li, S., You, G., 2011. Transmembrane peptide as potent inhibitor of oligomerization and function of human organic anion transporter 1. *Mol. Pharmacol.* 79, 569–574.
- Engeszer, R. E., Patterson, L. B., Rao, A. A., Parichy, D. M., 2007. Zebrafish in the wild: a review of natural history and new notes from the field. *Zebrafish* 4, 21–40.
- Gaborik, Z., Grindstaff, K., Zolnerciks, J., Oosterhuis, B. and Petro, N. *The transporter book*. 3rd edition, June 2017, Solvo Biotechnology, Budaors, Hungary.
- Gasiunas, G., Barrangou, R., Horvath, P., Siksnys, V., 2012. Cas9-crRNA ribonucleoprotein complex mediates specific DNA cleavage for adaptive immunity in bacteria. *Proc Natl Acad Sci USA* 109, E2579-E2586.
- Gekle, M., Mildenerger, S., Sauvant, C., Bednarczyk, D., Wright, S. H., Dantzler, W. H., 1999. Inhibition of initial transport rate of basolateral organic anion carrier in renal PT by BK and phenylephrine. *American Journal of Physiology: Renal Physiology* 277(2 Pt 2), F251–F256.
- Giacomini, K. M., Huang, S. M., 2013. Transporters in drug development and clinical pharmacology. *Clin Pharmacol Ther* 94, 3-9.

- Goodman & Gilman's The Pharmacological Basis of Therapeutics by. Joel Griffith Hardman, Lee E. Limbird, Alfred G. Gilman, 1994. 10th Ed.
- Groves, C. E., Suhre, W. B., Cherrington, N. J., Wright, S. H., 2006. Sex differences in the mRNA, protein, and functional expression of organic anion transporter (Oat) 1, Oat3, and organic cation transporter (Oct) 2 in rabbit renal proximal tubules. *Journal of Pharmacology and Experimental Therapeutics* 316, 743–752.
- Grundemann, D., Gorboulev, V., Gambaryan, S., Veyhl, M., Koepsell, H., 1994. Drug excretion mediated by a new prototype of polyspecific transporter. *Nature* 372, 549–552.
- Hagenbuch, B., Gui, C., 2008. Xenobiotic transporters of the human organic anion transporting polypeptides (OATP) family. *Xenobiotica* 38, 778–801.
- Hagenbuch, B., Meier, P. J., 2004. Organic anion transporting polypeptides of the OATP/SLC21 family: phylogenetic classification as OATP/SLCO superfamily, new nomenclature and molecular/functional properties. *Pflugers Arch.* 447, 653–65.
- Hamilton, F., 1822. *An Account of the Fishes Found in the River Ganges and Its Branches*. A. Constable and Company, Edinburgh.
- Haurwitz, R. E., Jinek, M., Wiedenheft, B., Zhou, K., Doudna, J. A., 2010. Sequence- and structure-specific RNA processing by a CRISPR endonuclease. *Science* 329, 1355–1358.
- Hill, A. J., Teraoka, H., Heideman, W., Peterson, R. E., 2005. Zebrafish as a model vertebrate for investigating chemical toxicity. *Toxicol. Sci.* 86, 6–19.
- Höglund, P. J., Nordström, K. J. V., Schiöth, H. B., Fredriksson, R., 2011. The solute carrier families have a remarkably long evolutionary history with the majority of the human families present before divergence of Bilaterian species. *Mol. Biol. Evol.* 28, 1531–41.
- Holtzman, N. G., Iovine, M. K., Liang, J.O., Morris, J., 2016. Learning to fish with genetics: a primer on the vertebrate model *Danio rerio*. *Genetics* 203, 1069 – 1089.
- Hwang, W.Y., Fu, Y., Reyon, D., Maeder, M. L., Kaini, P., Sander, J. D., Joung, J. K., Peterson R. T., Yeh, J.-R. J., 2013. Heritable and Precise Zebrafish Genome Editing Using a CRISPR-Cas System. *PLoS One* 8, oe68708.
- Ishikawa, T., 1992. The ATP-dependent glutathione S-conjugate export pump. *Trends Biochem Sci* 17, 463–468.
- Ishino, Y., Shinagawa, H., Makino, K., Amemura, M., Nakatae, A., 1987. Nucleotide sequence of the *iap* gene, responsible for alkaline phosphatase isozyme conversion in *Escherichia coli*, and identification of the gene product. *J. Bacteriol.* 169, 5429–5433.
- Jinek, M., Chylinski, K., Fonfara, I., Hauer, M., Doudna, J. A., Charpentier, E., 2012. A programmable dual-RNA-guided DNA endonuclease in adaptive bacterial immunity. *Science* 337,816–821.
- Joung, J. K., Sander, J.D., 2012. TALENs: a widely applicable technology for targeted genome editing. *Nat Rev Mol Cell Biol* 14, 49–55.

- Kell, D.B., Dobson, P.D. and Oliver, S.G., 2011. Pharmaceutical drug transport: The issues and the implications that it is essentially carrier-mediated only. *Drug Discovery Today* 16, 704–714.
- Keller, T., Egenberger, B., Gorboulev, V., Bernhard, F., Uzelac, Z., Gorbunov, D., Wirth, C., Koppatz, S., Dötsch, V., Hunte, C., et al., 2011. The large extracellular loop of organic cation transporter 1 influences substrate affinity and is pivotal for oligomerization. *J. Biol. Chem.* 286, 37874–37886.
- Kikuchi, R., Kusuhara, H., Hattori, N., Shiota, K., Kim, I., Gonzalez, F. J., Sugiyama, Y., 2006. Regulation of the expression of human organic anion transporter 3 by hepatocyte nuclear factor 1alpha/beta and DNA methylation. *Molecular Pharmacology* 70, 887–896.
- Kimura, H., Takeda, M., Narikawa, S., Enomoto, A., Ichida, K., Endou, H., 2002. Human organic anion transporters and human organic cation transporters mediate renal transport of prostaglandins. *Journal of Pharmacology and Experimental Therapeutics* 301, 293–298.
- Klaassen, C. D., Lu, H., 2008. Xenobiotic transporters: ascribing function from gene knockout and mutation studies. *Toxicol. Sci.* 101, 186–196.
- Kobayashi, D., Nozawa, T., Imai, K., Nezu, J., Tsuji, A., Tamai, I., 2003. Involvement of human Organic Anion Transporting Polypeptide OATP-B (SLC21A9) in pH-dependent transport across intestinal apical membrane. *J. Pharmacol. Exp. Ther.* 306, 703–708.
- Kobayashi, Y., Ohshiro, N., Sakai, R., Ohbayashi, M., Kohyama, N., Yamamoto, T., 2005b. Transport mechanism and substrate specificity of human organic anion transporter 2 (hOat2 [SLC22A7]). *Journal of Pharmacy and Pharmacology* 57, 573–578.
- Kobayashi, Y., Ohshiro, N., Shibusawa, A., Sasaki, T., Tokuyama, S., Sekine, T., Endou, H., 2002. Isolation, characterization and differential gene expression of multispecific organic anion transporter 2 in mice. *Molecular Pharmacology* 62, 7–14.
- Koepsell, H., 2013. The SLC22 family with transporters of organic cations, anions and zwitterions. *Mol. Aspects Med.* 34, 413–35.
- Koepsell, H., Endou, H., 2004. The SLC22 drug transporter family. *Pflugers Arch.* 447, 666–676.
- Koepsell, H., Lips, K., Volk, C., 2007. Polyspecific organic cation transporters: structure, function, physiological roles, and biopharmaceutical implications. *Pharm. Res.* 24, 1227–1251.
- Koepsell, H., Schmitt, B.M., Gorboulev, V., 2003. Organic cation transporters. *Rev. Physiol. Biochem. Pharmacol.* 150, 36–90.
- Kusuhara, H., Sekine, T., Utsunomiya-Tate, N., Tsuda, M., Kojima, R., Cha, S. H., Sugiyama, Y., Kanai, Y., Endou, H., 1999. Molecular cloning and characterization of a new multispecific organic anion transporter from rat brain. *Journal of Biological Chemistry* 274, 13675–13680.

- Kuze, K., Graves, P., Leahy, A., Wilson, P., Stuhlmann, H., You, G., 1999. Heterologous expression and functional characterization of a mouse renal organic anion transporter in mammalian cells. *Journal of Biological Chemistry* 274, 1519–1524.
- Leuthold, S., Hagenbuch, B., Mohebbi, N., Wagner, C. A., Meier, P.J., Stieger, B., 2009. Mechanisms of pH-gradient driven transport mediated by organic anion polypeptide transporters. *Am. J. Physiol. Cell Physiol.* 296, C570–82.
- Lin, J. H., Chiba, M., Baillie, T. A., 1999. Is the role of small intestine in first-pass metabolism overemphasized? *Pharmacol Rev* 51(2), 135-158.
- Ljubojevic, M., Balen, D., Breljak, D., Kusan, M., Anzai, N., Bahn, A., Burckhardt, G., Sabolic, I., 2007. Renal expression of organic anion transporter OAT2 in rats and mice is regulated by sex hormones. *American Journal of Physiology: Renal Physiology* 292, F361–F372.
- Ljubojevic, M., Herak-Kramberger, C. M., Hagos, Y., Bahn, A., Endou, H., Burckhardt, G., Sabolic, I., 2004. Rat renal cortical OAT1 and OAT3 exhibit gender differences determined by both androgen stimulation and estrogen inhibition. *American Journal of Physiology: Renal Physiology* 287, F124–F138.
- Louis, A., Muffato, M., Roest, C.H., 2013. Genomicus: five genome browsers for comparative genomics in eukaryota. *Nucleic Acids Res.* 41, 700–705.
- Lu, R., Chan, B. S., Schuster, V. L., 1999. Cloning of the human kidney PAH transporter: Narrow substrate specificity and regulation by protein kinase c. *American Journal of Physiology: Renal Physiology* 276, F295–F303.
- Mali, P., Yang, L., Esvelt, K.M., et al. 2013. RNA-guided human genome engineering via Cas9. *Science* 339, 823-826.
- Marger, M. D., Saier, Jr., M. H., 1993. A major superfamily of transmembrane facilitators that catalyze uniport, symport and antiport. *Trends Biochem. Sci.* 18, 13–20.
- Masereeuw, R., Russel, F. G., 2010. Therapeutic implications of renal anionic drug transporters. *Pharmacol. Ther.* 126, 200–216.
- McClure, M. M., McIntyre, P. B., McCune, A. R., 2006. Notes on the natural diet and habitat of eight danionin fishes, including the zebrafish *Danio rerio*. *J. Fish Biol.* 68, 1–18.
- Minuesa, G., Volk, C., Molina-Arcas, M., Gorboulev, V., Erkizia, I., Arndt, P., Clotet, B., Pastor-Anglada, M., Koepsell, H., Martinez-Picado, J., 2009. Transport of lamivudine [(-)-b-L-20,30-dideoxy-30-thiacytidine] and high-affinity interaction of nucleoside reverse transcriptase inhibitors with human organic cation transporters 1, 2, and 3. *J. Pharmacol. Exp. Ther.* 329, 252–261.
- Morrissey, K. M., Stocker, S. L., Wittwer, M. B., Xu, L., Giacomini, K. M., 2013. Renal transporters in drug development. *Annu. Rev. Pharmacol. Toxicol.* 53, 503–529.

- Motohashi, H., Sakurai, Y., Saito, H., Masuda, S., Urakami, Y., Goto, M., Fukatsu, A., Ogawa, O., Inui, K. I., 2002. Gene expression levels and immunolocalization of organic ion transporters in the human kidney. *J. Am. Soc. Nephrol.* 13, 866–74.
- Nakakariya, M., Shima, Y., Shirasaka, Y., Mitsuoka, K., Nakanishi, T., Tamai, I., 2009. Organic anion transporter OAT1 is involved in renal handling of citrulline. *Am. J. Physiol. Renal Physiol.* 297, F71–9.
- Nies, A.T., Koepsell, H., Damme, K., Schwab, M., 2010. Organic cation transporters (OCTs, MATEs), in vitro and in vivo evidence for the importance in drug therapy. *Handb. Exp. Pharmacol.* 201, 105–167.
- Nigam, S.K., Bush, K.T., Martovetsky, G., Ahn, S.-Y., Liu, H.C., Richard, E., Bhatnagar, V., Wu, W., 2015. The organic anion transporter (Oat) family: a systems biology perspective. *Physiol. Rev.* 95, 83–123.
- Nigam, S.K., 2018. The SLC22 Transporter Family: A Paradigm for the Impact of Drug Transporters on Metabolic Pathways, Signaling, and Disease
- Nakagawa, H., Hirata, T., Terada, T., Jutabha, P., Miura, D., Harada, K.H., Inoue, K., Anzai, N., Endou, H., Inui, K.-I., Kanai, Y., Koizumi, A., 2008. Roles of organic anion transporters in the renal excretion of perfluorooctanoic acid. *Basic Clin. Pharmacol. Toxicol.* 103, 1–8.
- Ogasawara, K., Terada, T., Asaka, J., Katsura, T., Inui, K., 2007. Hepatocyte nuclear factor-4{alpha} regulates the human organic anion transporter 1 gene in the kidney. *American Journal of Physiology: Renal Physiology* 292, F1819–F1826.
- Pardridge, W. M., 2002. Drug and gene targeting to the brain with molecular Trojan horses. *Nat Rev Drug Discov* 1(2), 131-139.
- Pasquier, J., Braasch, I., Batzel, P., Cabau, C., Montfort, J., Nguyen, T., Jouanno, E., Berthelot, C., Klopp, C., Journot, L., Postlethwait, J. H., Guiguen, Y., Bobe, J., 2017. Evolution of gene expression after whole-genome duplication: New insights from the spotted gar genome. *J Exp Zool (Mol Dev Evol)*. 2017, 1–13.
- Petzinger, E., Geyer, J., 2006. Drug transporters in pharmacokinetics. *Naunyn Schmiedeberg's Arch Pharmacol* 372, 465–475.
- Popovic, M., Zaja, R., Fent, K., Smital, T., 2013. Molecular characterization of zebrafish Oatp1d1 (Slco1d1), a novel Organic anion transporting polypeptide. *J. Biol. Chem* 288(47), 33894-33911.
- Popowski, K., Eloranta, J. J., Saborowski, M., Fried, M., Meier, P. J., Kullak-Ublick, G. A., 2005. The human organic anion transporter 2 gene is transactivated by hepatocyte nuclear factor-4{alpha} and suppressed by bile acids. *Molecular Pharmacology* 67, 1629–1638.
- Race, J. E., Grassl, S. M., Williams, W. J., Holtzman, E. J., 1999. Molecular Cloning and Characterization of Two Novel Human Renal Organic Anion Transporters (hOAT1 and hOAT3). *Biochemical and Biophysical Research Communications* 255, 508–514.

- Reyes, J. L., Melendez, E., Alegria, A., Jaramillo-Juarez, F., 1998. Influence of sex differences on the renal secretion of organic anions. *Endocrinology* 139, 1581–1587.
- Riordan, J. R., Rommens, J. M., Kerem, B-S., Alon, N., Rozmahel, R., Grzelczak, Z., Zielenski, J., Lok, S., Plavsic, N., Chou, J. L., Drumm, M. L., Iannuzzi, M. C., Collins, F. C., Tsui, L-C., 1989. Identification of the Cystic Fibrosis Gene: Cloning and Characterization of Complementary DNA. *Science* 245 (4922), 1066-1073.
- Rizwan, A. N., Burckhardt, G., 2007. Organic anion transporters of the SLC22 family: biopharmaceutical, physiological, and pathological roles. *Pharm. Res.* 24, 450–70.
- Robertson, E. E., Rankin, G. O., 2006. Human renal organic anion transporters: Characteristics and contributions to drug and drug metabolite excretion. *Pharmacology and Therapeutics* 109, 399–412.
- Sabolic, I., Asif, A. R., Budach, W. E., Wanke, C., Bahn, A., Burckhardt, G., 2007. Gender differences in kidney function. *Pflügers Archiv European Journal of Physiology* 455, 397–429.
- Saji, T., Kikuchi, R., Kusuhara, H., Kim, I., Gonzalez, F. J., Sugiyama, Y., 2008. Transcriptional regulation of human and mouse organic anion transporter 1 by hepatocyte nuclear factor 1 {alpha}/{beta}. *Journal of Pharmacology and Experimental Therapeutics* 324(2), 784–790.
- Sambrook, J. F., Fritsch, E.F., Maniatis, T. 1989. *Molecular Cloning - A Laboratory Manual*. Cold Spring Harbor Laboratory Press. Cold Spring Harbor, NY, USA.
- Sapranauskas, R., Gasiunas, G., Fremaux, C., Barrangou, R., Horvath, P., Siksnys, V., 2011. The *Streptococcus thermophilus* CRISPR/Cas system provides immunity in *Escherichia coli*. *Nucleic Acids Res.* 39, 9275–9282.
- Satlin, L. M., Amin, V., Wolkoff, A. W., 1997. Organic anion transporting polypeptide mediates organic anion/HCO₃⁻ exchange. *J. Biol. Chem.* 272, 26340–5.
- Sauvant, C., Holzinger, H., Gekle, M., 2002. Short-term regulation of basolateral organic anion uptake in proximal tubular OK cells: EGF acts via MAPK, PLA(2), and COX1. *Journal of the American Society of Nephrology* 13, 1981–1991.
- Sauvant, C., Holzinger, H., Gekle, M., 2003. Short-term regulation of basolateral organic anion uptake in proximal tubular opossum kidney cells: Prostaglandin E2 acts via receptor-mediated activation of protein kinase A. *Journal of the American Society of Nephrology* 14, 3017–3026.
- Sauvant, C., Holzinger, H., Gekle, M., 2006. Prostaglandin E2 inhibits its own renal transport by downregulation of organic anion transporters rOAT1 and rOAT3. *Journal of the American Society of Nephrology* 17, 46–53.
- Sekine, T., Cha, S. H., Tsuda, M., Apiwattanakul, N., Nakajima, N., Kanai, Y., Endou, H., 1998. Identification of multispecific organic anion transporter 2 expressed predominantly in the liver. *Federation of European Biochemical Societies Letters* 429, 179–182.

- Sekine, T., Miyazaki, H. and Endou, H., 2004. Molecular physiology of renal organic anion transporters. *Am. J. Physiol. Renal Physiol.* 290, 251-261
- Sekine, T., Watanabe, N., Hosoyamada, M., Kanai, Y., Endou, H., 1997. Expression cloning and characterization of a novel multispecific organic anion transporter. *Journal of Biological Chemistry* 272, 18526–18529.
- Shen, H., Lai, Y., Rodrigues, A. D., 2016. Organic anion transporter 2 (OAT2): an enigmatic human solute carrier. *Drug Metab. Dispos.* 45 (2), 228–236.
- Shuprisha, A., Lynch, R. M., Wright, S.H., Dantzler, W. H., 2000. PKC regulation of organic anion secretion in perfused S2 segments of rabbit proximal tubules. *American Journal of Physiology: Renal Physiology* 278, F104–F109.
- Simonson, G. D., Vincent, A. C., Roberg, K. J., Huang, Y., Iwanij, V., 1994. Molecular cloning and characterization of a novel liverspecific transport protein. *J. Cell Sci.* 107, 1065-72.
- Soodvilai, S., Chatsudthipong, V., Evans, K. K., Wright, S. H., Dantzler, W. H., 2004. Acute regulation of OAT3-mediated estrone sulfate transport in isolated rabbit renal proximal tubules. *American Journal of Physiology: Renal Physiology* 287, F1021–F1029.
- Spence, R., Fatema, M. K., Reichard, M., Huq, K. A., Wahab, M. A. et al., 2006. The distribution and habitat preferences of the zebrafish in Bangladesh. *J. Fish Biol.* 69, 1435–1448.
- Spence, R., Gerlach, G., Lawrence, C., Smith, C., 2008. The behaviour and ecology of the zebrafish, *Danio rerio*. *Biol. Rev. Camb. Philos. Soc.* 83, 13–34.
- Srimaroeng, C., Perry, J. L. and Pritchard, J. B., 2008. Physiology, structure, and regulation of the cloned organic anion transporters. *Xenobiotica* 38(7–8), 889–935.
- Sugano, K., Kansy M., Artursson, P., Avdeef, A., Bendels, S., Di, L., Ecker, G. F., Faller, B., Fischer, H., Gerebtzoff, G., Lennernaes H. and Senner, F., 2010. Coexistence of passive and carrier-mediated processes in drug transport. *Drug Discovery* 9, 597-614.
- Sugiyama, D., Kusuhara, H., Shitara, Y., Abe, T., Meier, P. J., Sekine, T., Endou, H., Suzuki, H., Sugiyama, Y., 2001. Characterization of the efflux transport of 17beta-estradiol-D-17beta-glucuronide from the brain across the blood–brain barrier. *Journal of Pharmacology and Experimental Therapeutics* 298, 316–322.
- Sun, W., Wu, R.R., Van Poelje, P.D., Erion, M. D. 2001. Isolation of a family of organic anion transporters from human liver and kidney. *Biochemical and Biophysical Research Communications* 283, 417–422.
- Swarts, D. C., Mosterd, C., van Passel, M. W. J., Brouns, S. J. J., 2012. CRISPR Interference Directs Strand Specific Spacer Acquisition. *PLoS One* 7, e35888.
- Sweet, D. H., Miller, D. S., Pritchard, J. B., Fujiwara, Y., Beier, D. R., Nigam, S. K., 2002. Impaired organic anion transport in kidney and choroid plexus of organic anion transporter 3 (Oat3 (Slc22a8)) knockout mice. *Journal of Biological Chemistry* 277, 26934–26943.

- Sweet, D. H., Wolff, N. A., Pritchard, J. B., 1997. Expression cloning and characterization of ROAT1: The basolateral organic anion transporter in rat kidney. *Journal of Biological Chemistry* 272, 30088–30095.
- Tahara, H., Shono, M., Kusuhara, H., Kinoshita, H., Fuse, E., Takadate, A., Otagiri, M., Sugiyama, Y., 2005. Molecular cloning and functional analyses of OAT1 and OAT3 from cynomolgus monkey kidney. *Pharmaceutical Research* 22,647–660.
- Takeda, M., Sekine, T., Endou, H., 2000. Regulation by protein kinase C of organic anion transport driven by rat organic anion transporter 3 (rOAT3). *Life Sciences* 67, 1087–1093.
- Tanaka, K., Zhou, F., Kuze, K., You, G., 2004b. Cysteine residues in the organic anion transporter mOAT1. *Biochemical Journal* 380, 283–287.
- Tanaka, Y., Xu, W., Zhou, F., You, G. F., 2004a. Role of glycosylation in the organic anion transporter OAT1. *Journal of Biological Chemistry* 279, 14961–14966.
- Tom, R., Bisson, L., Durocher, Y., 2008. Transfection of adherent HEK293-EBNA1 cells in a six-well plate with branched PEI for production of recombinant proteins. *Cold Spring Harb Protoc.* 3.
- Uwai, Y., Okuda, M., Takami, K. et al., 1998. Functional characterization of the rat multispecific organic anion transporter OAT1 mediating basolateral uptake of anionic drugs in the kidney. *FEBS Lett* 438, 321–324.
- Uwai, Y., Okuda, M., Takami, K., Hashimoto, Y., Inui, K., 1998. Functional characterization of the rat multispecific organic anion transporter OAT1 mediating basolateral uptake of anionic drugs in the kidney. *Federation of European Biochemical Societies Letters* 438, 321–324.
- Vallée, M., Mayo, W., Le Moal, M., 2001. Role of pregnenolone, dehydroepiandrosterone and their sulfate esters on learning and memory in cognitive aging. *Brain Research. Brain Research Reviews.* 37 (1–3), 301–312.
- Williams, R. T., 1959. *Detoxication Mechanisms. The Metabolism and Detoxification of Drugs, Toxic Substances and Other Organic Compounds.* 2nd edition. London: Chapman and Hall Ltd.
- Wolff, N. A., Thies, K., Kuhnke, N., Reid, G., Friedrich, B., Lang, F., Burckhardt, G., 2003. Protein kinase C activation downregulates human organic anion transporter 1-mediated transport through carrier internalization. *Journal of the American Society of Nephrology* 14, 1959–1968.
- Wright, S. H. and Dantzler, W. H., 2004. Molecular and cellular physiology of renal organic cation and anion transport. *Physiol. Rev.* 84, 987–1049.
- Wu, W., Jamshidi, N., Eraly, S. A., Liu, H. C., Bush, K. T., Palsson, B. O., Nigam, S. K., 2013. Multispecific drug transporter slc22a8 (oat3) regulates multiple metabolic and signaling pathways. *Drug Metab Dispos* 41, 1825–1834.

You, G., Kuze, K., Kohanski, R. A., Amsler, K., Henderson, S., 2000. Regulation of mOAT-mediated organic aniontransport by okadaic acid and protein kinase C in LLC-PK(1) cells. *Journal of Biological Chemistry* 275, 10278–10284.

Zhou, F., Xu, W., Hong, M., Pan, Z., Sinko, P. J., Ma, J., You, G., 2005. The role of N-linked glycosylation in protein folding, membrane targeting, and substrate binding of human organic anion transporter hOAT4. *Molecular Pharmacology* 67, 868–876.

7. Summary

Numerous endogenous compounds and xenobiotics are organic anions. Their disposition and elimination from the body depend on the function of polyspecific membrane transporters that belong to two subfamilies: SLC21 and SLC22 subfamily of the SLC (Solute Carriers) family. They are responsible for the uptake of various endogenous and xenobiotic compounds into the cell. Despite their crucial role in toxicological response in mammals, research on their ecotoxicological relevance and characteristics in non-mammalian species is still scarce. Therefore, the main goal of this study was identification and molecular characterization of organic anion transporters in zebrafish (*Danio rerio*). Additional goal of this study was to generate the first gene knockout in zebrafish, for a well characterized member of SLC21 family in zebrafish, *Oatp1d1*, by implementing CRISPR/Cas9 gene editing technology.

Using methods such as phylogenetic analysis, tissue expression analysis, and transfection in heterologous expression system, we developed transport assays based on fluorescent probes in order to identify potential substrates and inhibitors of ecotoxicological relevance and elucidate transport mechanism of zebrafish Oats as key elements in physiological and ADME processes of organic anions.

Phylogenetic analysis revealed specific clustering of vertebrate *Oat/oat* genes, with 3 main clusters: OAT1/Oat1, OAT2/Oat2 and OAT3/Oat3. Seven organic anion transporters are present in zebrafish: *Oat1*, *Oat2a*, *2b*, *2c*, *2d*, *2e* and *Oat3*, encoded by genes *slc22a6*, *slc22a7(a-e)* and *slc22a8*, respectively. Zebrafish *oat1* and *oat3* showed one-to-one orthology, while *oat2s* showed one-to-many orthology. Synteny analysis showed that zebrafish *oat2* genes are localized on two chromosomes, 11 and 17.

New model fluorescent substrates were identified for five zebrafish Oat proteins, lucifer yellow (LY) for *Oat1*, *Oat2a* and *Oat2d*; and 6-carboxyfluorescein (6-CF) for *Oat2b*, *Oat2d* and *Oat3*. Standardized high throughput in vitro assays for identification of interactors of these 5 proteins were developed.

Zebrafish Oats showed interaction with a variety of endogenous compounds including signaling molecules, Krebs's cycle intermediates, bile pigments, bile salts, steroid hormones and their conjugates; and various xenobiotics including NSAIDs, antineoplastics, diuretics

and industrials. Zebrafish Oat1 and Oat3, just as human OAT1 and OAT3, show overlapping substrate selectivity.

The first CRISPR/Cas9 zebrafish knockouts for the best in vitro characterized transporter of organic anions in zebrafish, organic anion transporting polypeptide 1d1 (Oatp1d1) were successfully generated in our group, and initial genotypization was performed on F1 generation embryos. Yet, more work has to be done before reaching F2 generation homozygotes ready for exposure experiments. Creation of the Oatp1d1 zebrafish knockouts will enable in vivo verification of the proposed Oatp1d1 function.

8. Sažetak

Brojni endogeni spojevi i ksenobiotici pripadaju skupini organskih aniona. Njihova raspodjela u organizmu, kao i eliminacija, ovisi o funkciji polispecifičnih membranskih prijenosnika koji pripadaju dvijema podobiteljima: SLC21 i SLC22, članicama obitelji SLC (eng. *Solute Carriers*). Ovi prijenosnici odgovorni su za unos raznih endo- i ksenobiotika u stanicu. Međutim, usprkos ključnoj ulozi u toksikološkom odgovoru kod sisavaca, njihova ekotoksikološka važnost i karakteristike su slabo istražene u ne-sisavaca. Glavni je cilj ovog istraživanja stoga bio identifikacija i molekularna karakterizacija prijenosnika organskih aniona kod zebrice (*Danio rerio*), a ovo istraživanje imalo je za cilj i stvaranje prvih genskih *knockout* zebrica za do sada najbolje istražen anionski prijenosnik zebrice *Oatp1d1*, i to korištenjem CRISPR/Cas9 pristupa editiranja genoma.

Koristeći se filogenetskom analizom, analizom tkivne ekspresije gena te transfekcijom u heterologni ekspresijski sustav, razvili smo transportne testove bazirane na fluorescentnim probama s ciljem otkrivanja potencijalnih supstrata i inhibitora od ekotoksikološke važnosti te kako bismo razjasnili transportni mehanizam Oat-a zebrice, kao ključnih elemenata fizioloških i ADME procesa u koje su uključeni organski anioni. Filogenetska je analiza pokazala specifično grupiranje *Oat/oat* gena kralježnjaka u 3 glavne skupine: OAT1/Oat1, OAT2/Oat2 i OAT3/Oat3. Kod zebrice je prisutno sedam Oat prijenosnika: *Oat1*, *Oat2a*, *2b*, *2c*, *2d*, *2e* i *Oat3*, a kodirani su genima *slc22a6*, *slc22a7(a-e)* i *slc22a8*. *oat1* i *oat3* zebrice pokazali su ortologiju jedan-ka-jedan, dok su *oat2* članovi pokazali ortologiju jedan-ka-više. Analiza sintenije pokazala je smještaj *oat2* gena na kromosomima 11 i 17 zebrice.

Identificirani su novi modelni fluorescentni supstrati za pet Oat-a zebrice, "Lucifer yellow" (LY) za *Oat1*, *Oat2a* i *Oat2d* te 6-karboksifluorescein (6-CF) za *Oat2b*, *Oat2d* i *Oat3*. Također su razvijeni i standardizirani visoko protočni in vitro testovi za identifikaciju interaktora ovih 5 proteina. Oat prijenosnici zebrice su pokazali interakciju s raznovrsnim endogenim spojevima, uključujući intermedijere Krebsovog ciklusa, žučne pigmente, žučne soli, steroidne hormone i njihove konjugate; kao i s raznim ksenobioticima poput NSPUL lijekova, kemoterapeutika, diuretika i industrijskih spojeva. *Oat1* i *Oat3* zebrice su pokazali preklapanje supstratne specifičnosti, koje pokazuju i OAT1 i OAT3 čovjeka.

Prve *knockout* zebrice za *Oatp1d1* su uspješno stvorene pomoću CRISPR/Cas9 pristupa. Napravljena je inicijalna genotipizacija embrija F1 generacije te slijedi rad na dobivanju homozigotne F2 generacije. Embriji i odrasle zebrice F2 generacije potom će biti korišteni za

izlaganje modelnim okolišno relevantnim spojevima i daljnju verifikaciju predložene funkcije Oatp1d1 prijenosnika *in vivo*.

9. Abbreviations

5-CF	5-carboxyfluorescein
6-CF	6-carboxyfluorescein
AA	Arachidonic acid
ABC	ATP Binding Cassette
Ac	<i>Anolis carolinensis</i>
ADME	Absorption, distribution, metabolism and elimination
BBB	Blood-brain barrier
BCSFB	Blood-cerebrospinal fluid barrier
BUT	n-Butyltin trichloride
BT	Benzotriazole
cAMP	Cyclic adenosine monophosphate
cDNA	complementary Deoxyribonucleic acid
cGMP	Cyclic guanosine monophosphate
CH	Cholate
Ci	<i>Ciona intestinalis</i>
COX I	Cyclooxygenase I
CRISPR	Clustered Regularly Interspaced Short Palindromic Repeats
DAPI	Diamidino-2-phenylindole
DBP	Dibutyl phthalate
DBT	Di-n-butyltin dichloride
DEHP	Bis(2-ethylhexyl)phthalate
DEP	Diethyl phthalate
DHEAS	Dehydroepiandrosterone sulfate
DHT	Dihydrotestosterone
DMEM	Dulbecco's modified Eagle medium
DMT	Dimethyltin dichloride
DPheT	Diphenyltin dichloride
DNA	Deoxyribonucleic acid
Dr	<i>Danio rerio</i>
DTT	Dithiothreitol
E3S	Estrone-3-sulfate
EDTA	Ethylenediaminetetraacetic acid
EGF	Epidermal growth factor
EF1 α	Elongation factor 1 α
ERK	Extracellular signal-regulated kinase
EtBr	Ethidium bromide
FBS	Fetal Bovine Serum
FITC	Fluorescein isothiocyanate
Ga	<i>Gastrosteus aculeatus</i>
GFP	Green fluorescent protein
Gg	<i>Gallus gallus</i>
Gm	<i>Gadus morhua</i>
HEK293	Human Embryonic Kidney 293
HNF	Hepatocyte nuclear factor

HEPES	Hydroxyethyl piperazineethanesulfonic acid
His	Histidine
HKG	Housekeeping gene
Hs	<i>Homo sapiens</i>
I	Inhibitor
IgG	Immunoglobulin G
IgG-HRP	Immunoglobulin G - horseradish peroxidase
LP	Loop
LY	Lucifer yellow
MATE	Multidrug and toxin compound extrusion
MEK	Mitogen-activated/extracellular-signal regulated kinase
MET	Methyltin trichloride
MFS	Multifacilitator superfamily
Mm	<i>Mus musculus</i>
MNE	Mean normalized expression
mRNA	messenger Ribonucleic acid
MTX	Methotrexate
NH ₄ Cl	Ammonium chloride
NP-40	Nonidet P-40
NSAID	Nonsteroidal anti-inflammatory drug
OAT/Oat	Organic anion transporter
OATP/Oatp	Organic anion transporting polypeptide
OCT/Oct	Organic cation transporter
OCTN/Octn	Organic carnitine transporter
OI	<i>Oryzas latipes</i>
ORCTL/Orctl	Organic cation like transporter
OTA	Ochratoxin A
PAH	p-aminohippurate
PBS	Phosphate-buffered saline
PCR	Polymerase chain reaction
PEI	Polyethyleneimine
PFOA	Perfluorooctanoic acid
PFOS	Perfluorooctanesulfonic acid
PGE2	Prostaglandine E2
PKC	Protein Kinase C
PLA2	Phospholipase A2
qPCR	Quantitative Real-Time polymerase chain reaction
RNA	Ribonucleic acid
S	Substrate
SD	Standard deviation
SDS	Sodium dodecyl sulphate
SE	Standard error
SLC	Solute carrier
T3	Triiodothyronine

T4	Thyroxine
TALEN	Transcription activator-like effector
TBA	Tetrabutylammonium
TBT	Tri-n-butyltin chloride
TC	Taurocholate
TCDC	Taurochenodeoxycholate
TCL	Total cell lysate
TEA	Tetraethylammonium
TET	Triethyltin chloride
TMT	Trimethyltin chloride
TMD	Transmembrane domain
Tn	<i>Tetraodon nigroviridis</i>
TPA	Tetrapentylammonium
TPheT	Triphenyltin chloride
TPrT	Tri-n-propyltin chloride
Tr	<i>Takifugu rubripes</i>
Tris	Tris(hydroxymethyl)aminomethane
WGD	Whole genome duplication
WT	Wild type
X-gal	5-bromo-4-chloro-3-indolyl- β -D-galactopyranoside
Xl	<i>Xenopus laevis</i>
ZFN	Zinc-finger nuclease

10. Supplement

Table S1. Protein annotation and accession numbers of protein sequences used in the phylogenetic analysis of OAT/Oat subfamily in vertebrate. Species abbreviations: Hs, *Homo sapiens*; Mm *Mus musculus*; Gg, *Gallus gallus*; Ac, *Anolis carolinensis*; Xl, *Xenopus laevis*; Dr, *Danio rerio*; Tn, *Tetraodon nigroviridis*; Tr, *Takifugu rubripes*; Ga, *Gastrosteus aculeatus*; Ol, *Oryzas latipes*.

Protein annotation	Accession number
HsOAT1	NP_004781.2
HsOAT2	NP_006663.2
HsOAT3	NP_004245.2
HsOAT4	NP_060954.1
HsOAT5	NP_001034841.3
HsOAT6	NP_001004326.4
HsOAT7	NP_543142.2
HsURAT1	NP_653186.2
MmOat1	NP_032792.2
MmOat2	NP_659105.2
MmOat3	NP_112471.3
MmOat5	NP_659034.1
MmOat6	NP_941052.1
MmUrat1	NP_033229.3
GgOat2	NP_001186367.1
AcOat1	ENSACAP00000006348
AcOat2	ENSACAP00000004498
AcOat3	ENSACAP00000013862
AcOatl1	ENSACAP00000008001
XlOat1	NP_001087663.1
XlOat3	NP_001087661.1
DrOat1	AAH95733.1
DrOat2a	NP_001077330.1
DrOat2b	XP_001340340.3
DrOat2c	XP_001337343.1
DrOat2d	XP_001337264.3
DrOat2e	NP_956643.1
DrOat3	NP_996960.1
GaOat1	ENSGACP00000027657
GaOat2b	ENSGACP00000015157
GaOat2c	ENSGACP00000023551
GaOat3	ENSGACP00000027316
OlOat1	ENSORLP00000015952
OlOat2e	ENSORLP00000024217
OlOat3	ENSORLP00000007641
TrOat1	ENSTRUP00000000970
TrOat2c	ENSTRUP00000035983

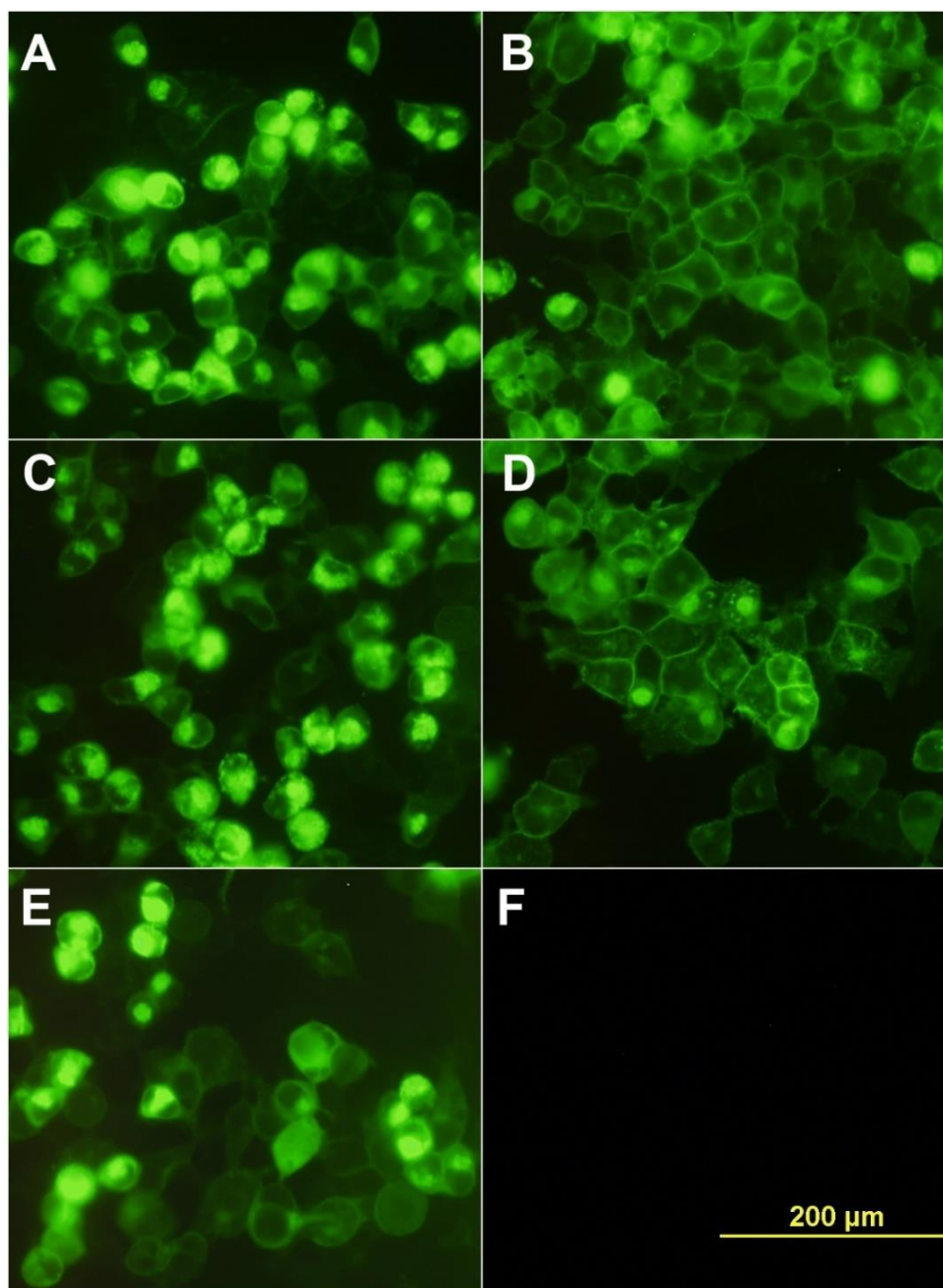


Figure S1. Live cell imaging on HEK293T cells transiently transfected with pDest-YFP vector containing specific zebrafish *oat2* gene: A) Oat2a, B) Oat2b, C) Oat2c, D) Oat2d, E) Oat2e, and F) mock transfected cells. YFP-labeled Oat2a-e fluorescence was observed with fluorescent microscope using the FITC filter.

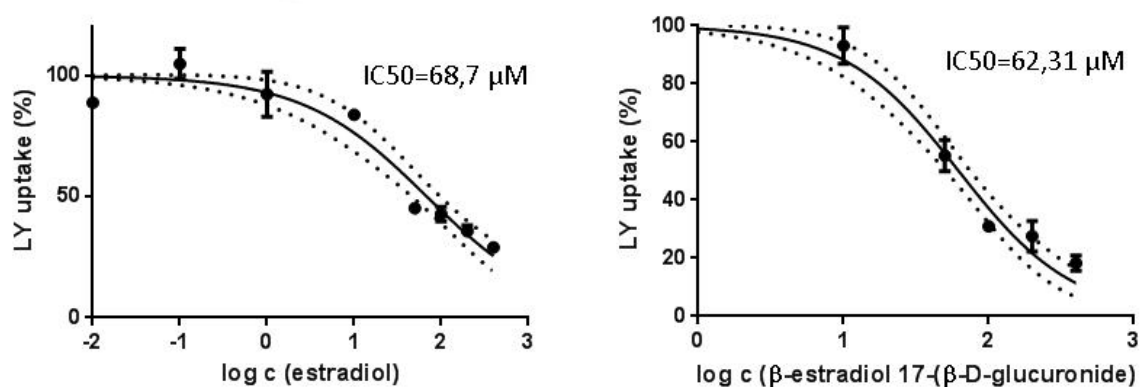


Figure S2. Concentration dependent inhibition of Oat1 mediated 6-CF uptake by estradiol and β -estradiol 17-(β -D-glucuronide) (μM). Values on X-axis were transformed to logarithmic scale ($\log X$). Each data point represents the mean \pm SD from triplicate determinations. Dotted lines represent confidence intervals.

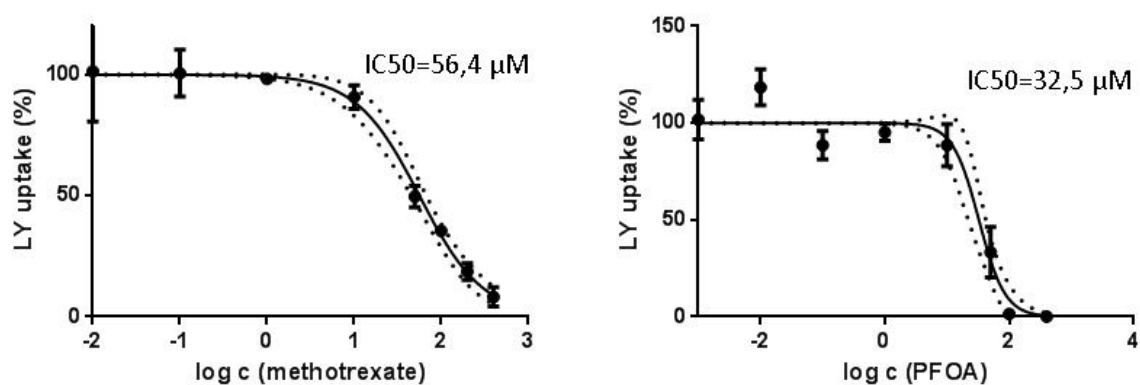


Figure S3. Concentration dependent inhibition of Oat1 mediated LY uptake by methotrexate and PFOA (μM). Values on X-axis were transformed to logarithmic scale ($\log X$). Each data point represents the mean \pm SD from triplicate determinations. Dotted lines represent confidence intervals.

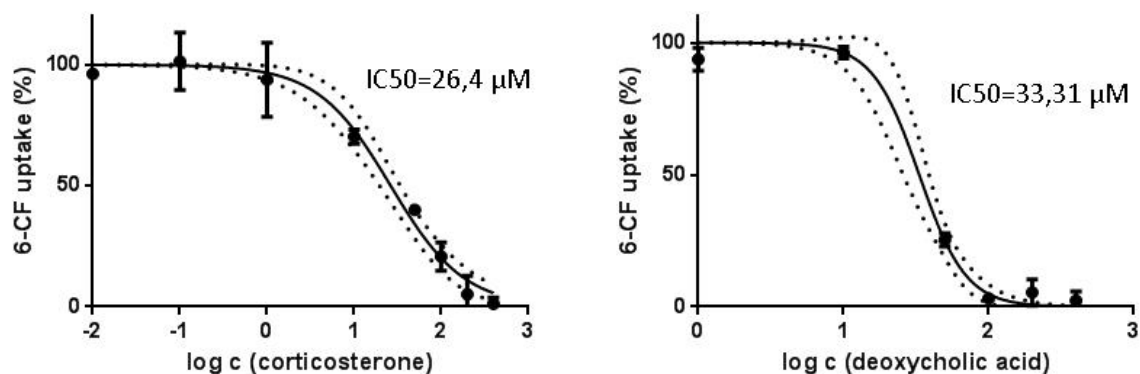


Figure S4. Concentration dependent inhibition of Oat3 mediated 6-CF uptake by corticosterone and deoxycholic acid (μM). Values on X-axis were transformed to logarithmic scale ($\log X$). Each data point represents the mean \pm SD from triplicate determinations. Dotted lines represent confidence intervals.

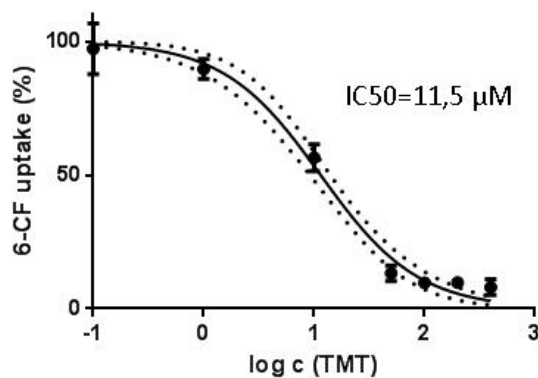


Figure S5. Concentration dependent inhibition of Oat3 mediated 6-CF uptake by TMT (μM). Values on X-axis were transformed to logarithmic scale ($\log X$). Each data point represents the mean \pm SD from triplicate determinations. Dotted lines represent confidence intervals.

11. Curriculum vitae

First name: Jelena

Family name: Dragojević

Date of birth: August 5th 1989

Place of birth: Virovitica, Croatia

Nationality: Croatian

Present position: Ph.D. student, Laboratory for Molecular Ecotoxicology, Division for Marine and Environmental Research, Ruđer Boskovic Institute, Zagreb, Croatia.

Education:

- PhD - Postgraduate Interdisciplinary Doctoral Study of "Molecular Biosciences", joint study of the J. J. Strossmayer University of Osijek, Ruđer Bošković Institute, Zagreb and University of Dubrovnik – in progress
- Master's degree in biology, J. J. Strossmayer University of Osijek, Department of biology, 2014
- Bachelors's degree in biology, J. J. Strossmayer University of Osijek, Department of biology, 2011

Projects:

- *Identification and functional characterization of (eco)toxicologically relevant polyspecific membrane transport proteins in zebrafish (*Danio rerio*)*. Croatian science foundation project (2014. - 2018.), Project leader Tvrtko Smital, PhD.
- *Identification and characterization of cyanobacterial toxins based on their interaction with basic cellular detoxification systems in zebrafish (*Danio rerio*) and zooplankton *Daphnia magna**. Swiss National Science Foundation (SNSF), SCOPES 2014-2016 Joint Research Project, Project leader Tvrtko Smital, PhD;
- *Ecotoxicological characterization of biologically active substances from marine environment*, funded within Center of excellence for science and technology integrating Mediterranean region (STIM) 2017-2021, Project leader Tvrtko Smital, PhD.

Platform presentations at scientific conferences:

1. FEBS 3+ Meeting, Molecules of Life, September 16-19, 2015, Portorož, Slovenia, Characterization of organic cation transporters in zebrafish (*Danio rerio*)
2. 13th Greta Pifat Mrzljak International School of Biophysics, October 1-10, 2016, Split – Zadar, Croatia, Functional characterization of organic anion transporters in zebrafish (*Danio rerio*): Oat2a-d
3. 10th European ZebraFish Meeting, July 3-7, 2017, Budapest, Hungary, Functional characterization of zebrafish (*Danio rerio*) organic anion transporter 2d (Oat2d)

4. Workshop: Cyanotoxins - toxicity, health and environmental impact, July 13-14, 2017, Novi Sad, Serbia, Interaction of zebrafish Organic anion transporters (Oats) with endo- and xenobiotics

5. 2nd International FishMed Conference on Zebrafish Research, March 25-27 2018, IIMCB, Warsaw, Poland, Characterization of zebrafish (*Danio rerio*) organic anion transporters Oat1 and Oat3

6. 10th Congress of Toxicology in Developing Countries, April 18-21, 2018, Belgrade, Serbia, Interaction of zebrafish (*Danio rerio*) organic anion transporter 2d (Oat2d) with xeno- and endobiotics

Publications:

1. Velki, M., Plavšin, I., Dragojević, J., Hackenberger, B.K., 2014. Toxicity and repellency of dimethoate, pirimiphos-methyl and deltamethrin against *Tribolium castaneum* (Herbst) using different exposure methods. Journal of Stored Products Research 59, 36-41.

2. Dragojević J., Mihaljević I., Popović M., Zaja R., Smital T., 2018. In vitro characterization of zebrafish (*Danio rerio*) organic anion transporters Oat2a-e. Toxicology in Vitro 46, 246-256.

Memberships:

Croatian society for biochemistry and molecular biology
Croatian biophysical society

Scholarships

Town scholarship for highschool and college students of Slatina, supported by town Slatina;
State scholarship supported by Ministry of science, education and sports of the Republic of Croatia.